THE MISCIBILITY AND THERMODYNAMICS

OF

CHLORINATED POLYETHYLENE BLENDS

SHAMSEDIN ROSTAMI

Department of Chemical Engineering and Chemical Technology

Imperial College

London

January 1983

Submitted for the Degree of Doctor of

Philosophy of the University of London

ABSTRACT

The miscibilities of solution chlorinated polyethylenes with
ethylene-vinyl acetate copolymers have been established using various
techniques.

The cloud point curves of the mixtures have been measured
using a light scattering turbidimeter. The heats of mixing of low
molecular weight analogues were found to be favourable for mixing.
The volume contractions on mixing for the analogues were measured using
a densimeter and that of a polymer blend was obtained indirectly from
the effect of pressure on the cloud point. Negative interaction
parameters were found for the blends below their cloud point temperatures
using the inverse gas chromatography technique.

Knowing all these experimental thermodynamic properties of
the mixtures it was possible to compare the results with the various
theories of polymer-polymer miscibility. A modified version of the
Flory-Huggins lattice model was used to calculate the interaction
parameters and also to simulate the phase boundaries. The disadvantages
of this model were discussed. Flory's equation of state theory with an
entropy correction factor was used to calculate the volume contraction
on mixing, the interaction parameters and the residual thermodynamic
quantities. This model was also used to simulate the spinodal curve
of the mixtures. The advantages and inherent difficulties of this
model were discussed. A need for a completely new model to explain
the thermodynamic quantities of blends with specific interaction is
recommended.

ACKNOWLEDGEMENTS

CONTENTS

CHAPTER FOUR

RESULTS

CHAPTER FIVE

SIMULATION OF PHASE BOUNDARIES

TABLES

FIGURES

CHAPTER ONE

1.1   INTRODUCTION

In the polymer literature the term compatibility is generally

used to describe the single phase behaviour of a mixture. In

commercial production processability is often used as a criterion

for compatibility, but this is not necessarily dependent on the

existence of a single phase. Miscibility is therefore better defined

in thermodynamic terms where the free energy of mixing provides an

unambiguous criterion for predicting miscibility and a true picture

of the equilibrium states of the polymer-polymer mixture, both

qualitatively and quantitatively.

The first attempt to treat the change in entropy and enthalpy

when two liquids are mixed was made in 1910 by van Laar (1910), who

based his work upon the van der Waals equation of state. A volume

additivity assumption was used and according to his expression, the

heat of mixing is always positive and can be zero in one special

condition. The theory also assumed that in a mixture, (a) the molecules

are arranged in a regular lattice, (b) the separate liquid components

have ordered structures of the same type and (c) the intermolecular

potential energy is the sum of contributions from nearest neighbours in

the lattice. The volume change in mixing is ignored by this theory.

The following equation, derived independently by Hildebrand

and Wood (1933), and Scatchard (1931, 1937), has formed the basis of

the theory of the regular solution (solubility parameter) developed

by Hildebrand et al. (1970)

$$\Delta E^M = (X_1 V_1 + X_2 V_2) \left\{ \left(\frac{\Delta E_1^V}{V_1} \right)^{\frac{1}{2}} - \left(\frac{\Delta E_2^V}{V_2} \right)^{\frac{1}{2}} \right\}^2 \Phi_1 \Phi_2 \qquad 1.1$$

where ΔE^M is the internal energy of mixing i.e. difference between

the energies of the solution and the components; X_1 and X_2 are the

molar fractions and Φ_1 and Φ_2 are the volume fractions of the

components. V_1 and V_2 are the molar volumes. $\frac{\Delta E^V}{V}$ is called the

energy of vaporization per unit volume, or more commonly, "the

cohesive energy density" and is related to the solubility parameter by:

$$\delta = \left(\frac{\Delta E^V}{V} \right)^{\frac{1}{2}} \qquad 1.2$$

The theory proves to be useful for thermodynamic considerations

of non-ideal mixtures (Hildebrand et al., 1970). This theory,

however, is only applicable to mixtures of non-polar molecules

with equivalent molar volumes and positive enthalpies of mixing. It

assumes an ideal entropy of mixing and ignores any volume change on

mixing.

The regular solution model has little practical value,

because very few mixtures are composed of two kinds of molecules whose

volumes are so nearly equal as to permit them to fit into even a

quasi-lattice, with a heat of mixing that is symmetrical in molar

composition. Despite these limitations, the theory proved to be able

to predict symmetrical phase diagrams, but failed to deal with

asymmetrical phase diagrams, caused by the difference in the molar

volumes of the components.

The first attempts to calculate the entropy of mixing of long chain molecules with segments occupying sites of a lattice and small molecules occupying single sites were made simultaneously and independently by Flory (1941, 1942) and Huggins (1941, 1942). They assumed that a chain molecule in solution may be regarded as built up from segments arranged on a regular array of sites, and that the intermolecular energy arises entirely from interactions between segments on neighbouring sites. The lattice model has been reasonably successful in interpreting the thermodynamic properties of polymer solutions, but the assumption of a lattice structure can scarcely be regarded as physically realistic. This method, however, has a wide range of usefulness as a first approximation in dealing with polymer solution properties. It also has a series of shortcomings, some of which will be briefly described here.

The restricted nature of the theory of regular solutions is one of the reasons for the limitation of the Flory-Huggins theory. The combinatorial entropy of mixing (i.e. a measure of the total number of molecular arrangements on the lattice) was calculated on the basis of that theory (Hildebrand, 1953), by assuming random distribution and no orientation for a solution in which the molecules of the components differ very considerably in size. The values obtained differ considerably from the ideal entropy of mixing. All the other assumptions of the theory are the same as in Hildebrand's theory i.e. it assumes equal volumes for polymer segments and solvent (therefore no change in volume on mixing) and that the enthalpy of mixing does not affect the magnitude of the entropy of mixing. These assumptions mean that the theory is applicable only for certain systems (Flory, 1942).

According to the original formulation, the Flory-Huggins interaction parameter χ, which arises from the mixing of n_2 moles of polymer with n_1 moles of solvent at constant temperature and pressure, is zero for athermal mixtures. Subsequent work proved that this is not true because both the excess entropy and the excess enthalpy contribute to χ:

$$\chi = \chi_S + \chi_H \qquad\qquad 1.3$$

where χ_S is the contribution from the excess entropy and χ_H is that from the excess enthalpy. It was also supposed that χ is independent of concentration, pressure, temperature and molecular weight. Experimental evidence has shown that these assumptions are over-simplifications and χ is now considered dependent on the above quantities.

A modified interaction parameter suggested by Tompa (1956) has several advantages over the Flory-Huggins interaction parameter and has been extensively used to describe binary mixtures:

$$\chi = \chi_1 + \chi_2 \Phi_2 + \chi_3 \Phi_2^2 + \ldots \qquad\qquad 1.4$$

where Φ_2 is the volume fraction of component two.

A similar empirical function, g, has been introduced by Koningsveld and Kleintjens (1971) to replace the Tompa and Flory-Huggins interaction parameter:

$$g = g_{K,1} + g_{K,2}/T + g_{K,3}T + g_{k,4}\ln T \qquad\qquad 1.5$$

$g_{K,i}$ in turn depends on measurable physical quantities such as the heat of mixing and molecular weight. This g function is related to X in the following way:

$$X = g \ (1- \Phi_2) \frac{\delta g}{\delta \Phi_2}$$ 1.6

and has been used (Koningsveld et al., 1974A) when only the second and third terms of Equation 1.5 are retained, to describe the phase boundaries of mixtures. However, no completely satisfactory molecular interpretations of g exist (Koningsveld et al., 1974A, 1980 and Koningsveld and Kleintjens, 1977) and the coefficients remain, at best, empirical.

Another shortcoming of the lattice theory was pointed out by Allen et al. (1960A, 1961) who found a bimodality on the cloud point curves of polyisobutene-poly(dimethylsiloxane) mixtures. Koningsveld et al. (1974A), by assuming a quadratic dependence of the interaction parameter on concentration, and combining it with Equation 1.5, managed to reproduce the observations of Allen et al. theoretically. In their theoretical simulation a restricted temperature dependence of g was used and polydispersity of the system was ignored. On this basis, Koningsveld et al. (1974A) drew the conclusion that the concentration dependence of the interaction parameter can outweigh the effect of the entropy of mixing, and the results of Allen et al. (1961A) can only be explained in this way.

The Flory-Huggins formulation does not take into account the effect of pressure on the miscibility of mixtures whereas experimentally introducing pressure to an oligomeric system with positive heat of mixing would result in elevation of the cloud point curves to higher temperatures. This effect was observed by Tripathi (1979) for the polystyrene-polybutadiene system for which positive heats of mixing were measured by Chong (1981). Here, one may conclude that if the spatial freedom for the mixture reduces due to applied pressure, then the configurational entropy increases to prevent an ordered arrangement of the mixture.

Finally, the present theory of polymer mixtures assumes that the force field around the molecules or polymer segments is isotropic. In other words, there are no orientation effects. However, clearly the interactional energy of two molecules depends on whether the molecules are "face to face" or "face to edge" or "edge to edge" or in any other mutual orientation. Hence, the mixing of two components will interfere with the state of each and will lead to an additional term in the enthalpy of mixing, which must take into account such factors as the shape and size of the molecules.

Rowlinson (1970) demonstrated that the idea of random mixing is an attractive and good approximation for mixtures of molecules of equal sizes and different energies. This makes it possible to specify exactly the configurational free energy of such a mixture in terms of that of one of the components, but it is quite inappropriate for mixtures of different sizes with steep Lennard-Jones potential energies. He concluded that the treatment of real mixtures must start from a position which at least does justice to the simple case of mixtures of hard spheres.

The inadequacies of the lattice model and its failure to predict the experimental results, has encouraged Flory and collaborators (Flory et al., 1964; Flory, 1965; Orwell and Flory, 1965; Abe and Flory, 1966; Eichinger and Flory, 1968) to initiate and develop a new so called "equation of state" theory by treating the molecules as hard spheres with equal volumes. In this new theory the hard core properties were introduced, which allowed calculation of all thermodynamic parameters and their corresponding excess values. Also for the first time a negative heat of mixing, interaction parameter and excess volume of mixing could be predicted by a theory.

The equation of state theory shows its superiority over the lattice model in many aspects, for example it predicts lower and/or upper critical solution phase boundaries for polymer mixtures whereas the lattice model can only predict upper critical solutions phase boundaries.

The present equation of state theory, however, although adequate in explaining early experimental results, was not completely capable of predicting the recent findings of Chahal et al. (1973) where theoretical prediction of χ are not matched with experimental ones. It therefore underwent some modification whereby an entropy correction parameter, Q_{12}, was introduced. This will be discussed in detail later on.

The original equation of state theory ignored polydispersity and its effect on the phase diagrams of the mixtures, and did not make any allowance for copolymers. It is also, like the corresponding equation of states theory of Prigogine et al. (1953) and the lattice-

fluid theory of Sanchez and Lacombe (1976), unable to give the exact

values of free energy, enthalpy and entropy change on mixing whereas

their corresponding partial molar quantities are accessible. In

addition, none of these theories considers the effect of polymer

tacticity on the miscibility of the polymer blends, as demonstrated

recently by Schurer et al. (1975) where changing the stero configuration

of poly(methyl methacrylate), PMMA, from isotactic to syndiotactic

causes it to become miscible with poly(vinylchloride), PVC.

One of the more interesting aspects of miscible blend studies

is the finding that many miscible systems with specific interactions

show cloud points on heating, which signal the existence of a lower

critical solution temperature, (LCST). The systems with LCST behaviour

have negative interaction parameters, and volume changes on mixing

below the LCST. For example, Olabisi (1975) has measured a negative

interaction parameter for PVC and Poly(ϵ. caprolactone) by inverse

gas chromatography, IGC. He proposed the possiblity of charge transfer

interactions between these two polymers which are weaker at higher

temperatures thus ensuring an LCST behaviour. Cruz et al. (1979)

have obtained negative heats of mixing for oligomeric systems with

specific interactions. They concluded that the polymer pairs whose

oligomeric analogues have negative heats of mixing are likely to form

miscible or partially miscible mixtures, and polymer pairs whose

oligomeric analogues show positive heats of mixing are invariably

immiscible. On the other hand, the miscibility due to a specific

interaction between PVC and the carbonyl oxygen of several polyesters

has been compiled by Ziska et al. (1981). Their findings indicate that

a negative interaction parameter exists between PVC and polyesters

when $3 \lesssim (CH_2)_x /COO \lesssim 12$, and it is more negative for linear polyesters compared to branched ones at the same value of $(CH_2)_x/COO$.

Nishi and Wang (1975) showed that the heat of mixing parameter in the classical theory of melting point depression is negative when it is applied to a miscible blend of poly(vinylidene flouride) (PVF_2) with PMMA. It is similarly negative for miscible blends of PVF_2 with poly(ethylmethacrylate), poly(methylacrylate), poly(ethylacrylate) and poly (vinylmethylketone), (Paul and Barlow, 1979). The LCST of these systems and also of PVF_2-PMMA was described by Bernstein et al. (1977).

The LCST behaviour of monodisperse poly(styrene) and poly (vinylmethylether PVME) with a molecular weight range of 10,000 to 20,000 was described by Nishi and Kwei (1975). These systems were studied in more detail by Davis and Kwei (1980) and Cowie and Saeki (1982) who found both LCST and UCST behaviour when polystyrene had the appropriate molecular weight. There are several other miscible systems which have already been documented by Krause (1978) and Olabisi et al. (1979) and more recently miscible pairs of PVC-solution chlorinated polyethylene (Doube and Walsh, 1979) solvent cast from 2-butanone and PVC with various polyacrylates and polymethylacrylates both solvent cast and prepared by in situ polymerization (Walsh and McKeown, 1980) were established and studied.

Lipatove et al. (1978) have found that the negative interaction parameters for poly(ethylene glycol), PEG 2,000-poly(ethylene glycol), PEG 40,000, a mixture with specific interactions, will become positive

at elevated temperatures. Nesterov et al. (1976) have also studied the

effect of temperature on the free energy of mixing of oligomers with

both UCST and LCST behaviour by the IGC technique. They found two

minima in the free energy of mixing for poly(propylene glycol), PPG

1050-poly(ethylene glycol adipate), PEGA 2,000 mixtures at all

compositions. They attributed the negative free energies to a miscible

region and positive free energies to immiscible regions, and thus

generated the phase diagrams of the system. Their calculation shows

that the heat of mixing is negative in the miscible region and remains

negative but small in the immiscible region. These considerations

commonly show that the most important factor for enhancing the

miscibility of high molecular weight polymers is the introduction of

specific interactions between constituents of individual chains, which

provide the necessary driving force for miscibility. Hydrogen bonding

is a specific interaction which has been proposed for many miscible

polymer systems as described by Paul and Newan (1978) and Olabisi et

al. (1979).

If we accept the concept of additivity of heats of mixing

given by Paul (1978) as

$$\Delta H_M = \Delta H_M(dis) + N\Delta H_M(sp) \qquad \qquad 1.6$$

where $N\Delta H_M(sp)$ is the contribution of specific interaction and $\Delta H_M(dis)$

is that of dispersive forces to the total heats of mixing, then for

a negative heat of mixing, the energy of the specific interactions

must exceed the positive contribution of $\Delta H_M(dis)$. Recent calculations

of Combs and Danne (1982) have predicted that the repulsive forces

between CH_2 and C atoms of two parallel and opposed paraffin molecules

to be 0.22 and 0.13 Kcal mol^{-1} respectively. The results are given at

separation distances where attraction forces vanish. According to

these results, a kind of specific interaction can bring about miscibility

of two polymers which can outweigh the repulsive energies.

The search for miscibility after all remains in the hands of

experimental findings. There are a number of examples given by

Krause (1978) indicating that preparation procedure and the method

used in studying the miscibility play a role in establishing a

miscible blend. For example, a transparent film, with a single glass

transition temperature, cast from cyclohexane was obtained by Kosai and

Higashino (1975) for EVA55 (and EVA with more than 55w% acetate content)

in PVC where two Tg's were detected by Marcincin et al. (1972) when

the blends were precipitated from 1% chlorobenzene solution. Storstom

and Randy (1971) and also Hedvig and Marossy (1981) without knowing

the cloud point temperature of EVA74-PVC have blended the sample at a

very high temperature in a two roll mill which gave a phase separated

blend. There are similar examples in other systems such as PMMA-PVC

as discussed by Walsh and McKeown (1980).

The aim of the present work is to establish miscible polymer

pairs and apply both the lattice and the equation of state models to

the mixtures to calculate their thermodynamic quantities and demonstrate

the advantages or disadvantages of each model in the light of experimental

results.

The mixtures presented here are blends of solution chlorinated

polyethylenes and ethylene-vinyl acetate copolymers. The miscibilities

and cloud point curves of the mixtures are established and the thermo-

dynamic parameters of the materials measured. The phase diagrams are

then simulated using the various theories.

CHAPTER TWO

THEORIES OF POLYMER-POLYMER MISCIBILITY

2.1   FLORY-HUGGINS LATTICE MODEL

There are two distinct statistical mechanical approaches to formulating a theory of chain molecular liquids and their mixtures. The first seeks to know the process by which the intermolecular forces determine the structure of the system. This is the method of radial distribution functions which is a correction factor applied to the random probability term of spherical, non-polar and non-interacting molecules (Hildebrand and Wood, 1933). The second proceeds from an assumed structure which usually resembles the regular lattice structure of crystalline solids. This is the so-called "lattice" method in which a polymer chain is conceptionally divided into segments of the same size as the lattice sites, and the size is set equal to that of the solvent molecules. In doing so, the most important features of the theory of strictly regular solutions, namely, maximum random mixing and no volume change on mixing were used by Chang (1939), Miller (1942), Huggins (1941, 1942) and Flory (1941, 1942).

2.1.1   The Entropy Change on Mixing

The combinatorial entropy of mixing of two monodisperse polymers with an arbitrary common segmental volume V^o and each consisting of N_i molecules with x_i segments, can be obtained by assuming that the segments are occupying cells (sites) of a three dimensional lattice with a total number of $N_1 x_1 + N_2 x_2$.

The number of moles of each polymer is $n_i = \dfrac{N_i}{N_A}$, the total volume

of the mixture is $(N_1 x_1 + N_2 x_2) V^o$, and the volume fraction, ϕ_i of

polymer i would be:

$$\phi_2 = \frac{n_2 x_2}{n_1 x_1 + n_2 x_2} \;, \quad \phi_1 = 1 - \phi_2 \qquad 2.1$$

By assuming that i_2 molecules of polymer 2 are already in the

lattice, the fraction of occupied sites is:

$$f_{i_2} = \frac{i_2 x_2}{N_1 x_1 + N_2 x_2} \qquad 2.2$$

and the fraction of unoccupied sites $= 1 - f_{i2}$ \qquad 2.3

The first segment of the $(i_2 + 1)$th polymer molecule can be

added in several ways in free places, i.e. $(1 - f_{i2})(N_i x_1 + N_2 x_2)$.

The second segment must be added in the adjacent and free places in

$(1 - f_{i2})Z$ ways where Z is the number of immediate neighbouring sites.

The third segment should occupy another neighbouring site which must

not be occupied by first segment of the molecule; in $(z - 1)(1 - f_{i2})$

ways. This will be true for the rest of polymer segments. Flory

and Huggins separately assumed that f_{i2} is independent of position

and the polymer is fully flexible. Hence, the number of distinguishable

ways of placing the $(i_2 + 1)$th segments on the lattice is a product

of the following series:

$$v_{i_2+1} = \tfrac{1}{2}(1 - f_{i2})^{x_2} Z(Z - 1)^{x_2 - 2} (N_1 x_1 + N_2 x_2) \qquad 2.4$$

The factor one half being introduced, since the two chain

ends are indistinguishable. Therefore, the number of ways, Ω_2, of

adding N_2 polymer molecules in the lattice is:

$$\Omega_2 = \frac{1}{N_2!} \prod_{i_2=0}^{N_2-1} v_{i_2+1} \qquad 2.5$$

By an analogous procedure the segments of polymer one are introduced into the remaining vacant sites, and one obtains:

$$\Omega_1 = \frac{1}{N_1!} \prod_{i_1=0}^{N_1-1} \nu_{i_1+1} \qquad 2.6$$

where

$$\nu_{i_1+1} = \tfrac{1}{2}(1-J_{i_1})^{x_1} Z(Z-1)^{x_1-2} (N_1 x_1 + N_2 x_2) \qquad 2.7$$

and

$$J_{i_1} = (N_2 x_2 + i_1 x_1)/(N_1 x_1 + N_2 x_2) \qquad 2.8$$

The total number of ways of introducing $N_1 x_1$ and $N_2 x_2$ segments into the lattice is:

$$\Omega = \Omega_1 \Omega_2 \qquad 2.9$$

From Boltzman's law the entropy of mixing is given by:

$$\frac{S_M}{k} = \ln \Omega_1 \Omega_2 = \ln \Omega_1 + \ln \Omega_2 \qquad 2.10$$

where $k = \dfrac{R}{N_A}$, Boltzman constant, R is the gas constant and N_A is Avogadro's number.

To obtain $\ln \Omega_1$, and $\ln \Omega_2$, the terms which are not dependent on i can be taken outside the product. Applying Stirling's approximation for the logarithmic factorial gives:

$$\frac{S_M}{k} = -N_2 \ln N_2 + N_2 - N_2 \ln 2 + N_2 \ln Z(Z-1)^{x_2-2} + N_2 \ln (N_1 x_1 + N_2 x_2)$$

$$-N_2 x_2 - N_1 \ln N_1 + N_1 - N_1 \ln 2 + N_1 \ln Z(Z-1)^{x_1-2} + N_1 \ln (N_1 x_1 + N_2 x_2)$$

$$-N_1 x_1 \qquad 2.11$$

The entropy of polymer 2 in a lattice of $N_2 x_2$ sites and the entropy of polymer 1 in a lattice of $N_1 x_1$ sites can be obtained easily by using $N_1 = 0$ for the former and $N_2 = 0$ for the latter, then in order to obtain the change in the entropy of mixing of the mixture the following relation must hold:

$$\frac{\Delta S_M}{k} = \frac{1}{k}(S_M - S_1 - S_2)$$ 2.12

therefore,

$$\frac{\Delta S_M}{k} = -N_1 \ln(N_1 x_1)/(N_1 x_1 + N_2 x_2) - N_2 \ln(N_2 x_2)/(N_1 x_1 + N_2 x_2)$$ 2.13

By replacing the number of molecules by the practical unit

of moles, the total volume of the mixture by $(n_1 x_1 + n_2 x_2)V^o$ and the

volume fraction of each component from Equation 2.1, then as a first

approximation for the combinatorial entropy of mixing per mole of

mixture, Equation 2.13 provides:

$$\Delta S^M_{comb.} = -R(n_1 \ln\phi_1 + n_2 \ln\phi_2)$$ 2.14

or $\quad \Delta S^M_{comb.} = -R \sum n_i \ln\phi_i$ 2.15

The partial molar entropy of each component[*] in the mixture

relative to its standard is,

$$\bar{S}_1 - S_1^o = -R \{\ln\phi_1 + (1-\frac{x_1}{x_2})\phi_2\}$$ 2.16

$$\bar{S}_2 - S_2^o = -R \{\ln\phi_2 + (1-\frac{x_2}{x_1})\phi_1\}$$ 2.17

and the combinatorial free energy of mixing of two components, for an

ideal mixture is:

$$\Delta G_{comb.} = -T\Delta S^M_{comb.} = RT(n_1 \ln\phi_1 + n_2 \ln\phi_2)$$ 2.18

---

* Partial molar quantities are designated by bars above the symbols for
  molar quantities and are defined as the rate of increase in the content
  of that particular quantity of the system while that particular
  component is being added at constant temperature, pressure and mole
  numbers of other components. The partial molar quantity of the
  free energy is called the chemical potential.

2.12   The Enthalpy Change on Mixing

The energy change involved in replacing neighbouring sites occupied by like segments by unlike segments may be calculated in terms of molecular pair contacts. If the attraction energy between like segments in polymer 1 and polymer 2 is assumed to be ε_{11} and ε_{22} respectively, that between unlike segments would be ε_{12}. The average number of polymer 1 segments surrounding each segment of this polymer in the mixture is $(Zn_1x_1)/(N_1x_1 + N_2x_2)$ and for segments of polymer 2 is $(ZN_2x_2)/(N_1x_1 + N_2x_2)$.

a.   The interaction energy of N_1x_1 segments by ZN_1x_1 is

$$-ZN_1^2 x_1^2 \varepsilon_{11}/2(N_1x_1 + N_2x_2) \qquad\qquad 2.19$$

b.   The similar interaction for the segments of polymer 2 is

$$-ZN_2^2x_2^2 \varepsilon_{22}/2(N_1x_1 + N_2x_2) \qquad\qquad 2.20$$

c.   This interaction between segments of polymer 1 and polymer 2 would be

$$-ZN_1x_1N_2x_2 \varepsilon_{12}/(N_1x_1 + N_2x_2) \qquad\qquad 2.21$$

The heat of mixing in the mixture will rise from the addition of these three terms, and the change in heat of mixing will be obtained by subtracting the heat involved if the pure components occupied the lattice individually from that or:

$$\Delta H_M = H_M - H_{pure} \qquad\qquad 2.22$$

where $$H_{pure} = (-ZN_1x_1\varepsilon_{11} - ZN_2x_2\varepsilon_{22})/2 \qquad\qquad 2.23$$

Substituting the corresponding terms in Equation 2.22 and simplifying yields:

$$\Delta H_M = n_1x_1\phi_2\Delta\varepsilon \qquad\qquad 2.24$$

where $\Delta\epsilon = ZN_A \{(\epsilon_{11} + \epsilon_{22})/2 - (\epsilon_{12})\} = \chi_{12}RT$ 2.25

and $\Delta H_M = RTn_1x_1\phi_2\chi_{12}$ 2.26

where χ_{12} is called the "interaction parameter".

2.13   The Gibbs Free Energy Change on Mixing

If the configurational entropy change is assumed to represent the total entropy change on mixing, then the free energy of mixing can be written as:

$$\Delta G_M = \Delta H_M - T\Delta S_M$$ 2.27

Equations 2.14, 2.26 and 2.27 yield

$$\Delta G_M = RT(n_1\ln\phi_1 + n_2\ln\phi_2 + n_1x_1\phi_2\chi_{12})$$ 2.28

This equation is not absolutely correct due to the fact that the contact energy associated with ΔH_M may change the non-interacting combinatorial entropy change on mixing. It was also shown by Longuet-Higgins (1953) that this is not dependent on the lattice model. He derived the same equations by starting from the free energy of mixing, in an entirely classical statistical manner. Koningsveld et al. (1971, 1974A, 1977, 1980) benefiting from the lattice model formulated an expression for the change in free energy of mixing of a quasi-ternary mixture consisting of a solvent, and two polydisperse polymers. A simple version of it for a linearly monodisperse mixture can be summarized as follows:

$$\frac{\Delta G_M}{RT} = \frac{\phi_1}{m_1}\ln\phi_1 + \frac{\phi_2}{m_2}\ln\phi_2 + g\phi_1\phi_2$$ 2.29

where the first two terms are the combinatorial entropy, and the term

$g\phi_1\phi_2$ represents any correction that might be needed to make

Equation 2.29 conform with experimental reality. m_1 and m_2 are

the polymer chain lengths respectively, expressed as the number of

lattice sites they occupy.

Various representations of g as a series function of ϕ_2 or as

a semi-empirical closed form, have been used (for example see

Equation 1.5). Another version with four constants has been used to

fit the critical temperature and composition data of Koningsveld and

Kleintjens (1972) for polystyrene in cyclohexane.

$$g = \alpha + (\beta_o + \frac{\beta_1}{T})/(1 - \gamma\phi_2) \qquad\qquad 2.30$$

where α, β_o, β_1 and γ are constants and can be obtained from the

phase boundaries of the system (Koningsveld and Kleintjens, 1972).

Although there is some foundation for this equation based

on detailed lattice calculations, the constants were used merely as

adjustable parameters to fit the data. This modification improved

the shape of the unmodified Shultz-Flory (1952) curves, but still cannot

predict the experimental results.

According to Huggins (1970, 1976) allowance must be made for

the influence of the immediate surroundings on a segment in the chain.

Setting the average allowed number of orientations of the segment

equal to v^o when it is at infinite dilution in the second polymer, and

correcting it to a value $v^o(1 - k_s)$ for a segment in the undiluted

polymer, Huggins calculated two orientational contributions to the

entropy of mixing. Inserting these two terms into Equation 2.29, one obtains:

$$\frac{\Delta G_M}{RT} = \frac{\phi_1}{m_1} \ln\phi_1 + \frac{\phi_2}{m_2} \ln\phi_2 + g\phi_1\phi_2$$

$$-\phi_1 \ln\{1 + K_1(1-\gamma)\phi_2 Q^{-1}\} \quad -\phi_2 \ln\{1 + K_2\phi_1 Q^{-1}\} \qquad 2.29.1$$

where the two parameters K_1 and K_2 are related to $K_{S,1}$ and $K_{S,2}$ by

$K_i = K_{s,}/(K-K_{s,i})$; $\quad Q = 1 - \gamma\phi_2$ and $\gamma = 1-S_2/S_1$; where s_i = interacting

surface of a segment i per unit volume.

This new correction, still based on random mixing, takes into account the effect of flexibility of one chain on the flexibility of its neighbours. K_1 and K_2 are also responsible for bimodality in the spinodal.

By definition, the thermodynamic limits of stability are called the spinodal and are characterized by a $\Delta G_M(\phi_2)$ function. The relation between $\Delta G_M(\phi_2)$ and the phase diagrams is illustrated in Figure 2.1. The $\Delta G_M(\phi_2)$ curve (Figure 2.1.B) for a two phase system has two inflection points where:

$$\left(\frac{\partial^2 \Delta G_M}{\partial\phi_2^2}\right)_{T,P} = 0 \qquad 2.31$$

The locus of these points in a $T(\phi_2)$ plot (i.e. phase diagram) is the spinodal. As the temperature changes (upwards for a UCST and downwards for an LCST) the two minima move together. The so-called consulate point or critical state occurs where the two points of inflection and the tangent points (coexisting phase compositions) coincide. Therefore

at the critical point:

$$(\frac{\partial^2 \Delta G_M}{\partial \phi_2^2})_{T,P} = (\frac{\partial^3 \Delta G_M}{\partial \phi_2^3})_{T,P} = 0 \qquad\qquad 2.32$$

Since $\Delta g_M = \phi_1 \Delta\mu_1 + \phi_2\Delta\mu_2$, then

$$\frac{\partial \Delta g_M}{\partial \phi_2} = \Delta\mu_2 - \Delta\mu_1 \qquad\qquad 2.33$$

where $\Delta\mu_1$ and $\Delta\mu_2$ are the chemical potential changes on mixing for

component 1 and 2 respectively. By this definition equality of $\Delta\mu_1 = \Delta\mu_1'$ and

$\Delta\mu_2 = \Delta\mu_2'$ for the whole composition range will produce the binodal curve

shown in Figure 2.1. The region between the binodal and the spinodal

is called the meta-stable region.

It has been shown (Chong, 1981) that the Flory-Huggins

expression for ΔG_M is useful in describing liquid-liquid mixtures.

The description is at least qualitatively correct. To ascertain this,

the ΔG_M function must be checked against experimental data, such as,

vapour pressure, osmatic pressure, etc. Such methods yield the chemical

potentials i.e. the first derivations of ΔG_M with respect to the concen-

tration, (Vink, 1975). On the other hand, the spinodal curve can be

obtained for liquid-liquid mixtures by the Pulse Induced Critical

Scattering (PICS) method which has been successfully applied by

various authors (Koningsveld et al., 1980; Kleintjens et al., 1980).

This can also give the critical point, i.e. $(\frac{\delta^3 \Delta G_M}{\delta \phi_2^3})_{P,T}$ from the

phase volume ratio:

$$r = (\phi_2'' - \phi_2)/(\phi_2 - \phi_2') \qquad\qquad 2.34$$

which at critical point gives $r = 1$.
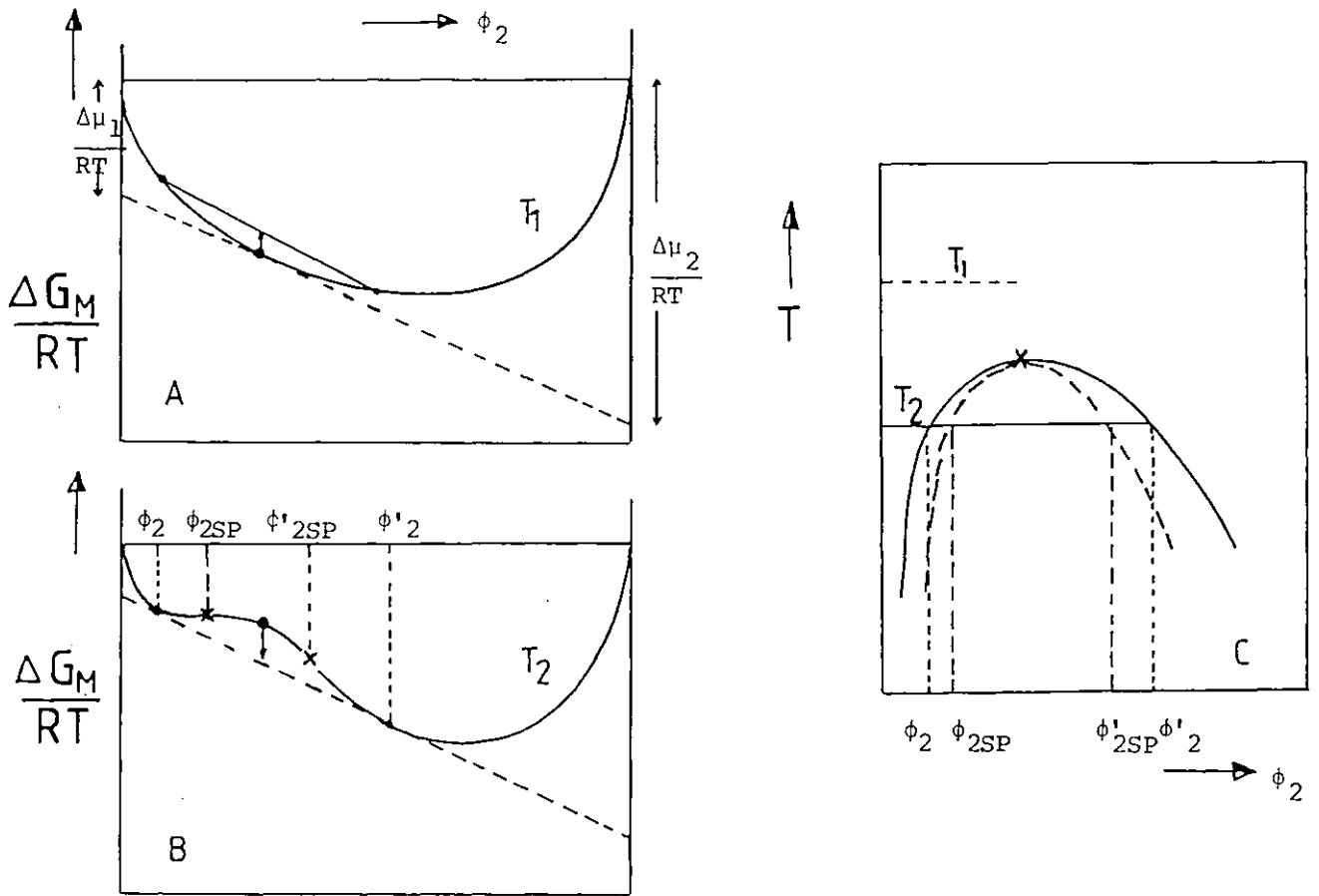
FIG. 2.1. The Gibbs free energy change on mixing as a function of volume fraction of component two showing
A. Complete, B. Partial miscibility.
Graph C is the phase diagram as a result of variation of free energy with temperature. Solid line in this graph represents the binodal curve and dashed line represents the spinodal curve.

Unfortunately there has not been a consistent series of measurements of binodal, spinodal and critical point on the same system to allow careful comparison with the Flory-Huggins theory. It is, however, certain that the original model is incapable of predicting lower critical solution temperature (LCST) phase diagrams which are common phenomena in high molecular weight polymer mixtures with a specific interaction (Bernstein et al., 1977). It also fails to deal with systems like polystyrene - poly(vinyl methyl ether) which exhibit both lower critical solution temperature (LCST) and upper critical solution temperature (UCST), for a selected range of molecular weights (Davis and Kwei, 1980 and Cowie and Saeki, 1982).

The lattice theory does not make allowance for an influence of pressure on the mixture because it ignores volume changes on mixing. However, if the g function of Koningsveld is used, one could assume g to depend on pressure as well as concentration.

Despite the corrections and new developments allowed in the theory, it cannot deal with all the new available data in the recent literature. Three major corrections in the theory are still necessary:

a.   Segment surface-area ratio

b.   Chain dimensions as a function of concentration, temperature and molar mass,

c.   Free volume.

In order to take into account all these corrections, and the contributions of the liquid state to the thermodynamics of mixtures in general, Flory and his collaborators, Flory et al. (1964), Flory (1965)

developed a new partition function. This partition function combines a geometrical factor for hard spheres (or any other shape) with an intermolecular energy of the van der Waals form, and also defines the equation of state and partial molar thermodynamic functions.

Although this new approach is an improvement over the classical Flory-Huggins formulation in terms of agreement between theory and experiments, the latter is still used by numerous workers due to its simplicity.

2.2 Flory's Equation of State Theory

In the equation of state model, Flory and co-workers abandoned the whole concept of a lattice, and characterised each pure component by three equation of state parameters, v^*, T^* and P^*, which may be evaluated from the pure component data, density, thermal expansion coefficient, and thermal pressure coefficient. In addition an interaction term, characterised by X_{12}, associated with a difference in chemical nature between the components was introduced in order to calculate the properties of the mixture.

This theory like other new theories (Patterson and Delmas, 1970, and Sanchez and Lacombe, 1978) benefits from the essential assumption of Prigogine et al. (1953) who divided a chain into "r-segments" and specified the number of external degrees of freedom.

We start with N molecules each one divided into r-segments
(the choice of a segment is arbitrary). The partition function for
non-attractive spherical molecules is given by:

$$\Omega = \{\gamma^{1/3}(v^{1/3} - v^{1/3}_*)e\}^{3Nrc} \quad , \ell^* \text{ is the hard-core length} \quad 2.35$$

where $\gamma = 1*^3/v^*$ is a purely geometrical factor, v is the volume and
v* is the hard-core volume of the molecule. The term 3 Nrc is interpreted
as follows: if Nr segments were independent of each other, then 3Nr would
be the number of degrees of freedom related to intermolecular motions.
Owing to the constraints of the chain this number is reduced, i.e. 3c
is the number of intermolecular degrees of freedom per segment:
$o < c \leq 1$. The total number of degrees of freedom is then divided
between internal and external. Flory ignored the contribution of
internal interaction and assumed c to be independent of temperature.
The derivation of Equation 2.35 is given in Appendix A-I.

Having formulated Equation 2.35 for non-attractive molecules,
a volume dependent "mean" intermolecular (attractive) energy, E_O,
is introduced:

$$E_O = -constant/v^m; \quad m \sim 1 \qquad\qquad 2.36$$

This gives a new partition function:

$$Z = \Omega \exp(-E_O/kT) \qquad\qquad 2.37$$

This expression is fundamental to the new theory which is
no longer related to a fixed volume. Provided only nearest-neighbour
interactions are important, E_O can be written

$$E_O = -(number of contacts).\eta/v = -NrS\eta/2v \qquad\qquad 2.38$$

where the number of contacts is $\frac{1}{2}$ NrS, and η/v is the intermolecular
energy per contact, S being the number of contact sites per segment,
proportional to the ratio of the surface area to the segmental volume.

Equation 2.38 can be expressed in terms of temperature by introducing the reduced volume, temperature and pressure as:

$$\tilde{v} = v/v^*, \quad T = \tilde{T}/T^*, \quad \tilde{P} = P/P^* \tag{2.39}$$

where the characteristic hard core parameters P^*, v^* and T^* satisfy the equation

$$P^*v^* = ckT^* \tag{2.40}$$

In further calculations it is convenient to define

$$\tilde{T} = T/T^* = 2v^*ckT/S\eta \tag{2.41}$$

therefore Equation 2.40 gives

$$P^* = S\eta/2v^{*2} \tag{2.42}$$

In Equation 2.37 where E_o is substituted from Equation 2.38 and $v = \tilde{v}.v^*$ we have:

$$Z = \Omega \exp(NrS\eta/2\tilde{v}v^*kT) \tag{2.42}$$

The exponential can be further simplified by using relation 2.41 to become:

$$Z = \Omega \exp(Nrc/\tilde{v}\tilde{T}) \tag{2.43}$$

Equation 2.35 can also be converted to:

$$\Omega = (\gamma v^* e^3)^{Nrc} . (\tilde{v}^{1/3} - 1)^{3Nrc} \tag{2.44}$$

Equations 2.43 and 2.44 will now yield the final partition function as

$$Z = \text{constant} (\tilde{v}^{1/3} - 1)^{3Nrc} \exp(Nrc/\tilde{v}\tilde{T}) \tag{2.45}$$

the constant being independent of T and v.

The pure component equation of state can be derived by differentiating Equation 2.45 for the pressure of the system, i.e.

$$P = (kT/Nr) . (\partial \ln Z/\partial v)_{T,N} \tag{2.46}$$

With the aid of Equations 2.39 and 2.40 this equation will become

$$\tilde{P} = (\tilde{T}/Nrc).(\partial \ln Z/\partial \tilde{v})_{\tilde{T},N} \qquad 2.46a$$

The resulting equation of state is:

$$\tilde{P}\tilde{v}/\tilde{T} = \tilde{v}^{1/3} / (\tilde{v}^{1/3} - 1) - 1 /\tilde{T}\tilde{v} \qquad 2.47$$

At atmospheric pressure $\tilde{P} \cong 0$ this equation yields:

$$\tilde{T} = (\tilde{v}^{1/3} - 1)/\tilde{v}^{4/3} \qquad 2.48$$

The equation of state parameters for a pure component may be obtained from its thermal expansion coefficient, α, and thermal pressure coefficient, γ, defined as:

$$\alpha = (1/v).(\delta v/\partial T)_{P,N} = (\partial \ln v/\partial T)_{P,N} \qquad 2.49$$

$$\gamma = (\partial P/\partial T)_{V,N} \qquad 2.50$$

from which it follows that

$$\tilde{v} = \{1 + (\alpha T)/3(1 + \alpha T)\}^3 \qquad 2.51$$

A derivation of this equation is shown in Appendix A-II. For a given α, Equation 2.51 gives $\tilde{v}$ and Equation 2.48 will provide $\tilde{T}$. Differentiation of Equation 2.47 followed by substitution from Equations 2.39 and 2.48 yields (see A-III)

$$P* = \gamma \, T\tilde{v}^2 \qquad 2.52$$

Evaluation of the equation of state parameters in this way enables one to obtain the other parameters such as c and $S\eta/2v$ (intermolecular energy per segment) etc.

2.2.1   Monodisperse Binary Mixtures

Adaptation of this theory to binary mixtures proceeds unambiguously from two premises, as follows:

a.   The core volumes of the pure components are additive, and the specification of a segment for each component remains arbitrary. Hence, it is convenient to choose segments of equal size so that $v_1^* = v_2^* = v^*$.

b.   The intermolecular energy depends on the surface area of contact between molecules and/or segments. The validity of this assumption rests on the fact that the intermolecular attractions are of short range compared with the molecular diameter of most liquids.

These assumptions were further discussed by Patterson and Delmas (1970).

The application of assumptions a and b leads at once to the following relations (fixing the parameters r, S and c applicable to the mixture)

$$N = N_1 + N_2 \qquad\qquad 2.53$$

$$\bar{r} = (\phi_1/r_1 + \phi_2/r_2)^{-1} \qquad\qquad 2.54$$

$$S = \phi_1 S_1 + \phi_2 S_2 = (r_1 N_1 S_1 + r_2 N_2 S_2)/\bar{r}N \qquad\qquad 2.55$$

$$\bar{c} = \phi_1 c_1 + \phi_2 c_2 = (r_1 N_1 c_1 + r_2 N_2 c_2)/\bar{r}N \qquad\qquad 2.56$$

It is necessary to redefine ϕ_1 and ϕ_2 as segment fractions, instead of volume fractions as introduced in the lattice model, i.e.

$$\phi_2 = 1 - \phi_1 = r_2 N_2/\bar{r}N \qquad\qquad 2.57$$

The molar hard-core volume is given by $V_i^* = rv_i^*$, thus $r_2/r_1 = V_2^*/V_1^*$, and we may write the segment fraction as

$$\phi_2 = N_2 V_2^* / (N_2 V_2^* + N_1 V_1^*) \qquad 2.58$$

or

$$\phi_2 = m_2 v_{SP,2}^* / (m_2 v_{SP,2}^* + m_1 v_{SP,1}^*) \qquad 2.59$$

where m_i is the mass of component i and $v_{SP,i}^*$ is the hard-core volume

per gram. These definitions will lead us to the following partition

function for the mixture,

$$Z = Z_{comb} \cdot (\gamma v^*)^{\bar{r}Nc} \cdot (\tilde{v}^{1/3} - 1)^{3\bar{r}N\bar{c}} \cdot \exp(-E_{O_M}/kT) \qquad 2.60$$

where Z_{comb} is the combinatorial factor for intermixing the two

components.

The intermolecular energy of the mixture E_{O_M} assumes a

similar form to that of the pure components, i.e.

$$E_{O_M} = -(A_{11}\eta_{11} + A_{22}\eta_{22} + A_{12}\eta_{12})/v \qquad 2.61$$

where A_{iJ} is the number of nearest neighbour contents of energy $-\eta_{iJ}/v$.

Assuming random mixing, it follows that (see Equation 2.38),

$$A_{12} = S_1 r_1 N_1 \theta_2 = S_2 r_2 N_2 \theta_1 \qquad 2.62$$

$$2A_{11} + A_{12} = S_1 r_1 N_1 \qquad 2.63$$

$$2A_{22} + A_{12} = S_2 r_2 N_2 \qquad 2.64$$

$$\Delta\eta = \eta_{11} + \eta_{22} - 2\eta_{12} \qquad 2.65$$

where θ_2 and θ_1 are site fractions and defined by:

$$\theta_2 = 1 - \theta_1 = S_2 r_2 N_2 / (S_2 r_2 N_2 + S_1 r_1 N_1) = (S_2/S_1) \cdot \phi_2 /$$
$$\{\phi_1 + (S_2/S_1)\phi_2\} = S_2\phi_2/S \qquad 2.66$$

Substitution of these equations into Equation 2.61 gives:

$$E_{O_M} = -(S\bar{r}N/2v)(\theta_1\eta_{11} + \theta_2\eta_{22} - \theta_1\theta_2\Delta\eta) \qquad 2.67$$

By an analogous definition to the energy of the pure component (see

Equations 2.38 and 2.42), the energy of the mixture can be defined as:

$$-E_{O_M}/\bar{r}N = P^*v^*/v \qquad 2.68$$

$$(\text{where } P_i^* = S_i\eta_{ii}/2v^{*2} \qquad 2.42)$$

Comparison of Equation 2.67 with Equation 2.68 and each individual

term with Equations 2.42 and 2.66 gives:

$$P^* = \phi_1 P_1^* + \phi_2 P_2^* - \phi_1 \theta_2 X_{12} \qquad 2.69$$

where $\quad X_{12} = S_1 \Delta\eta / 2v^* \qquad\qquad\qquad\qquad 2.70$

and is the interaction term, with dimensions of energy per unit

volume, and arises from the difference in chemical nature of the components.

Since Equation 2.40 is also applicable to the mixture, it

follows that:

$$P^* v^* = \bar{c} K T^* \qquad\qquad\qquad\qquad 2.71$$

and $\quad T^* = P^* / (\phi_1 P_1^* T_1^{*-1} + \phi_2 P_2^* T_2^{*-1}) \qquad 2.72$

Equations 2.69 and 2.72 show that the reduced parameters, $\tilde{P}$ and $\tilde{T}$,

for the mixture are composition dependent. Knowing $\tilde{T}$ for the mixture,

Equation 2.48 provides an important quantity, $\tilde{v}$, which is essential

in order to specify the binary mixture quantitatively.

2.2.2   The Enthalpy Change on Mixing

We now have all the quantities needed to calculate the

enthalpy change (i.e. excess enthalpy) on mixing which is equal to the

energy change on mixing at low pressure:

$$\Delta H_M = E_{o_{1,2}} - (E_{o_1} + E_{o_2}) \qquad 2.73$$

This can be expressed in terms of a subscripted version of Equation 2.68

as:

$$\Delta H_M = \bar{r} N v^* \{ \phi_1 P_1^* / \tilde{v}_1 + \phi_2 P_2^* / \tilde{v}_2 - P^* / \tilde{v} \} \qquad 2.74$$

Introducing P* from Equation 2.69 yields:

$$\Delta H_M = \bar{r} N v^* \{ \phi_1 P_1^* (\tilde{v}_1^{-1} - \tilde{v}^{-1}) + \phi_2 P_2^* (\tilde{v}_2^{-1} - \tilde{v}^{-1})$$
$$+ \phi_1 \theta_2 X_{12} / \tilde{v} \} \qquad 2.75$$

Since $\phi_i \bar{r} N = r_i N_i$ and $r_i v^* = V_i^*$, Equation 2.75 can be written as:

$$\Delta H_M = N_1 P_1^* V_1^* (\tilde{v}_1^{-1} - \tilde{v}^{-1}) + N_2 P_2^* V_2^* (\tilde{v}_2^{-1} - \tilde{v}^{-1})$$
$$+ N_1 V_1^* \theta_2 X_{12}/\tilde{v} \qquad\qquad 2.76$$

The latter form is preferred for mixtures of molecules which are comparable in size. The last term in each of these equations represents the contributions from contact interactions attributable to a difference between 1,2 pairs and the mean of 1,1 and 2,2 contact pairs. The terms preceding it, will be referred to as the equation of state terms. Their contribution to the enthalpy change on mixing depends on the reduced volume of the mixture. Eichinger and Flory (1968) wrote Equations 2.75 and 2.76 in a simple form as:

$$\Delta H_M = B N_1 \phi_2 \qquad\qquad 2.77$$

where B is assumed to be constant and independent of concentration. B is determined from the measured heat of mixing of one polymer with a large excess of the other. The important quantity X_{12}, in the limit of infinite dilution, may be obtained by series expansion of Equation 2.75 in powers of ϕ_2. This gives B in energy per mole as:

$$B = \lim_{\phi_2 \to 0} (\Delta H_M/N_1 \phi_2) = \lim_{N_2 \to 0} (\Delta H_M/N_2)(V_1^*/V_2^*)$$

$$= (V_1^*/\tilde{v}_1) \{P_2^* [(\tilde{v}_1/\tilde{v}_2 - 1) - \alpha_1 T(1 - \tilde{T}_2/\tilde{T}_1)] + (1 + \alpha_1 T)$$

$$(S_2/S_1)X_{12}\} \qquad\qquad 2.78$$

If $\tilde{T}_1 > \tilde{T}_2$, the equation of state contribution within the square brackets is negative, and the enthalpy change on mixing for a large excess of solvent will be negative unless X_{12} is large enough to dominate the terms in brackets. The negative enthalpy change on mixing will ensure a negative excess volume change on mixing defined as follows:

$$\tilde{v}^E = \tilde{v} - \tilde{v}^o, \quad \tilde{v}^o = \phi_1\tilde{v}_1 + \phi_2\tilde{v}_2 \qquad\qquad 2.79$$

or

$$\tilde{v}^E/v^o = \tilde{v}/(\phi_1\tilde{v}_1 + \phi_2\tilde{v}_2) - 1 \qquad\qquad 2.80$$

Equation 2.80 is related to the composition through $\tilde{T}$ or $T*$.
Measurements of the volume change on mixing ΔV_M and the unmixed V^o
gives $\tilde{v}^E/v^o = \Delta V_M/v^o$ directly.

Differentiating Equation 2.76 with respect to N_i will give
the partial molar heat of mixing of component i. In this derivation
the variation of $\tilde{v}$ with composition must be considered.

$$\Delta\bar{H}_1 = \bar{H}_1 - H_1{}^o = (\partial\Delta H_M/\partial N_1)_{\tilde{T},\tilde{P},N_2}$$

$$= (\partial\Delta H_M/\partial N_1)_{N_2,\tilde{T},\tilde{v}} + (\partial\Delta H_M/\partial\tilde{v})_{N_2,\tilde{T},N_1} \cdot (\partial\tilde{v}/\partial N_1)_{N_2,T,V} \qquad 2.81$$

This lengthy procedure is given in Appendix B-I, the final
result being:

$$\Delta\bar{H}_1 = P_1^*V_1^*\{(\tilde{v}_1{}^{-1} - \tilde{v}^{-1}) + (\alpha T/\tilde{v})(\tilde{T}_1-\tilde{T})/\tilde{T}\} +$$

$$(V_1^*X_{12}/\tilde{v})(1+\alpha T)\theta_2{}^2 \equiv RT\chi_H\phi_2{}^2 \qquad\qquad 2.82$$

where α, is the thermal expansion coefficient of the mixture and is
related to $\tilde{v}$ of the mixture according to Equation 2.51. Equation
2.82 serves as a definition of χ_H.

Expansion of the reduced partial molar residual (or excess)
enthalpy in powers of ϕ_2 leads to

$$\chi_H = \chi_{H,1} + \chi_{H,2}\phi_2 + \chi_{H,3}\phi_2{}^2 + \dots \qquad\qquad 2.83$$

The χ_H defined by Equation 2.82 can be used in the following equation
to evaluate the integral heat of mixing:

$$\Delta H_M = -N_1 (\phi_2/\phi_1) \int_1^{\phi_2} (\Delta\bar{H}_1/\phi_2{}^2)d\phi_2 \qquad\qquad 2.84$$

Substituting $\Delta\bar{H}_1/\phi_2{}^2 = RT\chi_H$ into the Equation 2.84 and integrating

yields:

$$\Delta H_M = RTN_1\phi_2\{\chi_{H,1} + (\chi_{H,2}/2)(1+\phi_2) + (\chi_{H,3}/3)(1+\phi_2 + \phi_2{}^2) + \ldots\}$$

2.85

This indicates that a measured heat of mixing at infinite dilution

can be used to obtain $\chi_{H,1}$, if $\chi_{H,2}$, $\chi_{H,3}$ etc. are known.

2.2.3 The Free Energy Change on Mixing

The factors of prime importance in the present theory are

the size, shape, contact interaction and the equation of state terms

of each component. According to the partition function (Equation 2.60)

and direct comparison with Equation 2.75 the free energy change on

mixing comprises a combinatorial term, $(\Delta G_{comb} = -T\Delta S_{comb} = -kT\ln Z_{comb})$,

equation of state terms and the contact interaction term. If the

molecules of the two components are comparable in size and shape, then

ΔG_{comb} should be given approximately by the ideal mixing expression,

and the remaining terms may be identified with the excess or residual

free energy, G^R. Therefore the residual free energy of mixing is

represented by a sum of the contact and equation of state terms

without limitation on the nature of the combinatorial expression.

This is also true in the case of the combinatorial and residual

entropy of mixing. Hence,

$$G^R = \Delta G_M - \Delta G_{comb}$$ 2.86

$$S^R = \Delta S_M - \Delta S_{comb}$$ 2.87

Neglecting the difference between the Helmholtz and the Gibbs free energy

at low pressure, the partition function will provide G as follows:

$$G = -kT\ln Z$$ 2.88

The details of this derivation are given in Appendix B-II, only the residual part, which we will be using in the present work will be treated here.

$$G^R = 3P_1^*V_1^*N_1\tilde{T}_1 \; \ln(\tilde{v}_1^{1/3} - 1)/(\tilde{v}^{1/3} - 1) + 3P_2^*V_2^*\tilde{T}_2$$

$$\ln(\tilde{v}_2^{1/3} - 1)/(\tilde{v}^{1/3} - 1) + \Delta H_M \qquad\qquad 2.89$$

The residual entropy of mixing arising from differences between the equation of state parameters for the pure components is implicit in the term of Equation 2.89. It may be written alternatively as:

$$S^R = -3 \; \{ (P_1^*V_1^*N_1/T_1^*) \; \ln(\tilde{v}_1^{1/3} - 1)/(\tilde{v}^{1/3} - 1) + (P_2^*V_2^*N_2/T_2^*) $$

$$\ln(\tilde{v}_2^{1/3} - 1)/(\tilde{v}^{1/3} - 1) \}$$

$$= -3\bar{r}Nv^* \; \{ (\phi_1 P_1^*/T_1^*) \; \ln(\tilde{v}_1^{1/3} - 1)/(\tilde{v}^{1/3} - 1) + (\Phi_2 P_2^*/T_2^*) $$

$$\ln(\tilde{v}_2^{1/3} - 1)/(\tilde{v}^{1/3} - 1) \qquad\qquad 2.90$$

The combinatorial part of the entropy is the one given in Equation 2.15. The partial molar residual entropy of mixing is obtained by the same method as was used to derive Equation 2.82, see Appendix B-III. Here we only write the final result:

$$T S_1^R = -P_1^*V_1^* \; \{ 3\tilde{T}_1 \; \ln(\tilde{v}_1^{1/3} - 1)/(\tilde{v}^{1/3} - 1) - (\tilde{T}_1 - \tilde{T}) . \; \alpha T/\tilde{T}\tilde{v} \}$$

$$+ \; \alpha T \; (V_1^*\theta_2^2 X_{12}/\tilde{v}) \equiv -RT\chi_S\phi_2^2 \qquad\qquad 2.91$$

The important feature of this equation is the relation between TS_1^R (or χ_S) and the reduced parameters of the mixture (i.e. $\tilde{v}$, $\tilde{T}$). It can be shown that when $\tilde{v} < \phi_1\tilde{v}_1 + \phi_2\tilde{v}_2$, χ_S will be smaller and that it becomes larger as $\tilde{v}$ approaches $\phi_1\tilde{v}_1 + \phi_2\tilde{v}_2$.

Addition of Equations 2.82 and 2.91 would yield the partial residual chemical potential of component one in the mixture. For derivation see Equations B.21, 22 and 23 in Appendix B-II.

$$(\mu-\mu_1^{\ o})^R = P_1^* v_1^* \left\{ 3\tilde{T}_1 \ln \frac{\tilde{v}_1^{1/3}-1}{\tilde{v}^{1/3}-1} + (\tilde{v}_1^{-1} - \tilde{v}^{-1}) \right\} +$$
$$v_1^* \theta_2^{\ 2} X_{12}/\tilde{v} \equiv RT X_t \phi_2^{\ 2} \qquad\qquad 2.92$$

This applies when the effect of the pressure on the mixture is neglected and the entropy correction factor, Q_{12}, has not been introduced. However, from the procedures used to obtain Equation 2.92 one can define:

$$X_t = X_H + X_S \qquad\qquad 2.93$$

In the same way as with Equation 2.83, X_t and X_S can be expanded to give:

$$X_t = X_{t,1} + X_{t,2}\phi_2 + X_{t,3}\phi_2^{\ 2} + \cdots \qquad\qquad 2.94$$
$$X_S = X_{S,1} + X_{S,2}\phi_2 + X_{S,3}\phi_2^{\ 2} + \cdots \qquad\qquad 2.95$$

Obviously the chemical potential of component one in the mixture is composed of a combinatorial and residual part. The combinatorial part is the one given by the Flory-Huggins theory. Therefore:

$$(\mu-\mu_1^{\ o}) = (\mu_1-\mu_1^{\ o})_{comb} + (\mu_1-\mu_1^{\ o})^R \qquad\qquad 2.96$$
$$(\mu-\mu_1^{\ o})_{comb} = RT \left\{ \ln\phi_1 + (1-r_1/r_2)\phi_2 \right\} \qquad\qquad 2.97$$

On these grounds, the chemical potential of component one in the mixture may be written as:

$$(\mu_1-\mu_1^{\ o})/RT = \ln(1-\phi_2) + (1-r_1/r_2)\phi_2 + \left\{ (\mu-\mu_1^{\ o})^R/RT\phi_2^{\ 2} \right\}\phi_2^{\ 2} \quad 2.98$$

By equating the chemical potentials from the two theories

an expression which relates X_{12} to the Flory-Huggins interaction

parameter can be obtained:

$$X_{12} = P_1^* V_1^* / RT \; \phi_2^2 \{ 3\tilde{T} \ln(\tilde{v}_1^{1/3} - 1) / (\tilde{v}^{1/3} - 1) + (\tilde{v}_1^{-1} - \tilde{v}^{-1}) + X_{12} \theta_2^2 / P_1^* \tilde{v} \}$$

2.99

2.2.4   The Entropy Correction Parameter

The configurational entropy of formation of a mixture may be

generally separated into two parts, an entropy of disorientation,

and an entropy of mixing of the disoriented molecules. The former,

has been disregarded in the discussion of polymer mixture by assuming

an equal molecular size for the components. However, inequality of

molecular sizes for the two components suggests a difference between

ΔS_{comb} and ΔS_{ideal} and also between the excess and the residual

entropy of mixing, i.e.

$$S^E = S^R + (\Delta S_{comb} - \Delta S_{ideal})$$

2.100

the value of $(\Delta S_{comb} - \Delta S_{ideal})$ goes to zero when $r_1 \rightarrow r_2$.

Discrepancies between S^R and S^E from calculated and

experimental values were observed by Abe and Flory (1966). This

directly reflects a difference between the calculated and observed values

of χ_t and χ_s. Furthermore, the predicted values of the χ_t and χ_s

parameters are much lower than the experimental values calculated

from experimental $\Delta \mu_1^R$ and S_1^R (Chalal et al., 1973). For instance,

the predicted χ_s parameter for PDMS in n-heptane is about 0.5

whereas its experimental value, obtained by a vapour sorption

technique, lies between 0.2 and 0.4. Similarly, the theoretical

X_S parameters are negative throughout the concentration range for

PDMS in xylene, whereas its experimental values are 0.3 (Chalal

et al., 1973).

Flory has overcome these differences by introducing a
purely entropy correction term into the free energy equation of the
mixture. The correction seems inevitable since the theory assumed
only contact interactions between neighbouring segments contribute
to X_{12} and treated X_{12} as an enthalpy parameter, while the interactions
between neighbours also affect the entropy. Such an entropy
contribution involving contacts of end and midchain segments, must
depend on the composition of the mixture in the same manner as the
interactional energy term.

On this basis, the entropy parameter Q_{12} is represented by
its contribution $-\tilde{v}TQ_{12}$ to the total exchange interaction parameter
X_{12} which consists of both an entropy and an enthalpy part. The enthalpy
interaction parameter is defined as: $\bar{X}_{12} = X_{12} - \tilde{v}TQ_{12}$ $\qquad$ 2.101

Thus, Equation 2.92 will be written in terms of $\bar{X}_{12}$ as:

$$(\mu_1 - \mu_1^\circ)^R = P_1^* v_1^* \{3\tilde{T}_1 \ln(\tilde{v}_1^{1/3} - 1)/(\tilde{v}^{1/3} - 1) + (\tilde{v}_1^{-1} - \tilde{v}^{-1})\}$$

2.102

$$+ v_1^* \theta_2^2 / \tilde{v} \cdot (X_{12} - T\tilde{v}Q_{12}) \equiv RT \chi_t \Phi_2^2$$

Q_{12} is reported to be positive for n-alkanes mixtures

(Orwall and Flory, 1967) and negative for natural rubber in benzene

(Eichinger and Flory 1968) and for PDMS in benzene, cyclohexane or

chlorobenzene (Shih and Flory, 1972).

From these examples and also relation 2.101, one may conclude

that when Q_{12} is positive the entropy of interaction between unlike

segments is favourable for mixing, while when it is negative the

entropy of interaction between unlike segments makes unfavourable

contribution to the mixing. The effect of Q_{12} on the phase boundaries

of mixtures will be discussed later.

In conclusion the theory under review appears to be more

successful in the treatment of the polymer mixtures than the classical

Flory-Huggins theory. It has a number of arbitrary parameters, but

in principal it overcomes the inadequacies of the conventional theory

of polymer solutions. For example, the concentration enthalpy and

entropy dependence of χ are approximated by the theory, the volume

change on mixing is brought within the scope of the treatment and the

phase diagrams of the polymeric systems have been treated more

realistically than any other existing theory. This theory is simple

to apply when the state parameters of the pure components are known.

Due to the reasons stated, this theory has been applied in the present

work to calculate χ values and other thermodynamic quantities. The

spinodal simulated on the basis of this theory will be presented

later.

McMaster (1973) has also carried out an extensive numerical
analysis of this theory for the phase stability of polymer blends.
Unlike Flory and co-authors, he has considered internal and external
degrees of freedom and also polydispersity of the polymers in his
derivations. In addition, the potential energy is assumed to be of
the form

$$E_o \, \alpha \, \frac{1}{v^n} \quad , 1 < n < 1.5 \qquad\qquad 2.103$$

His observation shows that the theory is well capable of predicting
both LCST and UCST behaviours with an LCST being the more common
in high molecular weight polymer mixtures. Also, negative or very small
positive values of the interaction parameter X_{12} favour miscibility.
The latter is responsible for both the UCST and LCST, whereas larger
positive values yield hourglass-type phase diagrams and larger negative
values give LCST behaviour. The effect of molecular weight, thermal
expansion coefficients, thermal pressure coefficients and the entropy
parameter on the phase boundaries of the mixtures are also considered.
His binodal, spinodal and critical point derivations have been
applied to other systems (ten Brinke et al., 1981) but they will not
be used in this work due to the possible error in evaluation of

$(\frac{\partial \tilde{v}}{\partial N_1})$ T,V,N_2 as was pointed out by Sanchez (1978).

Finally, the Prigogine "corresponding equation of state" and
the Sanchez "lattice-fluid" theories will briefly be compared with
the Flory equation of state theory. (Flory and collaborators
equation of state theory will from now on be referred to as Flory's
equation of state theory.).

2.3 The Corresponding Equation of State Theory

This theory is based on the treatment of quasi-spherical

molecule mixtures by Prigogine et al. (1953) who have considered the

effect of the volume change on mixing on the excess thermodynamic

functions. They applied the corresponding states principle of

Prigogine (1957), the concept of a division of the degrees of freedom of

the chain molecules into internal and external degrees of freedom, to

long chain molecular mixtures.

The free volume of a liquid is characterized by the reduced

temperature, which is the ratio of the thermal energy of the 3c

external degrees of freedom to the intermolecular contact energy, q *

$$\tilde{T} = \frac{c}{q} \circ \frac{KT}{\varepsilon^*} = \frac{T}{T^*} \qquad 2.104$$

and

$$P^* = \frac{U^*}{V^*} = \frac{q\varepsilon^*}{r\delta^3} = \frac{S\varepsilon^*}{\delta^3} , \qquad \tilde{U}^* = \frac{U}{\tilde{U}} = N_A q \varepsilon^* \qquad 2.105$$

Here ε^* and δ are the intermolecular energy and distance parameters

for the interaction between segments, U is the configurational energy

(essentially the negative of the energy of vaporization). For chain

molecules, the quantity q is obtained from r in the Prigogine treatment

by means of a lattice model:

$$S = \frac{q}{r} = \frac{Z-2}{Z} + \frac{2}{rZ} \qquad 2.106$$

where Z is the lattice coordination number.

The partial molar quantities of the mixtures are given by the

corresponding state approach in an identical form, (Patterson, 1972):

$$\Delta \mu_1{}^R \equiv RT\chi\phi_2{}^2 = P_1{}^*V_1{}^* \{ (\tilde{G}(\tilde{T}) - \tilde{G}(\tilde{T}_1)) + (\tilde{T}_1 - \tilde{T})(\partial\tilde{G}/\partial\tilde{T})_{\tilde{P}}\}$$

$$+ P_1^* V_1{}^* \{ -\tilde{G}(\tilde{T}) + \tilde{T}(\partial\tilde{G}/\partial\tilde{T})_{\tilde{P}} (X_{12}\theta_2{}^2/P_1{}^*) \} \qquad 2.107$$

where $\tilde{G} = G/rN\epsilon^*$.

The expressions for $\Delta\bar{H}_1{}^R \equiv RT\chi_H\phi_2{}^2$ and $T\bar{S}_1{}^R = -RT\chi_S\phi_2{}^2$ are

obtainable by replacing the reduced function $\tilde{G}$ by $\tilde{H}$ and $\tilde{T}S^R$

respectively. The first term in this equation corresponds to the

equation of state term and the second to the contact interaction term

of Flory. Prigogine used a lattice model to calculate X_{12} while

Flory's approach considers the actual molecular structures.

The following relations between the equation of state and the

corresponding equation of state exist   ,

$$P_1{}^*V_1{}^* = U_1, X_{12}/P_1{}^* = \nu^2 \qquad 2.108$$

$$\tilde{U} = -\tilde{V}^{-1}, -U_1 = P_1{}^*V_1{}^*\tilde{V}_1{}^{-1} \qquad 2.109$$

$$\tilde{S} = 3 \ln (\tilde{V}^{1/3} - 1) \qquad 2.110$$

$$\tilde{C}_p = \tilde{\alpha}/\tilde{V} = \alpha T/\tilde{V}\tilde{T} \qquad 2.111$$

which makes it possible to derive all corresponding expressions of

Flory's theory from Equation 2.107.

The corresponding state theory predicts χ and its relation

with X_{12} as follows:

$$\chi = -\frac{U_1}{RT}\nu^2 + \frac{C_{P,1}}{2R}\tau^2 \qquad 2.112$$

$$\chi = \frac{P_1{}^*V_1{}^*}{RT}\frac{1}{\tilde{V}_1} \{ (\frac{S_2}{S_1})^2 \cdot \frac{X_{12}}{P_1{}^*} + \frac{\alpha_1 T}{2}\{ \frac{P_2{}^*}{P_1{}^*}\tau - \frac{S_2}{S_1} \cdot \frac{X_{12}}{P_1{}^*}\}^2 \} \qquad 2.113$$

Since $-U_1 = P_1 * V_1 * / \tilde{V}_1$ and $\alpha_1 P_1 * V_1 * / \tilde{V}_1 = C_{P,1}$ and V^2 represented by $\left(\frac{S_2}{S_1}\right)^2 \cdot \frac{X_{12}}{P_1 *}$, these two equations will be similar if $\frac{S_2}{S_1}$ is set to unity.

As shown in Equation 2.113 the pressure effects on the χ is better illustrated in this case than with Flory's equation of state. theory. However, Patterson and Delmas (1970) have tested this theory against the precise thermal expansion coefficient and isothermal compressibility data for the normal alkanes given by Orwoll and Flory (1967) and Abe and Flory (1966). Their result shows that the model reproduces the data qualitatively, and the principle of corresponding state is well obeyed, but as $\tilde{T}$ or $\tilde{v}$ are increased, the predicted thermal expansion coefficient increases too rapidly and the isothermal compressibility too slowly.

By comparing ΔH_M, $T\Delta S_M$ and ΔV_M calculated from both theories, they pointed out that the predictions of Flory's theory are superior to those calculated from the original theory of Prigogine and his collaborators. This does not seem to be due to any marked superiority of Flory's model but rather to

a.   Fitting the reduction parameters of the pure components to the liquid state properties rather than using gas-phase data.

b.   The exaggeration by the corresponding equation of state model of the size differences in the mixture reduction parameter, e.g.

$V* = \phi_1 V_1 * + \phi_2 V_2 *$ in Flory's model

but $V* = \phi_1 V_1 * + \phi_2 V_2 * - \phi_1 \phi_2 (\rho^2/2 + 3\rho^3/4) V_1 *$ in the present model where a large positive "volume interaction" term is added for $V*$ which is probably incorrect, $(\rho = r^*_{22}/r^*_{11} - 1, r^*$ being the distance between two non-bonded segments at the potential minimum).

2.4   The Lattice-Fluid (LF) Theory

The LF theory developed by Sanchez-Lacombe (1976 and 1978) and

Sanchez (1978, 1980) departs markedly from the corresponding state theory

and does not require a separation of the internal and external

degrees of freedom, but divides a chain into r-segments. This theory

has much in common with the Flory-Huggins theory but differs in   one

important respect, that it allows   the lattice to be compressible.

The generalization is accomplished by allowing   an equilibrium number

of vacant sites to exist in the lattice. Thus the compressible lattice

theory is capable of describing volume change on mixing as well as

LCST and UCST behaviours.

Three equation of state parameters are required to describe

the LF equation of state and they are related to three molecular

parameters ε^*, v^* and r as

$$\varepsilon^* = KT^* = P^*v^* \tag{2.114}$$

$$r = MP^*/KT^*\rho^* = Mv^*_{SP}/v^* \tag{2.115}$$

As with Flory's model, negative heats of mixing will yield a negative

volume change on mixing, although a negative ΔV_M is not a sufficient

condition for negative ΔH_M.

Unlike Flory's theory the hard core volume of the mixture is

obtainable from the close-packed volumes of the pure components:

$$v^*_{SP} = m_1/\rho_1^* + m_2/\rho_2^* \tag{2.116}$$

$$\tilde{v} = \rho^*/\rho = 1/\tilde{\rho} \tag{2.117}$$

where ρ_i^* is the close-packed mass density of component i and ρ is

the density of the mixture which is required to obtain $\tilde{v}$. Characteristic

pressures are pairwise additive in the close-packed mixture, i.e.

$$P^* = \phi_1 P_1^* + \phi_2 P_2^* - \phi_1 \phi_2 \Delta P^* \qquad 2.118$$

$$\Delta P^* = P_1^* + P_2^* - 2P_{12}^* \qquad 2.119$$

$$\phi_1 = r_1 N_1 / \bar{r} N = 1 - \phi_2 \qquad 2.120$$

Like Flory's theory X_{12} (which is proportional to the change in

energy that accompanies the formation of a 1-2 contact from a 1-1 and

a 2-2 contact) is obtainable from the experimental values of $\Delta H_M(\infty)$,

similarly a negative ΔH_M yields a negative X_{12}. Knowing X_{12} and $\nu =$

$v_1^*/v_2^* = (S_2/S_1)^3$ yield T^* of the mixture.

X_{12} has the following relation with χ and is the only parameter

required to characterise a binary mixture, therefore this theory can

be called a one parameter theory.

$$X_1 = r_1 \tilde{\rho}_1 \{ X_{12} + \tfrac{1}{2} \Psi_1^2 \tilde{T}_1 P_1^* \beta_1 \} \qquad 2.121$$

where ψ_1 is a dimensionless function given by Sanchez and Lacombe

(1978) and β_1 is the isothermal compressibility of component one. The

first term is the energetic contribution and the second one is an

entropic contribution as with $\chi_1 = \chi_{H,1} + \chi_{S,1}$, which is similarly defined

in Flory's theory.

The phase stability and the spinodal equation are more

illustrative in this case than with Flory's theory, i.e. the following

inequality must hold for a binary system to be miscible.

$$\frac{\delta (\Delta \mu_1 / kT)}{\delta \phi_1} = \tfrac{1}{2} (\frac{1}{r_1 \phi_1} + \frac{1}{r_2 \phi_2}) - \tilde{\rho} \{ X_{12} + \frac{1}{2} \psi^2 \tilde{T} P^* \beta \} > 0 \qquad 2.122$$

where the first term is combinatorial contribution, $\tilde{\rho}\,X_{12}$ is an

energetic contribution and $\frac{1}{2}\tilde{\rho}\,\Psi^2 TP*\beta$ is an entropic contribution from

the equation of state. It is significant to note that this entropic

contribution makes an unfavourable contribution to the miscibility.

The temperature dependence of the three terms in the spinodal is

illustrated in Figure 2.2. The combinatorial entropy makes a larger

contribution on both sides of the spinodal curve, Figure 2.3. To

relax this effect a correction factor of Q_{12} which has been ignored

by the LF theory is inevitable.

The LF theory is in an early stage of its development, which

makes it difficult to compare with Flory's theory .Its advantage is

in inequality (2.122), where the first term is negligible and the

term $\tilde{T}\Psi^2 P*\beta$ is always positive, then miscibility for high molecular

weight polymers can only be predicted when ΔH_M or X_{12} is negative..

Some other comparisons of both the theories are given by Sanchez (1978).

The main disadvantage of the present theory is the prediction

of ΔV_M from the close-packed densities. Most of the $\rho*$ values

predicted by the theory are about 10% smaller than their known crystalline

densities, which is most probably due to the packing factor of the

lattice.

Finally, the LF theory is intended to describe the fluid

(disordered) and not crystalline (ordered) state, even though a

lattice is used in the formation of the theory.
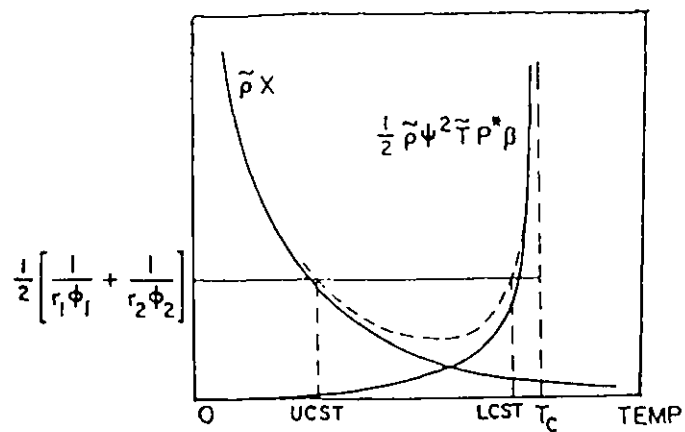
FIG. 2.2. Schematic behaviour of the three terms in the spinodal inequality. The inequality is satisfied between the UCST and LCST.
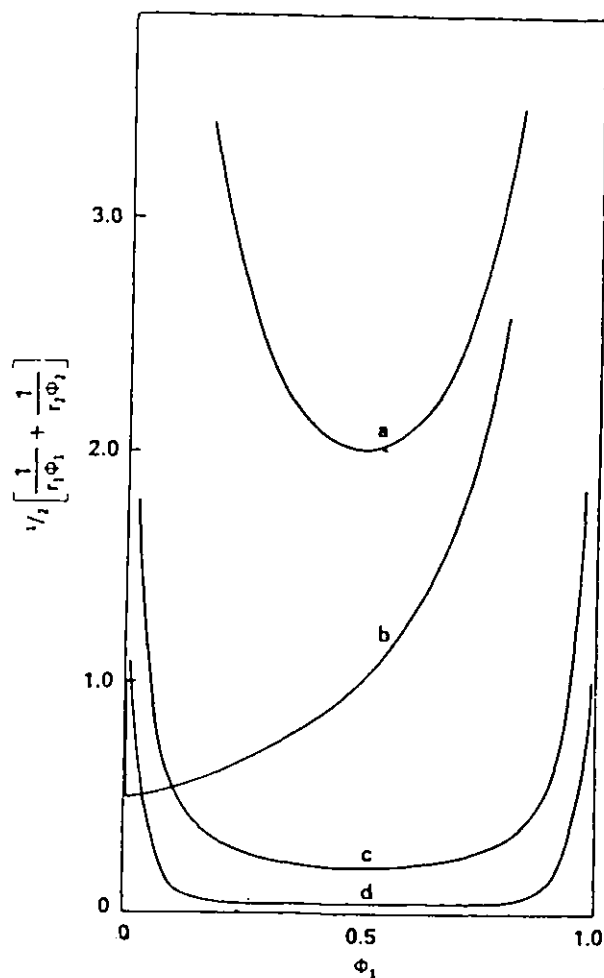
FIG. 2.3. Combinatorial entropy contribution to the spinodal against close-packed volume fraction ϕ_1.

  a. $r_1=r_2=1$ b. $r_1=1$, $r_2 \gg 1$ c. $r_1=r_2=10$ d. $r_1=r_2=50$

CHAPTER THREE

EXPERIMENTAL DETERMINATION OF MISCIBILITY

AMONG CHLORINATED POLYETHYLENES AND

ETHYLENE-VINYL ACETATE COPOLYMERS

3.1   MATERIALS

Polyethylene possesses several outstanding electrical and chemical properties, and is made from a low cost monomer. There is an attraction in trying to make a rubber using a chain backbone related to that of polyethylene, but less regular, in order to inhibit or at least restrict crystallization. It is also desirable that neither interchain interaction nor chain stiffness should be greatly increased. There are two ways of achieving these aims:

I   Copolymerization of ethylene with either alkenes such as in ethylene-propylene rubbers, or non-hydrocarbon monomers, such as vinyl acetate and methylacrylates.

II   Modifications of already formed polyethylene, for example by chlorination and chlorosulphonation.

The ethylene-vinyl acetate copolymers (EVA) have been available for some years under the commercial names of EVATONE (ICI), LEVAPREN (Bayer) and EVA (Wacker kemie). Introducing polar monomers into polyethylene chains increases the rubber like elasticity and reduces the crystallinity. The procedures for preparation of these copolymers are given by ICI and Reynolds and Conterine (1961) patents, their modified procedures are explained by German and Heikens (1971, 1975).

The chlorination of polyethylene may be carried out either in solution or suspension. The former gives reasonably random and uniform chlorination, while the latter is more uneven (Brydson, 1978). The introduction of chlorine groups into the polyethylene molecules has two opposing effects:

I   It reduces chain regularity restricting and eventually eliminating the ability of the polymer to crystallize.

II   It increases interchain attractions (and barriers to rotation) causing the T_g to be raised eventually to a point where the amorphous polymer is no longer rubbery.

The physical forms of chlorinated polyethylene (CPE) related to their chlorine content are compared in Table 3.1 as given by Brydson (1978) and Abu-Isa and Myers (1973).

TABLE 3.1

EFFECT OF CHLORINE CONTENT ON THE PHYSICAL PROPERTIES OF CHLORINATED POLYETHYLENE

Cl% Content	Structure at Ambient Temperature	Physical Form at Ambient Temperature
8	Mainly crystalline	Flexible
25	25% "	Rubbery
35	<6% "	Rubbery
40	<2% "	Soft, Flexible
45	<2% "	Flexible, Leathery
54	<2% "	Rigid

Ibu-Isa and Myers (1973), using the statistical treatment of

Frensdorff and Ekiner (1967) and the NMR and IR spectrum of several

chlorinated polyethylenes, have shown that the presence of a chlorine

in the polymer chain hinders the substitution of another chlorine

atom, up to a 52 weight percent degree of chlorination. On this

basis the chlorinated polyethylenes used in this work (higher than

35 W% Cl content) are assumed to be randomly chlorinated and contain

no appreciable amount of crystallinity. In the present work two types

of commercial chlorinated polyethene supplied by DuPont under the trade

name of Hypalon 40 and Hypalon 48 were used. These are essentially

chlorinated polyethylene and possess a small amount of $(-SO_2 Cl)$

side chains (~1.5 w% sulphur). These samples are designated H 40 and

H 48 respectively in this work.

The other solution chlorinated polymer made specifically for

this study is designated as CPE3.

As the other blending component, two types of EVAs were used,

EVATONE 40 with a nominal 40% w/w vinyl acetate content hence called

EVA40 and LEVAPREN 45 with a nominal 45% w/w vinyl acetate hence

called EVA45.

3.1.1   Preparation of CPE3

Polyethylene can be chlorinated in solution or in suspension

(Billmeyer, 1971). Solution chlorination is preferred due to the

random substitution of the chlorine along the polyethylene chains.

Chlorination is by means of a radical reaction in the presence of

light. High density polyethylene (HDPE) with a nominal molecular weight

of 10,000 was used in order to avoid chain branching in the products.

HDPE (20 grams) was dissolved in analar chlorobenzene (400 cm^3) by

stirring and gradually heating up to 130^oC. A flow of chlorine gas was

conducted into the solution at an average flow rate of 30 $cm^3.min^{-1}$,

after passing it through concentrated sulphuric acid. A visible light

source was used as a radical initiator, and to avoid any oxidation the

solution was kept under a nitrogen blanket. The chlorination process

was carried on for six and a half hours at 130^oC while the solution

was stirred.

The following radical substitution reactions are presumed to

occur under these conditions:

$$Cl_2 \xrightarrow{\hspace{0.3cm} h\nu \hspace{0.3cm}} 2 \; Cl^o$$

$$RH + Cl^o \longrightarrow R^o + HCl \hspace{3cm} 3.1$$

$$R^o + Cl_2 \longrightarrow RCl + Cl^o$$
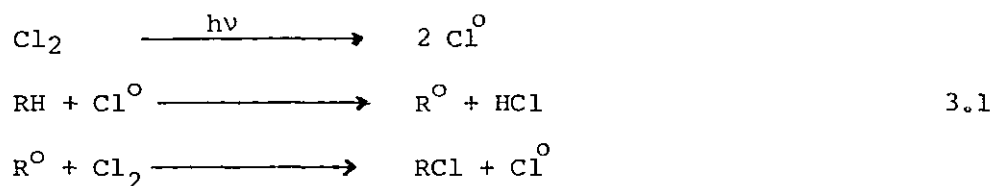
where RH stands for polyethylene and RCl for chlorinated polyethylene.

At the end of the chlorination time the flow of chlorine gas was

stopped, and the light source turned off. The reaction product was

cooled and precipitated into a ten times excess of methanol (A.R.),

washed with methanol and dried for two weeks at 50^oC in a vacuum oven

at 0.1 mm Hg. This product gives a transparent film by moulding.

The intrinsic viscosity of CPE3 in THF at 25^oC is 1.41 and its elemental

analysis is given in Table 3.3.

In order to measure the heat of mixing of the CPEs and EVAs, two commercial chlorinated paraffins, ceroclor 45 and ceroclor 52 (ICI) were used as low molecular weight analogues of chlorinated polyethylenes.

3.1.2   Preparation of Sec-Octyl Acetate (Oc.Ac.)

Secondary octyl acetate (1-methyl heptyl acetate) was used as a low molecular weight analogue for ethylene-vinyl acetate copolymers. It was prepared by the reaction of octan-2-ol with acetic anhydride as follows:

The octane-2-ol (A.R., BDH) was distilled at 64°C and 20 mm Hg prior to use, all other reagents were Analar grade and were used as supplied. Octan-2-ol (100 cm^3, 0.77 moles) and Pyridine (80 cm^3, 1.008 moles) were placed in a flask fitted with a stirrer and reflux condenser. Acetic anhydride (86 cm^3, 0.91 moles) was slowly added to the flask via a dropping funnel while the contents were refluxed. The mixture was then refluxed for a further four hours, it was cooled and 100 cm^3 of ether   added to the contents of the flask. After mixing 100 cm^3 of distilled water was also added. Pyridine was separated from the organic phase which contained the acetate. The ether solution was washed three times, with 10% of concentrated sulphuric acid (40 cm^3) to remove the remaining pyridine, followed by a saturated sodium carbonate solution in order to remove any acid. The ether solution was then dried over anhydrous sodium sulphate, filtered, and the ether evaporated off. The acetate was distilled and the product was collected at 68-70°C and 20 mm Hg pressure.

Gas chromatography analysis showed the product to be greater

than 98% pure, the only observable impurity being unreacted octan-2-ol

which has an $11^{O}C$ difference in boiling point compared with the acetate at 20 mm Hg.

Elemental analysis of the product given below is compared with the

theoretical values.

Elemental Analysis   c = 69.86,   H = 11.65,   O = 18.60

Theoretical   c = 69.77,   H = 11.63,   O = 18.60

3.1.3   Physical Properties of the Components

The degrees of chlorination of the low molecular weight

materials, ceroclor 45 (designated as S45) and ceroclor 52 (designated

as S52) were determined by elemental analysis.   The molecular weights

were determined by vapour phase osmometry (VPO) at $37^{O}C$ using

butanone as a solvent.   The results are given in Table 3.2.

TABLE 3.2

Material	Chlorine Content w%	$\bar{M}n$ V.P.O.
Ceroclor 45	45.74	395
Ceroclor 52	53.08	437

The chlorine, carbon and hydrogen content of the chlorinated

polyethylenes and the carbon and hydrogen content of the EVAs were

also determined by elemental analysis, and their molecular weight

examined by gel permeation chromatography (G.P.C.) in tetrahydrofuran,

relative to polystyrene.   The number average molecular weight $\bar{M}_{n}$,

and weight average molecular weight $\bar{M}_{w}$, relative to polystyrene, were

computed from the following expressions:

$$\bar{M}_n = \frac{\Sigma N_i M_i}{\Sigma N_i} = \frac{\Sigma W_i}{\Sigma (W_i/M_i)}, \quad \bar{M}_w = \frac{\Sigma N_i M_i^2}{\Sigma N_i M_i} = \frac{\Sigma W_i M_i}{\Sigma W_i} \qquad 3.2$$

where N_i is the number of species i of molecular weight M_i and $W_i = N_i M_i/N_A$, with N_A being Avogadro's number. The results of these computations, together with the elemental analysis results for CPEs and EVAs are given in Table 3.3.

TABLE 3.3

Material	w% Cl	w% C	w% H	$\bar{M}_n \times 10^{-4}$	$\bar{M}_w \times 10^{-5}$	$\dfrac{\bar{M}_w}{\bar{M}_n}$
H40	35.41	54.26	8.18	2.06	1.88	9.12
H48	44.05	47.16	6.68	2.39	1.82	7.61
CPE3	52.65	42.25	5.50	3.22	2.56	7.95
EVA40	–	74.46	11.55	2.29	1.19	5.20
EVA45	–	71.72	11.04	3.77	2.56	6.79

When the Mark-Houwink-Sakurada parameter, K and α, (Brandrup and Imergut, 1975) for the polymers are not known, the actual molecular weights can be approximated by a so-called one parameter method.

Busnel (1982) has explained that macromolecules eluted from G.P.C. at one elution volume have the same "hydrodynamic volumes", V_h, or:

$$V_{h(v)} = \{[\eta]_x M_x\}_{(v)} \qquad 3.3$$

where $[\eta]_x$ and M_x are the intrinsic viscosity and molecular weight of the species x eluted at volume v. It is, therefore, possible to accept that:

$$\left\{ \frac{[\eta]_{PS}}{[\eta]_X} \right\}_{(v)} = B \qquad\qquad 3.4$$

where B is the "Benoit factor" and is constant for the family of x for

a given element (PS stands for polystyrene).

On this basis,

$$M_{ix} = B \, M_{iPS} \quad \text{or} \quad \bar{M}_{nx} = B\bar{M}_{nPS}, \quad \bar{M}_{Wx} = B\bar{M}_{WPS} \qquad 3.5$$

The intrinsic viscosity of polystyrene in THF at $25^{\circ}C$ is given by

Busnel (1982) as:

$$[\eta]_{PS} = 0.9 \times 10^{-3} \, M^{0.5}, \quad M < 10,000 \qquad\qquad 3.6$$

$$[\eta]_{PS} = 0.145 \times 10^{-3} \, M^{0.7}, \quad M > 10,000 \qquad\qquad 3.7$$

The intrinsic viscosities of CPE3 and EVA45 in THF at $25^{\circ}C$

were found to be 1.415 and 1.07 $dl.g^{-1}$ respectively. The B value,

obtained for CPE3 is 0.625 and that of EVA45 is 0.827. The

approximated molecular weights are:

CPE3 $\qquad \bar{M}_W \simeq 1.6 \times 10^5$

EVA45 $\qquad \bar{M}_W \simeq 2.1 \times 10^5$

The more precise methods for molecular weight determination of the

polymers are explained by Collins et al. (1973).

The crystallinity of the polymers was checked using Guinier

and Philips cameras (Alexander, 1965). The monochromatic X-ray

beam ($CuK_{\alpha}, \lambda = 1.54\text{Å}$) with a nickel filter was used in each case.

No crystallinity was detected in either case, therefore we are

essentially dealing with amorphous polymers in this work.

Densities of the polymeric compounds were measured by the
equal volume titration method at $25^{\circ}C$ (ASTM, 1971). Water-sodium
bromide and n-propanol-water mixtures were used for CPEs and EVAs
respectively. The equivalent density of the titrated solutions were
measured by a digital densimeter DMA46 (Anton, Paar, Austria) at
the same temperature. The densities of low molecular weight compounds
were directly measured by the densimeter. The results of these
measurements are given in Table 3.4. The error in the density of
solid polymers is ±0.0005 g.cm^{-3} and that of liquids is ±0.0002 g.cm^{-3}.

TABLE 3.4

DENSITIES AT $25^{\circ}C$

Material	Oc.Ac.	S45	S52	H40	H48	CPE3	EVA40	EVA45
Density g.cm^{-3}	0.8554	1.1640	1.2592	1.1220	1.2556	1.296	0.9498	0.9530

3.2   BLEND PREPARATION

The miscibility of the following six binary polymer-polymer
systems were studied:

1. EVA40-H40   2. EVA45-H40   3. EVA40-H48

4. EVA45-H48   5. EVA40-CPE3   6. EVA45-CPE3

Mixtures of each individual binary system were found to be
transparent at room temperature when they were cast from a 5 w/v% solution
in tetrahydrofuran (A.R., BDH).

A total amount of one gram of the two components was dissolved in THF (20 cm^3) with stirring over one day. The clear solution obtained was poured into a petri dish (2" diameter) which had been treated by washing with a 2V/V% solution of 1.1.1-trimethyl chlorosilane (BDH) in 1.1.1-trichloroethane, to ease removal of the film. Slow evaporation of THF left a clear film of 200 to 300 μm thickness. The films were kept under vacuum at room temperature for one week before being used and kept in a desiccator until required.

3.2.1   Determination of THF Residue in the Blends

The weight loss of a blend (50 w% H40 in EVA45) during the removal of the residual THF was measured continuously by means of an Oertling microbalance, Model 146. The weight of the blend reached a constant value after eight days, as shown below. No further weight losses were observed after further evacuations.

day	1st	2nd	3rd	6th	8th
weight lost %	7.57	0.58	0.29	0.074	0.029

Infra-red spectroscopy did not detect any peak due to THF in this blend. In another experiment, one gram of 50/50w/w% of EVA40 in CPE3 and one gram of 50/50 w/w% of EVA40 in H40, which had been dried for eight days as above, were separately dissolved in 40 cm^3 of toluene. 1 μl of these solutions were injected in the column of a PYE Unicam gas chromatograph, with a thermal conductivity detector. The chromatograph was calibrated to detect up to 0.01 w/w% of tetrahydrofuran in toluene. A trace of tetrahydrofuran less than 0.08 w/w% in both blends was observed.

3.3   METHODS FOR ESTABLISHING MISCIBILITY

Optical, mechanical, electrical, morphological and thermo-
dynamic properties of various polymer mixtures are often used as
criteria for establishing miscibility. The methods to determine these
properties with their limitations have been extensively reviewed by
MacKnight et al. (1978) and Olabisi et al. (1979).

When a viscous polymer is cooled, the transition from a
soft elastomer to a rigid glass occurs at a temperature or over a
range of temperatures known as the glass transition temperature, Tg.
Since all polymers exhibit a glass transition temperature, any
miscible blend which behaves as one homogeneous phase will show a
single glass transition temperature, which is generally between the
Tg's of the individual polymers. In dynamic mechanical studies, the
storage modulus of a blend decreases rapidly, and the loss modulus
exhibits a maximum in the neighbourhood of Tg. The physical properties
also change near Tg. For example, the line width in nuclear magnetic
resonance undergoes an abrupt narrowing at this temperature. In
polar polymer blends, the dielectric loss tangent and the imaginary
part of the complex dielectric constant passes through a maximum in
the region near Tg. The refractive index shows a change at Tg. The
thermal expansion coefficient, and the heat capacity also change
at Tg.

For miscible blends, many attempts have been made by
researchers to correlate the Tg with the blend composition as is
frequently done with random copolymers. Several miscible blends
(Hammer, 1971 and Hichman and Ikada, 1973) exhibit composition
dependence of Tg which can be predicted by the simple Fox (1956)
relationship.

$$\frac{1}{Tg_b} = \frac{W_1}{Tg_1} + \frac{W_2}{Tg_2} \qquad \qquad 3.8$$

where W_1 and W_2 are the weight fraction of the respective components and Tg_b, Tg_1 and Tg_2 are the Tg's of the blend component one and component two respectively. A logarithmic form of this equation is given by Pochan et al. (1979). Other polymers are reported to follow the Wood (1958) equation (Fried et al. 1978). Some others (Prest and Porter, 1972) follow the more detailed Kelley-Bueche (1961) expression. None of these relationships including the Gordon-Taylor (1952) and Dimarzio-Gibbs (1959) equations specifically take into account the interaction term of the blend. The equation of Pochan et al. (1979) remains at an empirical level. The Tg of a blend having specific interactions, however, may follow the general form:

$$Tg_b = \phi_1 Tg_1 + \phi_2 Tg_2 + \lambda \phi_1 \phi_2 \qquad \qquad 3.9$$

where ϕ_1 and ϕ_2 are the volume fractions of component one and two and λ is related to the interaction term and the flexibility of one chain relative to the other. The presence of a single glass transition alone may not be a definitive test of miscible blends, as there are some circumstances under which the Tg criterion may not be applicable (MacKnight et al., 1978). Other difficulties associated with the glass transition temperature are discussed by Cowie and McEwen (1979).

Different techniques measure different motions of a miscible blend, and the detection and position of a relaxation maximum would be expected to depend on the particular measurement technique. A full assessment of blend homogeneity may require the use of several techniques for comparison. The following techniques are considered as reliable methods for establishing polymer-polymer miscibility in the present work.

3.3.1 Dynamic Mechanical Relaxation

Dynamic mechanical analysis involves the determination of the dynamic mechanical properties of polymers and their mixtures. In viscoelastic studies of polymeric materials the method of sinusoidal excitation and response have been widely used (Murayama, 1978). In this case, the applied and resulting deformation both vary sinusoidally with time, the rate being specified by the frequency, f, in cycles per second or $\omega = 2\pi f$ in radians per seconds.

For linear viscoelastic behaviour the strain will alternate sinusoidally but will be out of phase with the stress as shown in Figure 3.1.
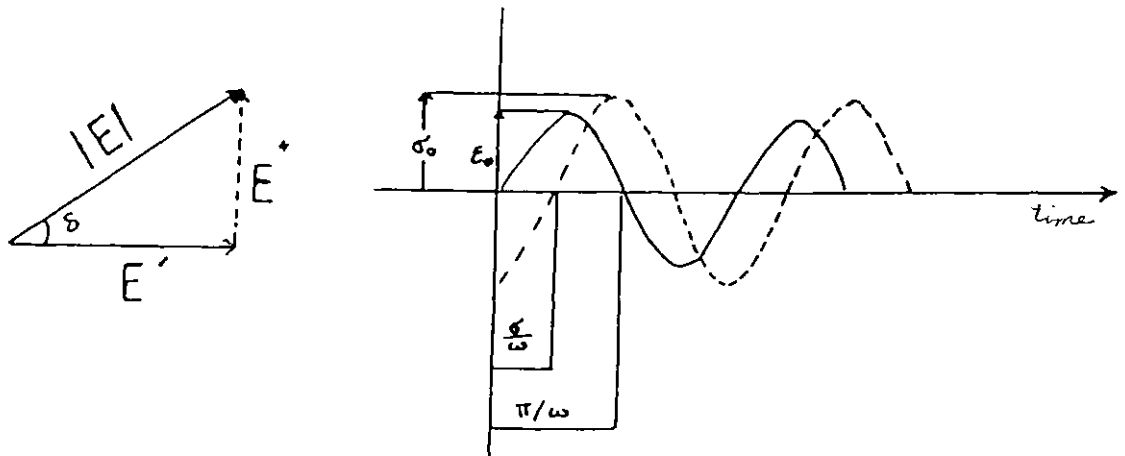

Figure 3.1. Schematic relation between various parameters in dynamic mechanical relaxation measurement ε_o is the input strain and σ_o the output stress.

A phase lag results from the time necessary for molecular rearrangements which is associated with the relaxation phenomena (McCrum et al., 1967). The stress, σ, and the strain ε, can be expressed as follows

$$\sigma = \sigma_o \sin(\omega t + \delta), \quad \varepsilon = \varepsilon_o \sin \omega t \qquad 3.10$$

where ω is the angular frequency and δ is the phase angle. Expanding σ

$$\sigma = \sigma_o \sin \omega t \cos \delta + \sigma_o \cos \omega t \sin \delta \qquad 3.11$$

Hence stress can be considered to consist of two components, one in phase with the strain, $\sigma_o \cos \delta$, and the other 90° out of phase, $\sigma_o \sin \delta$. When these are divided by the strain, the modulus can be separated into in phase (real) and out of phase (imaginary) components, i.e.

$$\sigma = \varepsilon_o E' \sin \omega t + \varepsilon_o E'' \cos \omega t \qquad 3.12$$

$$E' = \frac{\sigma_o}{\varepsilon_o} \cos \delta \text{ and } E'' = \frac{\sigma_o}{\varepsilon_o} \sin \delta \qquad 3.13$$

where E' is the real part of the modulus (storage modulus) and E'' is the imaginary part (loss modulus). The energy loss per cycle or damping in the system, can be measured from the "loss tangent" $\tan \delta$ defined as:

$$\tan \delta = \frac{1}{\omega \tau} = \frac{E''}{E'} \qquad 3.14$$

When $\tan \delta$ is near the maximum the molecular motion of the chain molecules starts, but with a larger phase angle delay to the stress, which causes the mechanical damping.

The exponential representation of the moduli, yields the complex dynamic modulus, E^*, as:

$$E^* = E' + iE'' \qquad 3.15$$

A Rheovibron dynamic viscoelastomer at a constant oscillating frequency of 11 Hz was used (Model DDV-II, Toyo Measuring Instruments). The temperature was scanned at 1°C.min^{-1} and direct tan δ values were recorded. The sample dimensions were 20 x 5 x 0.3 mm. A plot of loss tangent against temperature was constructed.

3.3.2 Dielectric and Depolarization Measurements

The dielectric propoerties of polymers are analogous to the mechanical properties in that the dielectric constant, ε', is similar to mechanical storage and the dielectric loss factor, ε'', is similar to the mechanical loss. In dielectric experiments an alternating electric field produces an alternating electric polarization which, in the case of polar solids, will lag behind the applied field by some phase angle. The loss factor or tan $\delta = \dfrac{\varepsilon''}{\varepsilon'}$ is commonly used to determine the glass transition. The main advantage of this technique over the dynamic mechanical testing is the wide range of frequencies available. This permits the loss factor to be determined either as a function of temperature over many frequencies or as a function of frequency at selected temperatures. The latter is particularly important because blend miscibility may be studied at temperatures below or **above** CPCs permitting a study of systems showing LCST or UCST miscibility (Wetton et al., 1978). In this case, if one presents the dipole of a polar polymer by a single relaxation time, τ, then the constituents of the complex dielectric content, ε^*, are defined by Hedvig (1977) as:

$$\varepsilon^* = \varepsilon' - i\varepsilon'' \hspace{4cm} 3.16$$

$$\varepsilon' = \varepsilon_\infty + (\varepsilon_o - \varepsilon_\infty)/(1 + \omega^2\tau^2) \qquad\qquad 3.17$$

$$\varepsilon'' = (\varepsilon_o - \varepsilon_\infty)\omega\tau/(1 + \omega^2\tau^2) \qquad\qquad 3.18$$

and $\qquad \tan \delta = (\varepsilon_o - \varepsilon_\infty)\omega\tau/(\varepsilon_o + \varepsilon_\infty\omega^2\tau^2) \qquad\qquad 3.19$

where ε_o and ε_∞ are the limits of ε' at zero frequency and infinite

frequency. The ε'' and $\tan \delta$ go through a maximum when $\omega\tau = 1$.

The dielectric relaxation measurement has been used by Wetton

et al. (1978) for establishing the miscibilities of polymer blends.

Its practical application is not as common as mechanical relaxation

measurements. The conductivity effects such as the Maxwell-Wagner-

Sillars (MWS) phenomena have made this method less attractive. The

MWS effect has been discussed by Hedvig (1977) and Wetton et al. (1978).

It is a polarization effect which occurs as a result of the accumulation

of charges at an interface of two media of different conductivities.

Dielectric relaxation measurements are normally performed

by means of a radio-frequency bridge, which gives the conductance

and capacitance of an unknown capacitor, polymer or blend, in digital

numbers. A 1621 General Radio Precision Capacitance Instrument was

used to measure the loss tangent in this work. A conventional PTFE

insulated two-terminal cell with a working electrode diameter of 3 cm

was used as a sample holder. All the measurements were performed at

a constant frequency of 37 Hz and a temperature range of -50 to 80°C

was used unless stated. The heating rate was approximately 1.5°C

per minute and readings were taken every 2 or 3 degrees.

An alternative form of spectra can be obtained by recording

the short-circuit current during warming-up after the blend has been

polarized at a constant d.c. field above the transition temperature.

This method has been referred to as the thermostimulated current

depolarization or electric depolarization current method. The scheme

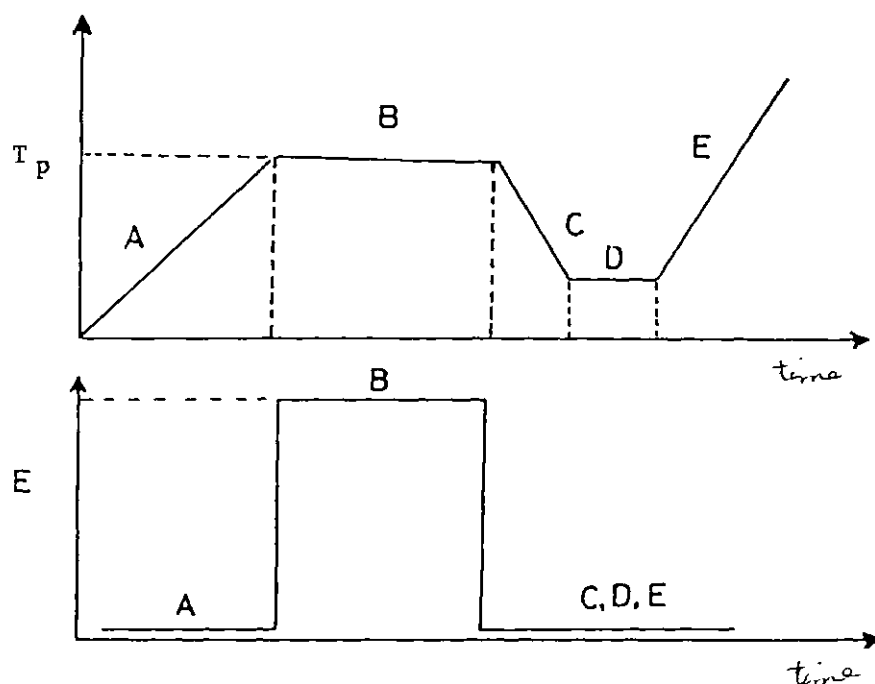of the dielectric depolarization process is shown in Figure 3.2.

Figure 3.2. Schematic presentation of depolarization method T_p is the polarization temperature.

A blend of approximately 25 μm thickness was cast onto an

aluminium coated glass slide which acts as one electrode. The sample

was kept under vacuum at 0.1 and then 3×10^{-5} mm Hg for 48 hours

before polarization (Zambrand, 1981). A 30-40 volts d.c. supply was

used for polarizing the blend for 30-60 minutes at the polarizing

temperature, T_p, below phase separation and above the transition temperatur

(stage B in Figure 3.2). It was cooled to -80°C and the external

field was removed (stage C). Using a temperature program unit the

polarized sample was heated at a rate of 2^{O}C.min^{-1} (stage E) where

an electrometer was connected to it to record the circuit current.

The current peaks recorded in this way are found to correlate with the

transition temperatures measured by the dielectric technique. The

reproducibility of the peak intensity was found to be excellent when

the same thermal history was repeated.

Part of the dielectric depolarization current may be attributed

to (a) thermal depolarization of the dipoles attached to the polymer

chain, with a decay rate of polarization, P, expressed as:

$$\frac{dP}{dt} = -P/\tau \qquad\qquad 3.20$$

where τ is the relaxation time, (Sharama et al., 1980).For dipolar

relaxation, the dielectric loss is a maximum at the resonance

frequency.

and   part to (b) the depolarization of the dipoles of Maxwell-Wagner-Sillars

type and detrapping of the charges above the transition temperature.

3.3.3   Differential Scanning Calorimetry

This technique measures the amounts of heat required to

increase the sample temperature by a value of ΔT over that required to

heat a reference material by the same ΔT. The variation in power

necessary to maintain this level during a transition is monitored

and recorded. The technique has been reviewed by MacKnight et al.

(1978), Olabisi et al. (1979) and Rabek (1980). It has been shown

that the method is suitable for studying polymer-polymer miscibility.
A detailed application of this method has been shown by Fried et al.
(1978). The utility of the differential scanning calorimeter, DSC, for
measuring the melting point depression in order to calculate the
interaction parameter between PVF_2 and PMMA was demonstrated by Nishi
and Wang (1975). In this work, the DSC measurement of the blends
were performed in a DuPont, 990 thermal analyser with a DSC cell at
a sensitivity of 0.2 mcal.sec^{-1} and a heating rate of 5°C.min^{-1}. The
heat flow as a result of a power difference between ~20 mg of a sample
in an aluminium pan and a similar empty one was recorded.

3.3.4   Phase Contrast Microscopy

In this type of microscopy the beam from the interference
diffraction maxima of the light passing through a specimen is split
into two parts, by a beam splitting prism. Each part contains the
full object information. These beams combine again in an interferometer
and by shearing one beam vertically against the other the two waves
hit each other sheared, and interference will occur depending on the
phase difference of the components.

The difference in phase between the two light waves depends
on the difference in optical path length. The optical path length
is defined as the product of the geometrical path and refractive
index.

Sections from the blend, 20-30 μm thick, were illuminated
by the transmitted light of a mercury lamp in an interference phase
contrast microscope (Carl Zeiss Jena Ltd.). The structure of the
blend was observed before heating,as a function of the temperature
as it was heated, and after heating using a Cambion heating
stage. A series of colour photographs were taken as the morphology
of the specimen changed. The advantage of this technique is that it
avoids the possibility of artefacts due to staining.

More details and other applications of   phase contrast
microscopy are given by Bennett (1951) and Doube (1979).

3.3.5   Transmission Electron Microscopy

The resolving power of a light microscope is limited by the
wave nature of the light. The minimum spacing, d, which can be
resolved by a good microscope is of the order of the wavelength of
the radiation source, λ, and is given by:

$$d = \frac{\lambda}{n \sin \theta}$$ 3.21

where θ is the angle of acceptance of the lens and n is the refractive
index of the specimen. For better resolution, larger values of   θ
and shorter wavelength radiations are required.

Transmission Electron Microscopy (T.E.M.) has provided
resolution of 2 to 10 A°. It is basically analogous to visible light
microscopy but uses an electron beam instead of a light beam, and
electrostatic or electromagnetic lenses instead of glass ones. The
technique and its application to polymers are described by Rabek (1980)
and Collins et al. (1973). Other specific applications of electron

microscopy are given by McMaster (1975) and Meyer et al. (1978).

Rabek (1980) and Collins et al. (1973) have given details of the considerations for sample preparation. In this work an Ultramicrotome equipped with a liquid nitrogen cooled cold chamber (L.K.B. Sweden) was used. Glass knives were freshly prepared for each section. The specimen temperature was set at $-80^{\circ}C$ and the glass knife at $-150^{\circ}C$. Thin sections of the blends around 900 A° in thickness were made and placed on a supporting copper grid.

A JEM, 100B, Transmission Electron Microscope with $3.5A^{\circ}$ resolution was used to investigate the structure of the blends which were heat treated for different lengths of time and at different temperatures. The heat treated samples were quenched down below their glass transition temperature on the surface of a cold metal before ultramicrotoming. The blend before heat treatment provided a basis against which the other blends could be compared. A number of blends were compared in this way.

The method is limited by the sample preparation and the stability of the polymers in the electron beam. Other limitations of the method are described by Christner and Thomas (1977).

3.3.6   Infra-red Spectroscopy

Infra-red spectroscopy is an attractive method for examining the interactions of different polymers in a blend using the specific vibrations of the chemical groups. There are a number of descriptions in the literature of the vibrational spectra of polymer blends with

specific interactions. Coleman and Zarian (1979) have studied the

Fourier-transform infra-red spectrum (FTIR) of poly (ε-caprolactone), PCL-

poly (vinyl chloride) blends. They have observed a band shift to a

lower frequency in the C=O absorption of PCL as a function of PVC

concentration. They also noticed that the width at half-height of the

carbonyl band varies with PVC composition in an S-shape manner. These

findings indicate the existence of a specific interaction between these

materials which is responsible for the miscibility. A shift in the

C=O stretching frequency of PMMA in the presence of poly (vinylidene

fluoride), PVF_2, was observed by Coleman et al. (1977). Tabb and

Koening (1975) studied the FTIR spectra of plasticized PVC and

proposed that interactions between the carbonyl bands and the carbon-

chloride band may occur in the amorphous regions of this polymer.

Varnell et al. (unpublished A) have considered the shifts to a lower

frequency of the C=O stretching band to be a consequence of a

weakening of the carbonyl band by a hydrogen bonding type interaction.

They also draw the conclusion that the carbonyl groups are planar,

hence carbonyl stretching vibration is a highly localized mode (i.e.

> 90% (C=O)) and any frequency shifts for this bond in a mixture

arise from chemical interactions. On the other hand, Varnell et al.

(unpublished B) believe that a small change in the frequency of the

carbon-chlorine stretching vibrations cannot be assumed to be definitive

evidence for direct involvement of the chlorine atoms in any specific

interaction.

The energy of hydrogen bonding in carbonyl groups may be estimated by considering the equilibrium constant for the dissociation of the hydrogen bonded group. This involves estimating the extinction coefficients of pure and blended components at various temperatures, and thus constructing the van't Hoff plot by Equation 3.22.

$$- \ln K_d = \frac{\Delta H}{RT} - \frac{\Delta S}{R}$$

3.22

A similar suggestion was made by Senich and MacKnight (1980) and Earnest and MacKnight (1980).

Preliminary studies of the infra-red spectra of EVA45-CPE3 blends using a Perkin-Elmer Model 631 spectrometer with 0.3 cm^{-1} resolution at 1000 cm^{-1}, have indicated a considerable shift of the C=O stretching band of EVA45 in the presence of CPE3 at room temperature. Shifts to a lower frequency of the C-Cl stretching band of CPE3 were also observed in the region 620 to 660 cm^{-1}. The shifts in C=O and C-Cl stretching bands have been attributed to a specific interaction between these materials.

3.3.7 Light Scattering Turbidimetry

A stable homogeneous mixture is transparent, whereas an unstable inhomogeneous mixture is turbid unless (a) the components of the mixture have identical refractive indexes or (b) a phase separation smaller than the resolution of the technique used occurs. Given a stable homogeneous mixture, the transition from the transparent to the turbid state may be brought about by variation of temperature, pressure or composition of the mixture. The cloud point corresponds

to this transition point - the initial point of phase separation.

The cloud point can be established by light scattering turbidimetry

or microscopy etc. The basis of light scattering turbidimetry was

described by Stein (1978) and Olabisi (1979). A light wave

incident upon a sample may be transmitted, absorbed or scattered.

These phenomena can be generally described by

$$I_t = I_o \exp \{-(\varepsilon + \tau) \, 1\} \qquad\qquad 3.23$$

where I_t and I_o are the transmitted and incident intensities of a

sample of thickness 1, ε is the absorption coefficient and τ is the

turbidity. τ is related to the Rayleigh ratio for scattering angles

θ and μ, shown in Figure 3.3, by Equation 3.24

$$\tau = \int_{\theta=0}^{\Pi} \int_{\mu=0}^{2\Pi} R \, (\theta, \mu) \, \sin \, (\theta, \mu) \, d\mu \, d\theta \qquad\qquad 3.24$$

Turbidity measurements are used in studying cloud point

curves (CPC) of solutions (Cowei and Saeki, 1982), oligomers (Chong,

1981) and solid mixtures (Reich and Cohen, 1981).

The instrument used in the present work was fully described

by Chong (1981). It measured the intensity of scattered light of

a blend by means of a photodiode at a scattering angle of $\theta = 45^{\circ}$.

μ is equal to zero in this particular machine. The temperature of

the sample can be controlled and programmed to change at a constant

rate either on cooling or heating. The incident light is from a 12 volts

tungsten lamp and is focussed onto the sample and then onto the

detector after scattering. A data logger is used to take readings

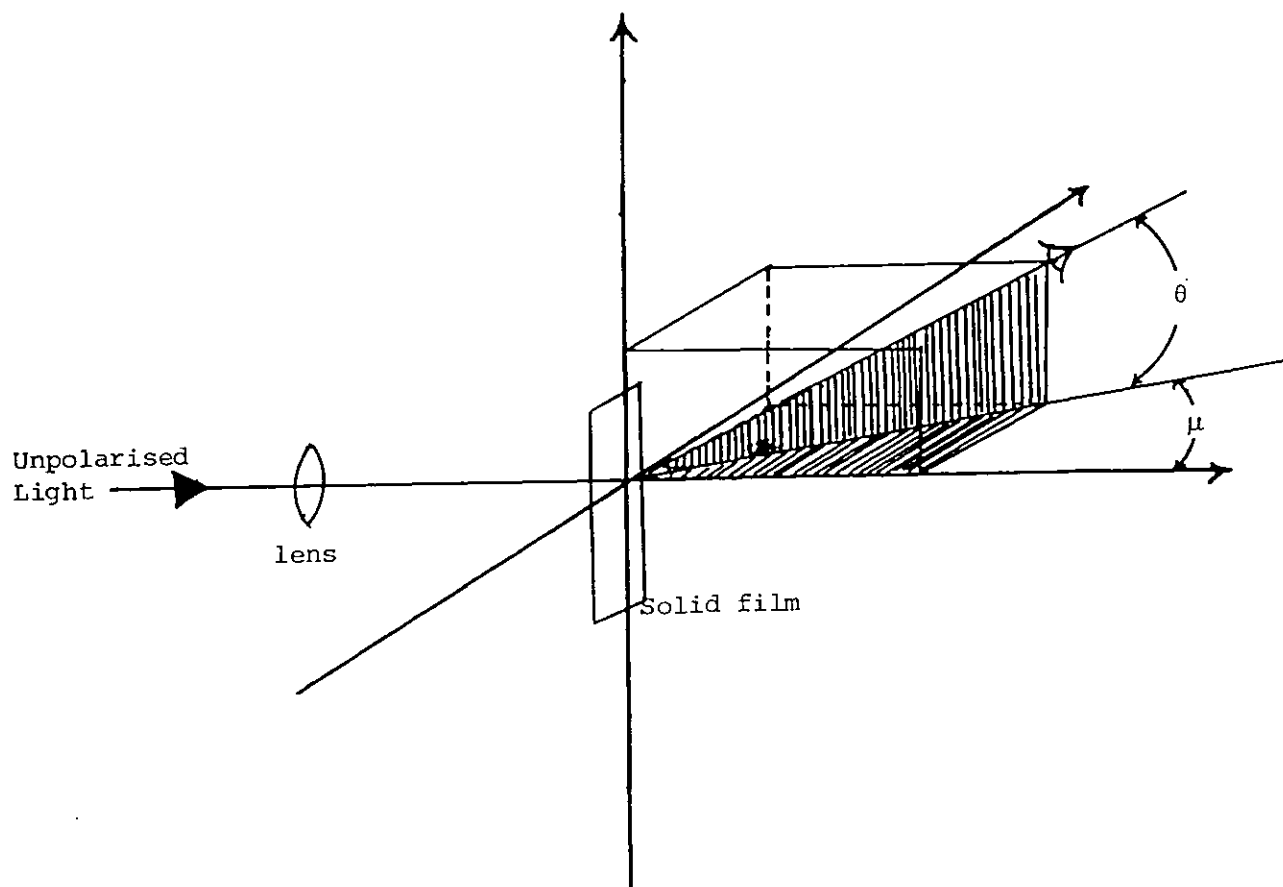at periodic intervals of the temperature and intensities.

FIG. 3.3. Scattering angles θ and μ for an unpolarised light after passing through a sample.

In order to obtain the cloud point of each blend a thin film (100-300 μm thickness and 5 x 20 mm) was screwed into a brass sample holder and then located in the turbidimeter. The sample was heated at 0.2^OC.min^{-1}. The data logger was programmed to take readings at one minute intervals. Typical traces of scattering intensity as a function of temperature obtained for blends of 65 and 55 w% H48 in EVA40 are shown in Figure 3.4. The corresponding temperature of the first deflection point was taken as the cloud point temperature. This was repeated for the whole range of concentrations for each pair of polymers and the cloud point curves were thus constructed. These curves for all the six systems are of the LCST types and are accurate within 5 to 10°C depending on the system and the blend itself.

In order to determine whether a blend was undergoing phase separation or merely domain ripening, where the larger domains are growing at the expense of the small ones, the scattering intensity at an angle of 45° was observed as a function of time. This is equivalent to the light scattering invariant, at a fixed angle, as defined by Koberstein et al. (1979):

$$Q_{LS} = \int_0^\infty R\underset{\sim}{h}\,'d\underset{\sim}{h} \qquad\qquad 3.25$$

where R is the Rayleigh ratio and $\underset{\sim}{h} = \dfrac{4\,\Pi}{\lambda\,\sin\dfrac{\theta}{2}}$ is scattering vector.

In the spinodal decomposition or nucleation and growth mechanisms of phase separations, Q_{LS} increases with time, whereas in the domain ripening mechanism it remains constant with time. An example of the continuous increases in scattering intensities with time for blend of H48-EVA40 = 55-45 and 65-35 is given in Figure 3.4. The figure shows an increase in the intensity of the light scattered at temperatures
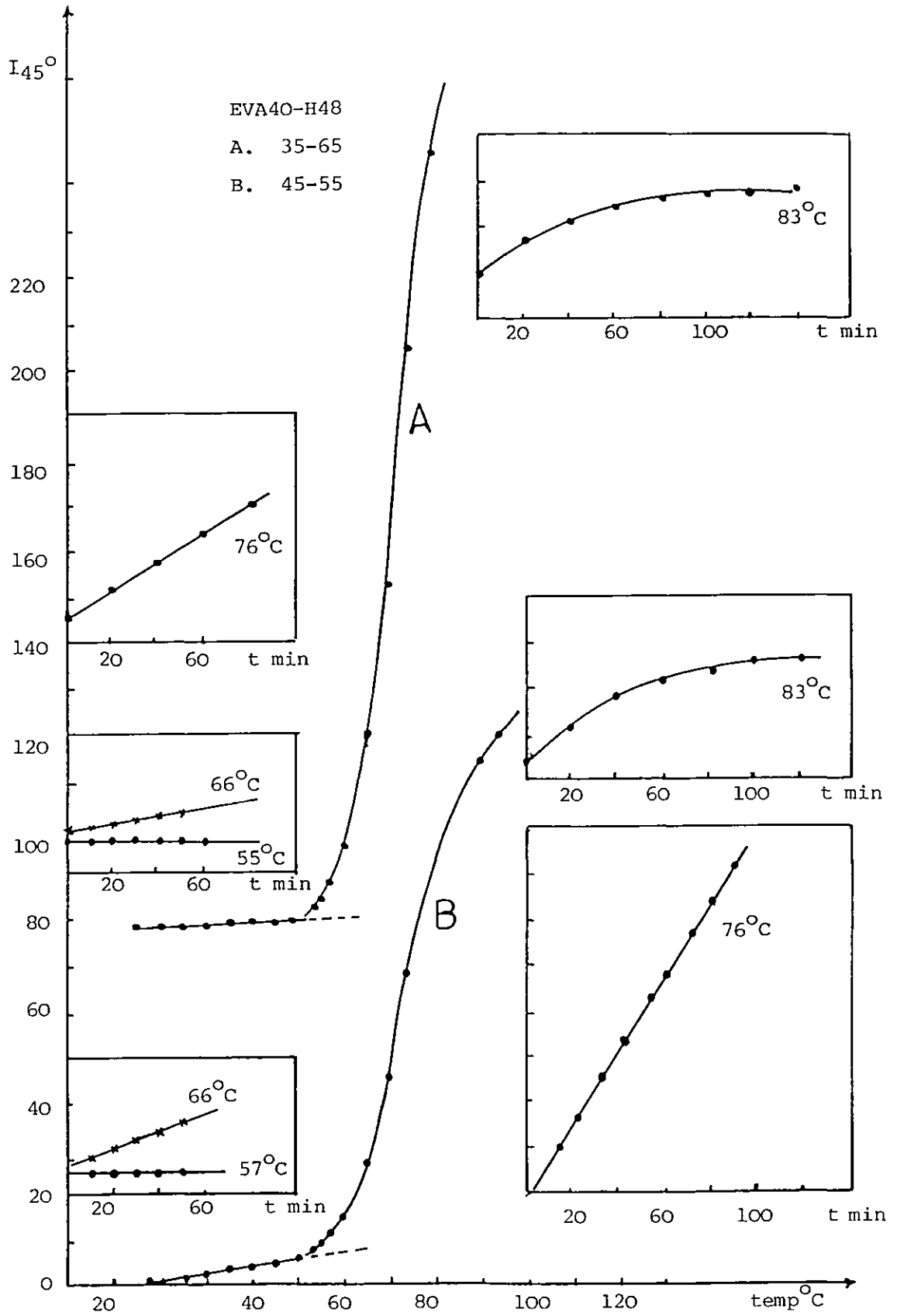
FIG. 3.4. Scattered intensity versus temperature and time.

above the cloud point and a constant value below this point. These observations show that the phase separation mechanism is not by domain ripening and give an alternative way of finding the cloud point of the blends. Following these observations the blends were heated up at a rate of $0.2^{\circ}C.min^{-1}$ to a certain temperature which was kept constant and the intensity of the scattered light recorded as time passed. This gave additional confirmation to the cloud points of the blends which were previously determined by scanning the temperature. Figure 3.4 also indicates that the growth rate of phase separation is faster at higher temperatures and the phase separated domains grow initially in a linear manner which becomes exponential at higher temperatures as thermodynamic equilibrium is approached. This confirms the findings of McMaster (1973) and Gilmer et al. (unpublished). These latter authors have given an exponential form for the domain growth as

$$D_m = a \exp (bt) \hspace{4cm} 3.26$$

where D_m is the fluctuation spacing at an angle of maximum intensity θ_m and a and b are constant at any given temperature.

3.4   MEASUREMENTS OF THE THERMODYNAMIC QUANTITIES

3.4.1   Heats of Mixing Measurements

Experimental values of heats of mixing are normally obtained by direct calorimetric measurements at constant pressure. The combination of calorimetric data, preferably at several temperatures, with other state parameters of the pure components leads to the determination of all the excess properties given in Chapter Two with high precision. The sign and magnitude of the heat of mixing, which is a function of nearest neighbour contacts, is crucial in the miscibility study of two polymers.

Cruz et al. (1979) have shown that polymers with negative heats of mixing are likely to be miscible or partially miscible, whilst Patterson (1968) has shown that the heats of mixing change sign in the region corresponding to two phases. The approach of Tager et al. (1975) in applying Hess's law to calculating the heats of mixing of solid polymers was considered more carefully by Weeks et al. (1977). Substantial errors are reported in the heat of mixing measured for PS and PPO by the latter authors, which arise from the subtractions inherent in Hess's law. The correction required to obtain the enthalpy of mixing in the liquid state was also discussed by these authors.

Allen et al. (1960A) have measured the heats of mixing of oligomeric materials by direct mixing. The same procedure was also followed by Cooper and Booth (1977). The usefulness of the measurement of heats of mixing of model compounds was demonstrated by Cruz et al. (1979).

We have measured the heats of mixing of sec-octyl acetate, as an analogue of EVA45, and ceroclor 45 and 52, as analogues of H48 and CPE3 respectively, in a modified NBS batch type microcalorimeter. The microcalorimeter used is fully described by Chong (1981). The instrument has an accuracy of $\pm$ 0.002 $J.g^{-1}$ as determined by an acid-base reaction. The stability of the temperature is within $0.001^{\circ}C$. Total weight of the two components which were mixed at 64.5, 73.08 and $83.5^{\circ}C$ at atmospheric pressure was about 1.5 grams. The microcalorimeter was electrically calibrated using a resistor immersed in a 50/50 w/w% mixture of the system under investigation. To account for the temperature dependence of thermal conductivity and the heat capacity
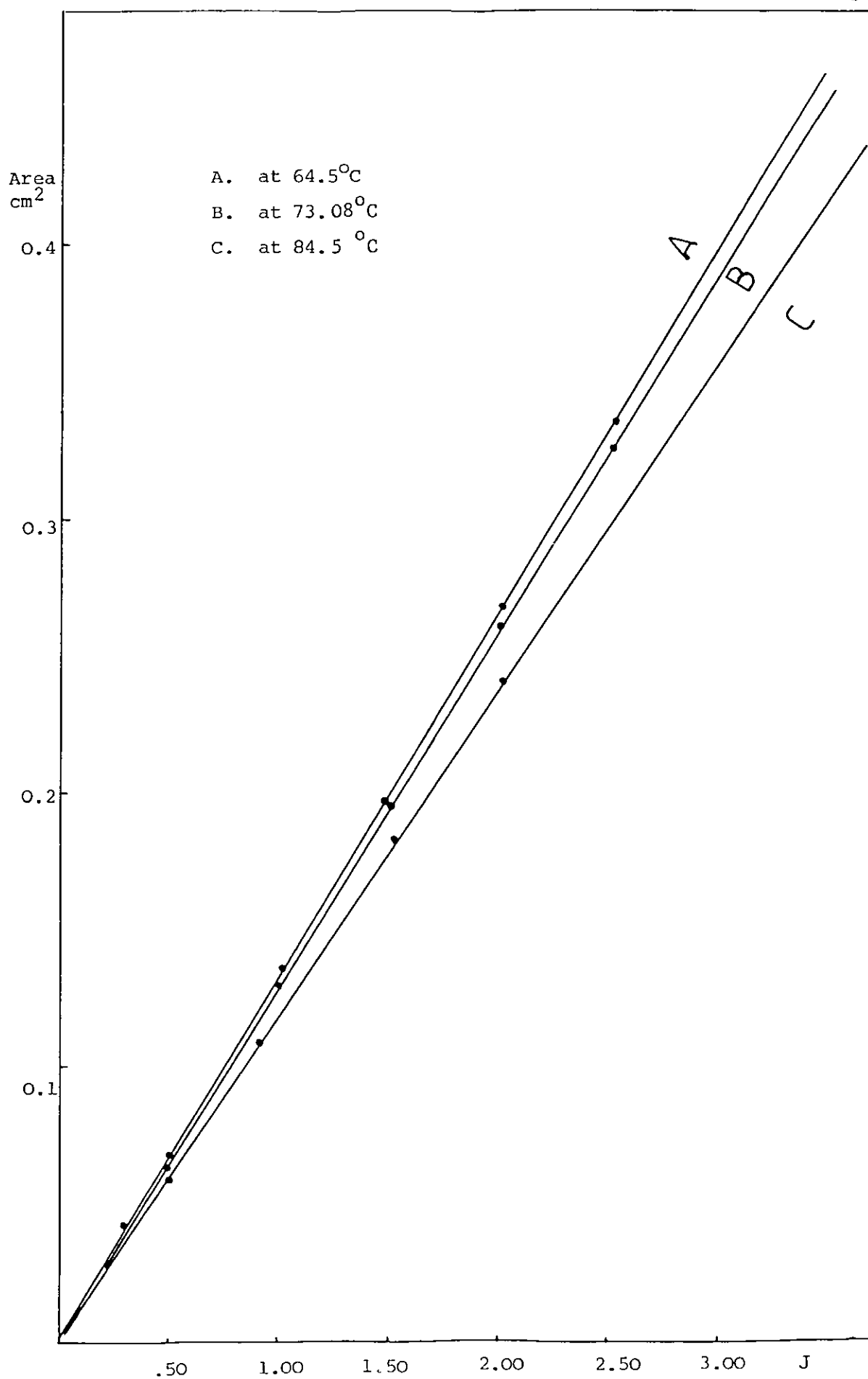
of the mixture this was repeated at each operating temperature. An example of such a calibration curve for 50/50 w% mixture of sec-octyl acetate and ceroclor 52 is shown in Figure 3.5. The horizontal axis shows the electrical energies given to the mixture and the vertical axis gives the areas of the resulting peaks.

The required amounts of the pure liquids were kept at the operating temperature for 3-6 hours before mixing. The measurements were repeated three or four times for each composition and an average value taken. The results were reproducible within the range of 0.004 to 0.009 $J.g^{-1}$ depending on the system, composition and temperature.

3.4.2   Inverse Gas Chromatography

Conventional gas liquid chromatography determines the property of an unknown sample in the moving phase with a known stationary phase. The inverse method, however, determines the property of the stationary phase using a known volatile solute in the moving phase. The volatile molecules are referred to as probe molecules.

Since the initial work of Smidsrod and Guillet (1969) numerous investigators have used inverse gas chromatography (IGC) to determine physicochemical parameters characterizing the interaction of small amounts of volatile solutes with polymers (Olabisi et al., 1979).

Area
cm^2

A. at 64.5^{o}C

B. at 73.08^{o}C

C. at 84.5 ^{o}C

0.4

0.3

0.2

0.1

.50   1.00   1.50   2.00   2.50   3.00   J

FIG. 3.5. Calibration curves for sec-octyl acetate/ceroclor 52 = 50/50.

Baranyi (1981) has shown that infinite dilution weight fraction activity coefficients, interaction parameters and excess partial molar heats of mixing can be readily determined with this technique. Partial molar heats of mixing, partial molar free energies of mixing and solubility parameters of a wide variety of hydrocarbons in PS and PMMA have been determined by this technique by Baranyi and Guillet (1977). The temperature dependence of the interaction parameter between PS and PVME has been studied by Robard and Patterson (1977). Hydrogen-bonding polymer-solute interactions have been studied by IGC by Baranyi et al. (1980). Doube and Walsh (1980) have utilized this technique to measure the interaction parameter between PVC and CPE.

A PYE Unicam GCD chromatograph with a flame ionization detector was used to measure the solvent-polymer and polymer-polymer interaction parameters for the polymers used in this work. Nitrogen was used as a carrier gas. The column supporter was 30-40 mesh porous PTFE and the coating procedure was as explained by Doube and Walsh (1980).

The link between IGC measurements and interaction parameters is the infinite-dilution activity coefficient, which is obtainable directly from the specific retention volume, Vg, data. The latter was computed using the relation given by Baranyi (1981):

$$Vg = (t_s - t_m) Q. \frac{J. 273.16}{W \quad T} \qquad\qquad 3.27$$

where t_s is the retention time for the solvent and t_m is that of a non-interacting gas, methane. W is the weight of stationary phase, T is the operating temperature and J is a correction factor for gas compressibility as described by Cruickshank et al.(1966). The values of Vg were extrapolated to zero flow rate to obtain Vg^o.

The weight fraction activity coefficient at infinite dilution

of the probe $(\frac{a_1}{W_1})^\infty$ and the solvent-polymer interaction parameters,

χ_{12} and χ_{13}, were then calculated from the equations given by Deshpande

et al. (1974).

$$\ln\left(\frac{a_1}{W_1}\right)^\infty = \frac{273.16R}{Vg^O P_1^O M_1 Z} , \quad Z = \exp P_1^O \cdot (B_{11} - V_1)/R\,T \qquad 3.28$$

$$\chi_{12} = \ln\frac{273.16R\,v_{2\,SP}}{Vg_2^O P_1^O V_1 Z} - (1 - \frac{V_1}{V_2})\,\Phi_2 \qquad\qquad 3.29$$

and

$$\chi_{13} = \ln\frac{273.16R v_{3\,SP}}{Vg_3^O P_1^O V_1 Z} - (1 - \frac{V_1}{V_2})\,\Phi_3 \qquad\qquad 3.30$$

where V_1, M, P_1^O and B_{11} refer to the solute molar volume, molecular

weight, saturation vapour pressure and second virial coefficient

respectively. R is the gas constant and T is the column temperature.

$v_{i\,SP}$, V_i and ϕ_i are the specific volume, molar volume and volume fraction

of component i. The densities of the solvents were obtained from

Timmermans (1960) as were values of P_1^O except those for tetrahydrofuran

and butanone which were calculated using the method of Ambron (1980).

Second virial coefficients were taken from Dymond and Smith (1980),

those for tetrahydrofuran and butanone being estimated from critical

constants by the method of McGlashen and Potter (1962).

Knowing χ_{12} and χ_{13} the interaction between a solvent and a

column containing a homogeneous mixture of two polymers, $\frac{\chi_{23}}{V_2}$, can be

obtained from (see Olabisi et al., 1979)

$$\{\frac{\chi_{12}}{V_1}\Phi_2 + \frac{\chi_{13}}{V_1}\Phi_3 - \frac{\chi_{23}}{V_2}\Phi_2\Phi_3\}V_1 = \ln\frac{273.16R\,(W_2 v_{2SP} + W_3\,v_{3SP})}{P_1^O Vg_{23}^O V_1 Z}$$

$$- (1 - \frac{V_1}{V_2})\Phi_2 - (1 - \frac{V_1}{V_3})\Phi_3 \qquad\qquad 3.31$$

This equation was converted to a simpler and more useful form in this work to facilitate the calculation of $\frac{\chi_{23}}{V_2}$ and also to eliminate the error contribution of Z, χ_{12} and χ_{23}. The simplified equation for $\frac{\chi_{23}}{V_2}$ is:

$$\frac{\chi_{23}}{V_2} = \frac{1}{V_1} \left\{ \frac{1}{\phi_3} \ln \frac{v_{2SP}}{Vg_2^O} + \frac{1}{\phi_2} \ln \frac{v_{3SP}}{Vg_3^O} - \frac{1}{\phi_2\phi_3} \ln \frac{W_2 v_{2SP} + W_3 v_{3SP}}{Vg_{23}^O} \right\} \quad 3.32$$

where ϕ_2 and ϕ_3 are the volume fractions and W_2 and W_3 are the weight fractions of polymers '2' and '3', V_1, V_2 are the molar volumes of solute and polymer '2' and v_{2SP}, v_{3SP} are the specific volumes of the polymers. Vg_2^O, Vg_3^O and Vg_{23}^O refer to the single component and mixed column values.

The $\frac{\chi_{23}}{V_2}$ calculated from Equation 3.32 should be more accurate than the one calculated from Equation 3.31. The $\frac{\chi_{23}}{V_2}$ obtained from IGC measurements, however, contains a contribution from the non-combinational entropy of mixing. We have reservations about the quantitative reliability of IGC results because of the problem of removing the effect of surface adsorption and diffusion limitation with stationary phase as discussed by Doube and Walsh (1980). No attempt, therefore, was made to calculate the interaction term, χ_{23}, of the mixed column as done by Olabisi et al. (1979).

3.5   THE VOLUME CHANGE ON MIXING

3.5.1   Density Measurements

In the absence of electron-donor-acceptor interactions, normal

liquids expand upon mixing, as illustrated by numerous workers.

Densification, however, mostly occurs in mixtures with specific

interactions.   An example of this for PS in PPO mixtures is given

by Jacques and Hapfenberg (1974) and for that of PS in PVME by

Kwei et al. (1974).

The volume changes of mixing of sec-octyl acetate with

Ceroclor 45 and 52 at $25^{\circ}C$ were measured using a DMA46 (Anton Paar,

Austria) densimeter. The principle of the density measurement in

this method is based on the change of the natural frequency of a

hollow oscillator tube when filled with different liquids or gas.

The densities of pure liquids and their mixtures were measured

using the following procedure:

Prior to each experimental series, the instrument was

calibrated at $25^{\circ}C$, with dry air at atmospheric pressure and with

doubly distilled water. The temperature was controlled constantly

by a $\pm$ $0.25^{\circ}C$ thermometer. All mixtures were prepared by weighing

the components to $\pm$ 0.1 mg. The solutions (approximately 2.5 cm^3)

were heated and mixed and after cooling were transferred to a syringe

and injected through the densimeter. Measurements were repeated

three or four times and average values were taken. The experimental

errors of the densities measured are estimated to be $\pm$ 0.0002 g .cm^{-3}

in the regions richer in the acetates and $\pm$ 0.00035 g .cm^{-3} in the

regions richer in ceroclors. The volume change of mixing for these

mixtures was calculated from the following relation:

$$\frac{\Delta V_M}{V^o} = \frac{v_{SP}}{W_1 v_{1SP} + W_2 v_{2SP}} - 1$$

3.33

where v_{1sp}, v_{2SP} and v_{SP} are the specific volumes of component one, two and their mixture respectively, and W_1 and W_2 are the weight fraction of the corresponding components.

This method is becoming a standard method for obtaining the excess volume of mixing as reported by Pikkarainen (1982) and Kokkonen (1982).

3.5.2   The Effect of Pressure on Mixing

Patterson and Robard (1978) by using a combination of the Prigogine and Flory equation of state theories have related the interaction parameter, χ_{12}, between solvent-polymer or polymer-polymer to two terms, one interactional and the other free volume, as given below.

$$\frac{\chi_{12}}{V_1^*} = \frac{P_1^*}{RT_1^*} \left\{ \underbrace{\frac{\tilde{v}_1^{1/3}}{\tilde{v}_1^{1/3} - 1} \cdot \frac{\chi_{12}}{P_1^*}}_{\substack{\text{interactional} \\ \text{term}}} + \underbrace{\frac{\tilde{v}_1^{1/3}}{(\frac{4}{3} - \tilde{v}_1^{1/3})} \cdot \frac{\tau^2}{2}}_{\substack{\text{free volume} \\ \text{term}}} \right\}$$

3.34

where τ is related to the volume difference between two components in a system and given by $\tau = 1 - T_1^* / T_2^*$ The other terms in Equation 3.34 have the same meanings as defined in Chapter Two.

The effect of increasing temperature on the free volume

and interaction terms of EVA45-CPE3 mixture calculated from this

equation are illustrated in Figure 3.6. This shows that increasing

temperature causes the negative interactional term to decrease and

also the positive free volume to increase. Applying pressure to

this system is expected to reduce $\tilde{v}$ and make X_{12} more negative, hence

the misicibility of the system increases in a similar manner to that

which has been observed by Saeki et al. (1975, 1976). A lowering of

the LCST by pressure is extremely rare and has not so far been

seen in a nonaqueous system.

According to the thermodynamic analysis given by Prigogine

(1957) in the vicinity of the critical point the pressure dependence of

the critical solution temperature is related to the ratio of volume

change on mixing and enthalpy of mixing as below.

$$(\frac{dT}{dP})_c = - \frac{(\partial\chi/\partial P)_T}{(\partial\chi/\partial T)_P} = \frac{T\Delta V_M}{\Delta H_M} \qquad 3.35$$

This equation implies that for positive values of $(\frac{dT}{dP})_c$ and negative

values of ΔH_M, the system undergoes contraction. In the case of a

UCST, ΔV_M can be either negative or positive depending on the sign

of $(\frac{dT}{dP})_c$ which in turn is affected by the nature of the mixture.

Saeki et al. (1975) have found that the value of $(\frac{dT}{dP})_c$ for PS in

cyclohexane (with a UCST) is positive when molecular weight of PS is

3.7×10^4 and it becomes negative for solutions of PS of a higher

molecular weight range of $11-145 \times 10^4$. Tripathi (1979) has also

found that by increasing the pressure on two mixtures (methoxylated

poly(ethylene glycol) in methoxylated poly(propylene glycol) and

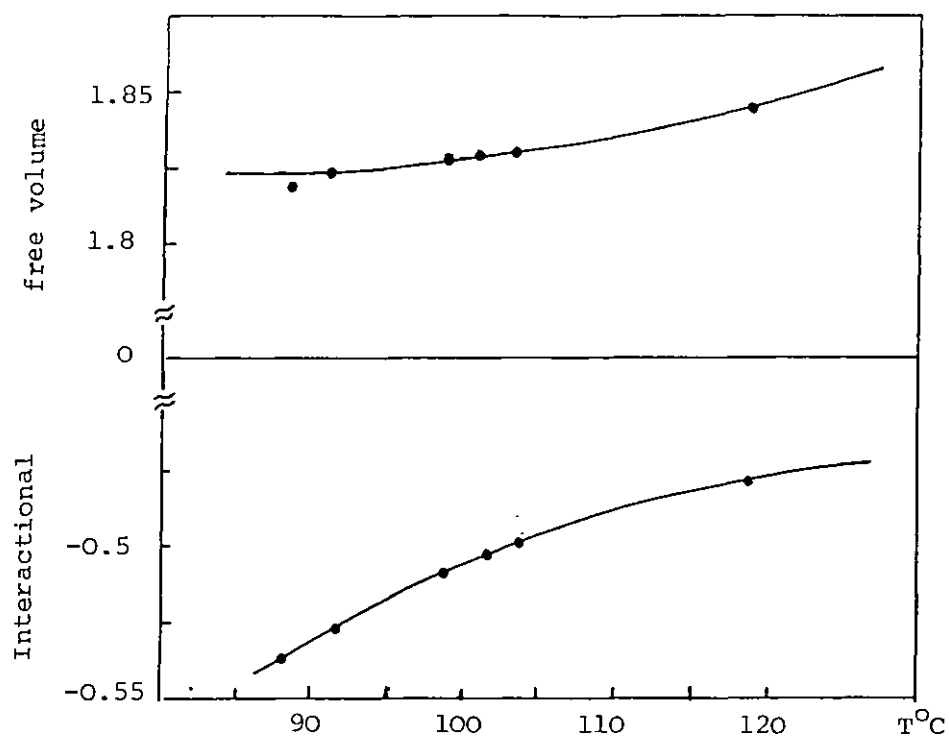polystyrene in poly(butadiene)), which exhibit UCST behaviour, the

FIG. 3.6. The free volume term and interactional term calculated for EVA45-CPE3 at different temperatures.
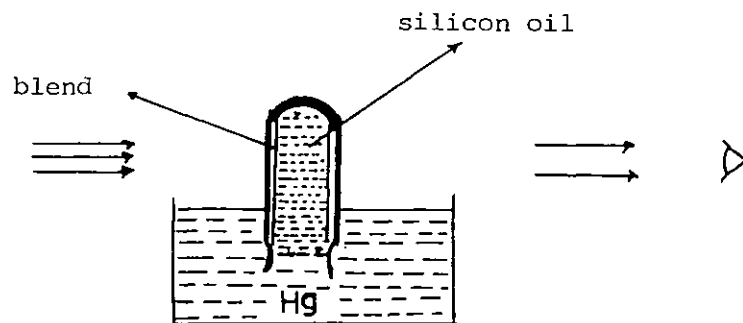

FIG. 3.7. Position of the sample in silicon oil and Hg under pressure.

miscibilities decreased. Using the Flory-Huggins model he has shown

that χ values increase on increasing the pressure for the above

mentioned mixtures.

It is possible to use equation 5.39, without its combinatorial

part, for the total interaction parameter to calculate $(\frac{\partial \chi}{\partial p})_T$ and

$(\frac{\partial \chi}{\partial T})_P$ individually. This procedure, however, may not give a precise

answer to $(\frac{dT}{dP})_c$ because of complications in pressure and temperature

dependence of χ_{12}.

A film of 50 w% EVA45 in CPE3, about 300 μm thick, was placed

around a specially designed glass sample holder of 7.00 mm O.D. and

16.00 mm height to be tested under the pressure. The rest of the

sample holder was filled with chromatography grade silicon oil (see

Figure 3.7).

The pressure apparatus used was described by Tripathi (1979)

and was capable of studying the effect of pressure on polymer-polymer

miscibility up to 150°C and in the pressure range of 1 to 1000 atm.

Its pressure vessel was mounted in a thermostat controlled bath ($\pm$0.1°C).

The optical arrangement was such that the transmitted light was

detected by a photodiode set at zero angle to the incident light beam.

The blend was heated gradually with an average heating rate

of 0.17°C.min^{-1} at atmospheric pressure. The cloud point of the

sample was found in a similar manner to that explained in Section 3.3.7.

The result is almost the same as given by the turbidimeter if allowance

is made for the detection angles. The experiment was repeated

at various pressures each time on a newly mounted sample. The

pressure dependence of the cloud points obtained is reported in

Chapter Four.

It is worth mentioning that the silicone oil acts as a

pressure transferring medium and this has been found to have virtually

no effect on the cloud point of the blend.

CHAPTER FOUR

RESULTS

4.1   THE ESTABLISHMENT OF MISCIBILITY AND THE PHASE BOUNDARY

4.1.1   Dynamic Mechanical Relaxation

The relaxation peaks obtained, using a rheovibron at a

frequency of 11 HZ, for EVA45, CPE3, and some of their blends are given

in Figure 4.1. The temperature was scanned at a rate of $1^{O}C$ min^{-1}.

Similar results for EVA40 and CPE3 and some of their blends are shown

in Figure 4.2. The mechanical relaxation of EVA45-H48 blends and

EVA40-H48 blends are given in Figures 4.3 and 4.4 respectively.

The rheovibron has given a single transition temperature to

all the blends studied. The rheovibron was also used to estimate the

phase separation temperature of the blends. The blends were heated

up to a certain temperature and quenched down on a surface of cooled

metal, in order to freeze in the probable structure. They were then

tested as usual. An example of the results for a blend of 65 w% EVA40

in H48 is given in Figure 4.5. According to this result the blend

will phase separate in the temperature region of 62 to $82^{O}C$. This was

proved to be consistent with other methods of determination for this

blend. The rheovibron failed to detect any phase separation of EVA40

in H40 and EVA45 in H40 blends when they were similarly heat treated.

The difference between the transition temperatures of the pure

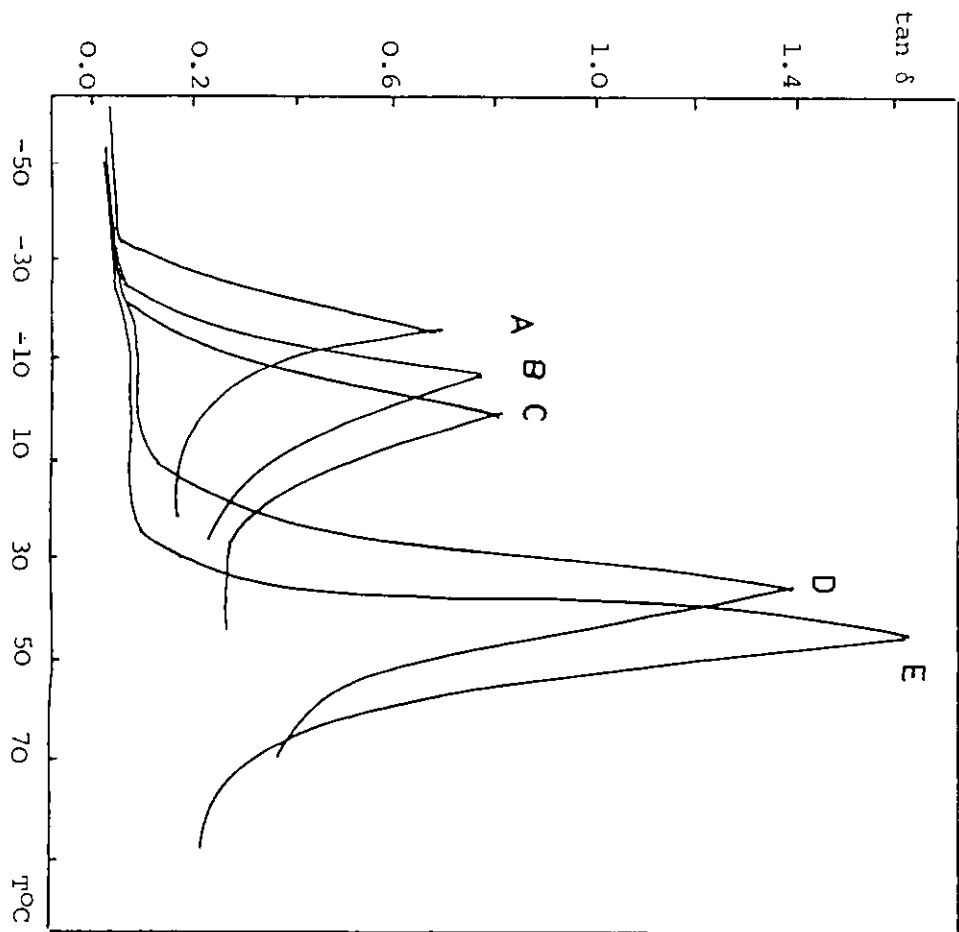components of these blends is only about $20^{O}C$.

FIG. 4.2. The dynamic mechanical relaxation curves
for EVA40, CPE3 and their blends.
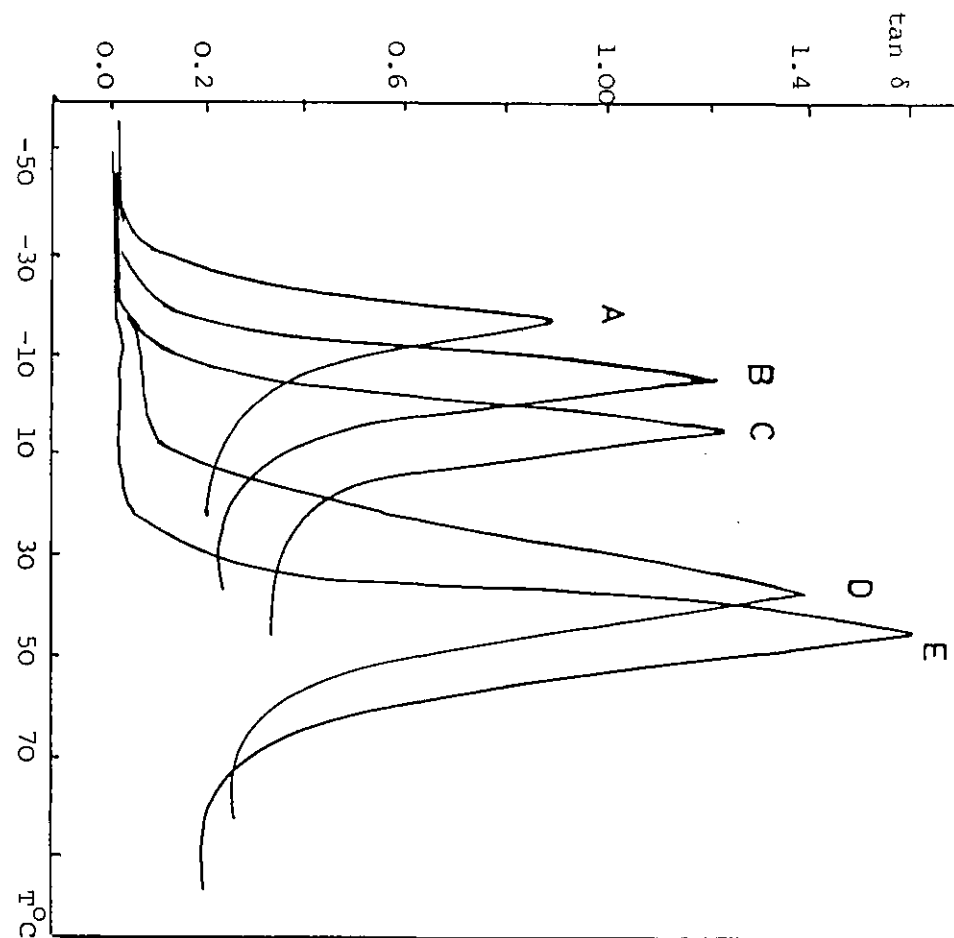A. 100% EVA40 C. 40% EVA40 E. 100% CPE3
B. 80% EVA40 D. 20% EVA40

FIG. 4.1. The dynamic mechanical relaxation curves for
EVA45, CPE3 and their blends.
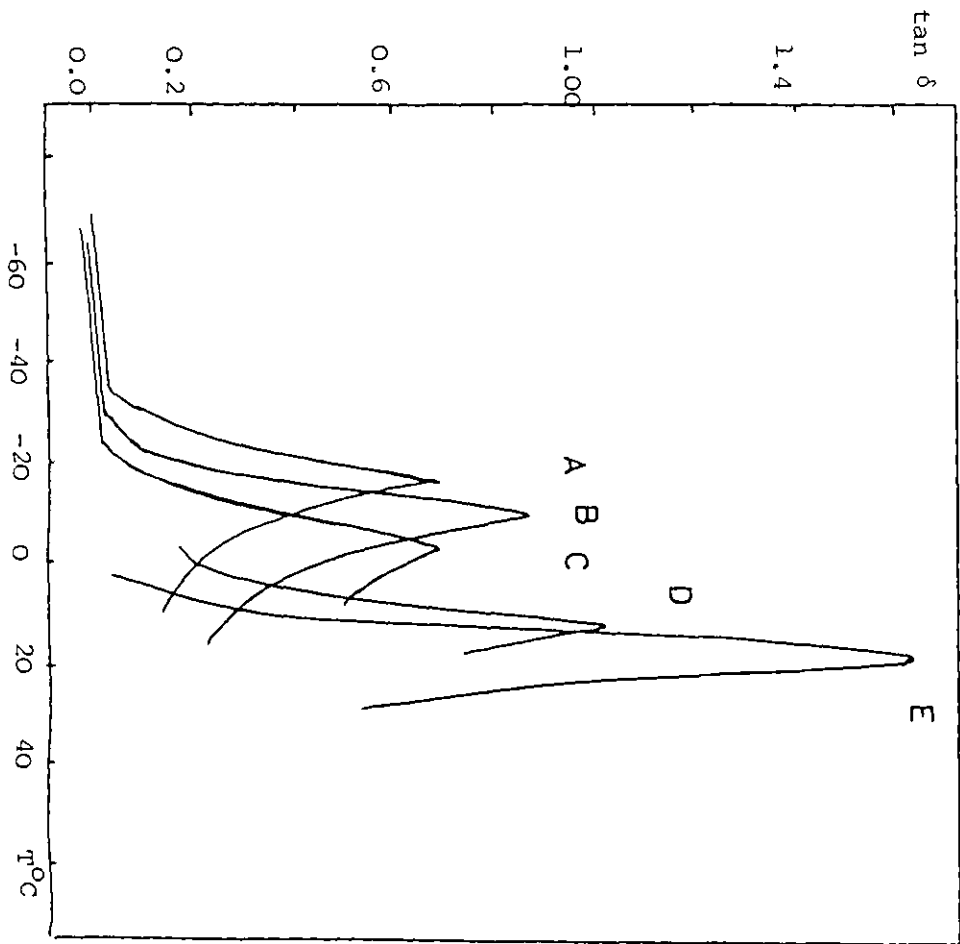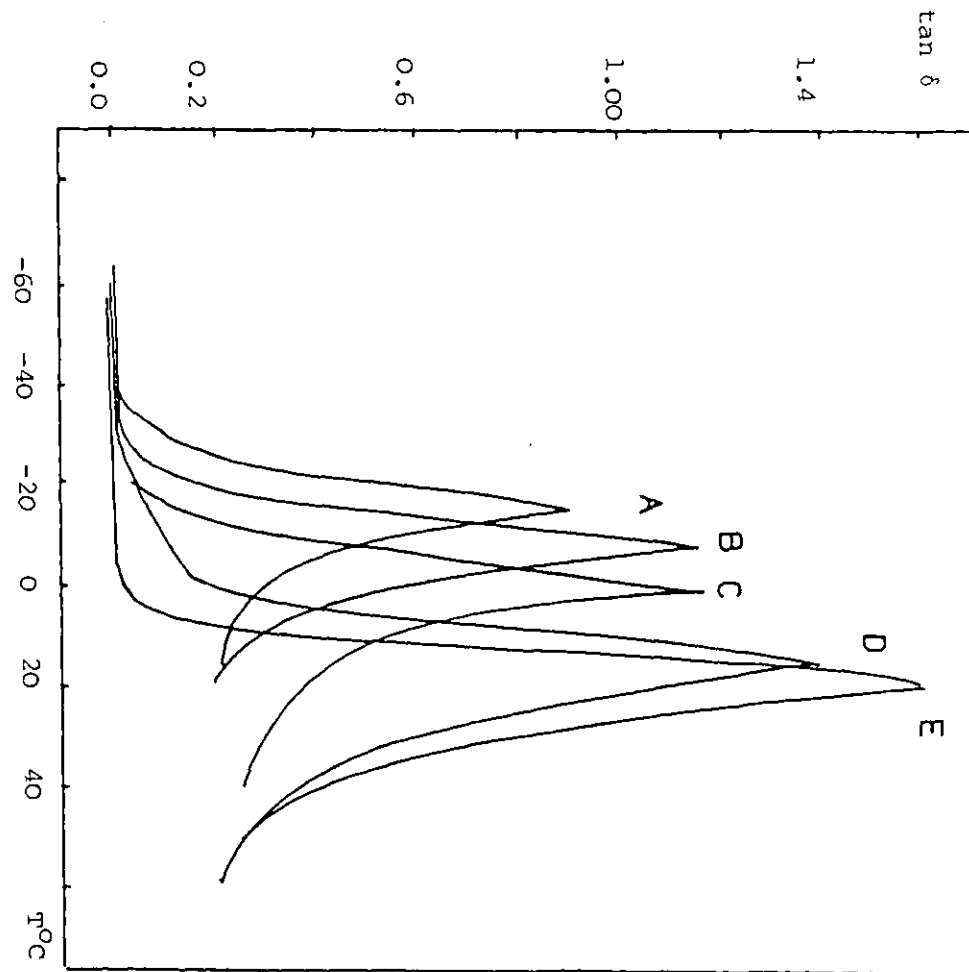A. 100% EVA45 C. 50% EVA45 E. 100% CPE3
B. 80% EVA45 D. 20% EVA45

FIG. 4.4. The dynamic mechanical relaxation curves for EVA40, H48 and their blends.
A. 100% EVA40   C. 50% EVA40   E. 100% H48
B. 80% EVA40   D. 30% EVA40

FIG. 4.3. The dynamic mechanical relaxation curves for EVA45, H48 and their blends.
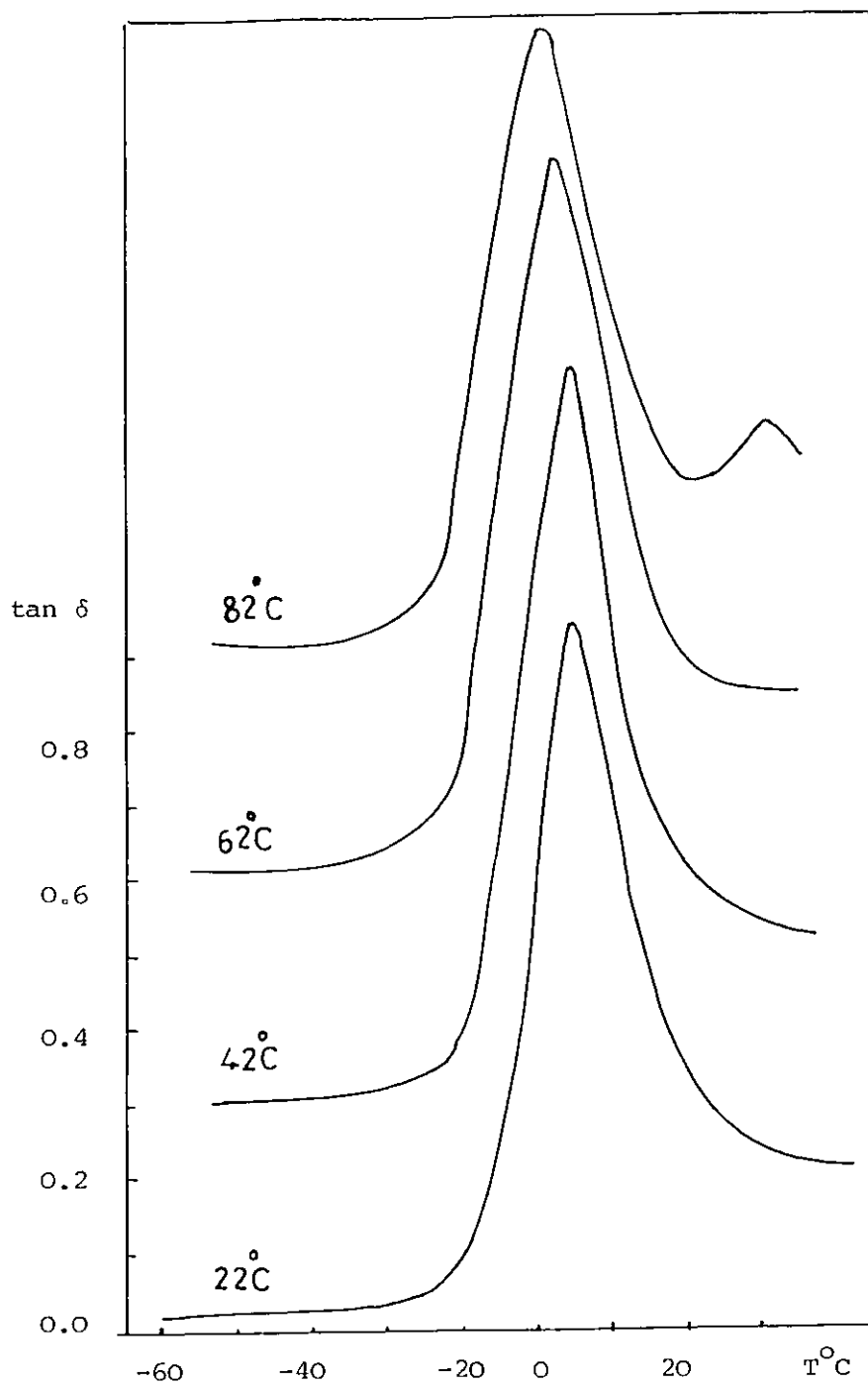A. 100% EVA45   C. 50% EVA45   E. 100% H48
B. 80% EVA45   D. 20% EVA45

98

FIG. 4.5. Phase separation temperature of 65 w% EVA40 and H48 as
determined by dynamic mechanical relaxation testing.

The results in Figures 4.1 to 4.4 show that the temperatures of the relaxation peaks of EVA45 and EVA40 are almost identical at -17°C. This relaxation is associated with the beta relaxation of EVA. The transition temperature remains constant until the vinyl acetate content increases to 55 w% of the polymer. At higher acetate contents, the transition temperature increases, approaching the value for pure polyvinyl acetate. More details of this behaviour are given by Nielsen (1960). Hammer (1971) has shown that the gamma transition of the copolymers around -110°C is due to a more limited type of rotational motion of a few CH_2 groups. This transition remains entirely unaffected by the presence of C-Cl groups. The beta transition, therefore, is used to judge the presence or absence of pure EVA40 or EVA45 in the blends.

The relaxation of the chlorine containing groups in amorphous chlorinated polyethylene has been attributed to the alpha relaxation which increases with temperature as the degree of chlorination increases. The other relaxations of chlorinated polyethylene were studied in more detail by Perena et al. (1980).

4.1.2   Dielectric and Depolarization Relaxation

The dielectric relaxation peaks obtained for EVA45, CPE3 and some of their blends are given in Figure 4.6. The Maxwell-Wigner-Sillared effect is also shown in this figure. Similar results for EVA40-CPE3 and EVA45-H48 mixtures are shown in Figures 4.7 and 4.8 respectively. The MWS effect is not plotted in these figures.
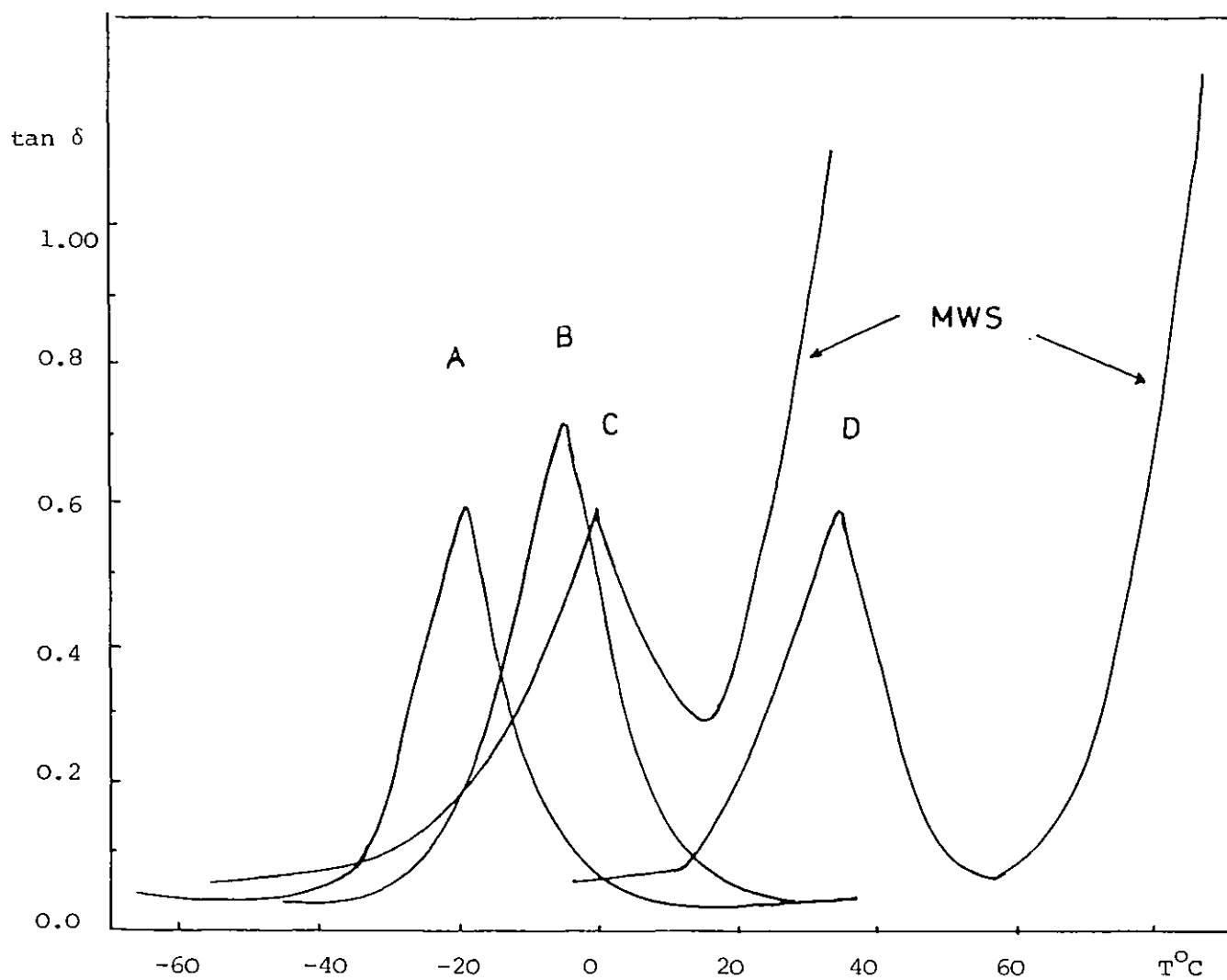
FIG. 4.6. The dielectric relaxation curves for EVA45, CPE3 and their
mixtures at 37 Hz. The MWS effect in pure CPE3 and 30 w%
EVA45 in CPE3 is exhibited.
A. 100% EVA45   C.   30% EVA45
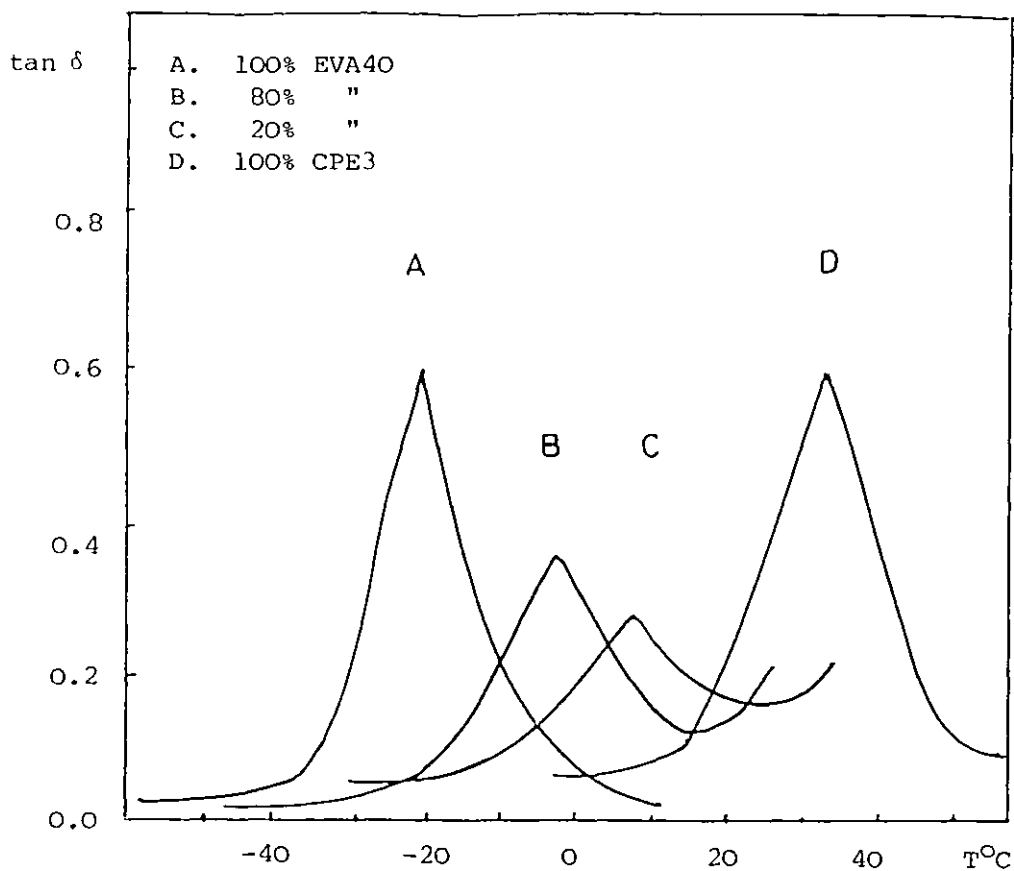B.   70% EVA45   D.   100% CPE3

FIG. 4.7. The dielectric relaxation curves for EVA40, CPE3 and
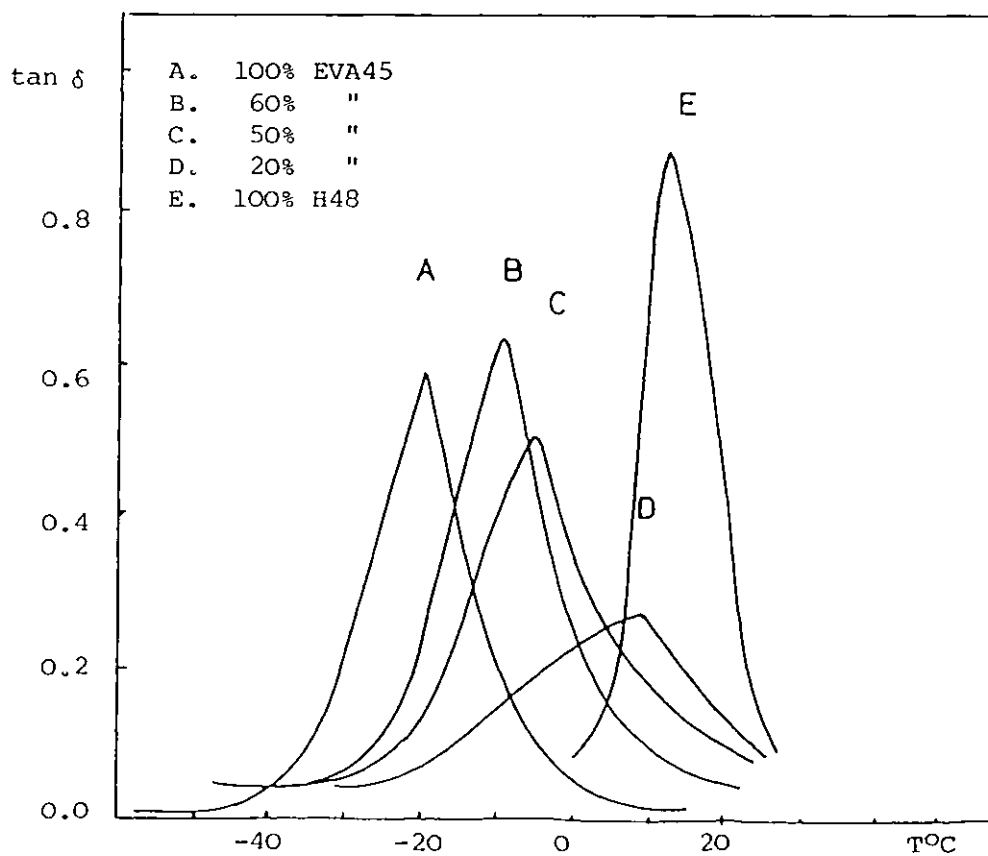their mixtures at 37 Hz.

FIG. 4.8. The dielectric relaxation curves of EVA45, H48 and their
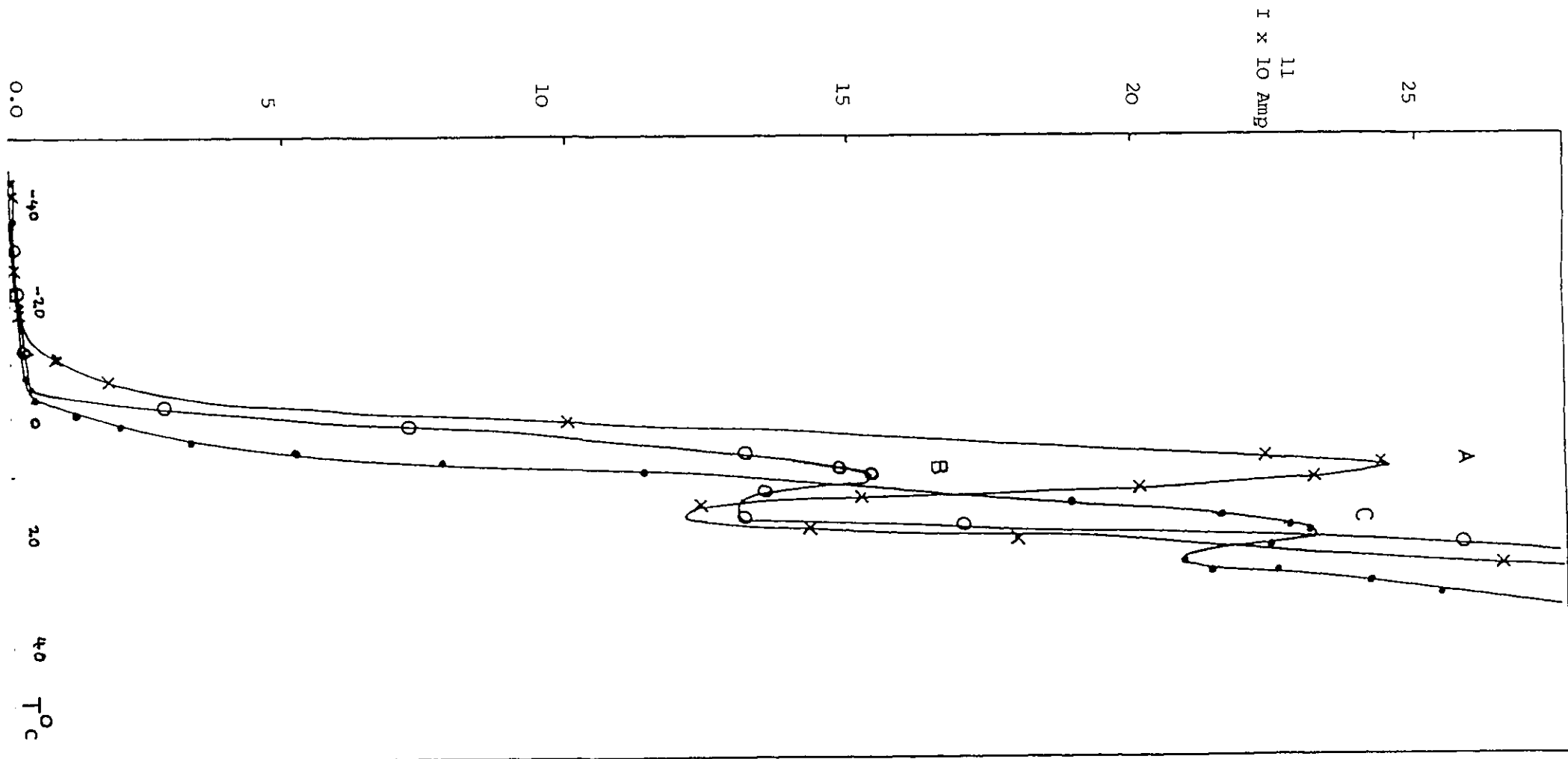mixtures at 37 Hz.

FIG. 4.9. The depolarization currents of some blends obtained when they were charged whilst above their glass transition temperatures. A. 60-40 = EVA40-H48 B. 70-30 = EVA45-CPE3 C. 50-50 = EVA40-CPE3

The depolarization traces of some blends are given in Figure 4.9. The samples had a thickness of 20μm and were charged at 35 V for 50 minutes at 25°C (blend A), 60 minutes at 47° (blend B) and 42 minutes at 50°C (blend C). The heating rate during the charge release was 2°C min^{-1}.

The depolarization current detected for some of the blends studied shows single transitions. The transition temperatures are higher than those given by dielectric or dynamic mechanical relaxations. This is partially due to the non-frequency dependence of depolarization and also to the complication of the depolarization peak as discussed by Hedvig (1977).

4.1.3   Differential Scanning Calorimeter

The results for EVA40-H48 blends with a heating rate of 5°C min^{-1} are given in Figure 4.10. Similar results for EVA40-CPE3 blends are also presented in Figure 4.11.

The transitions obtained by this technique are not generally sharp. This may be due to the nature of the blend constituents and also to the unreliability of the particular instrument used. Lower heating rates could also give sharper transitions especially when the Tg's of the pure components were well separated. Annealing the blends at a rate of 1°C min has improved the resolution of the transitions, but this technique was not considered useful for this study.
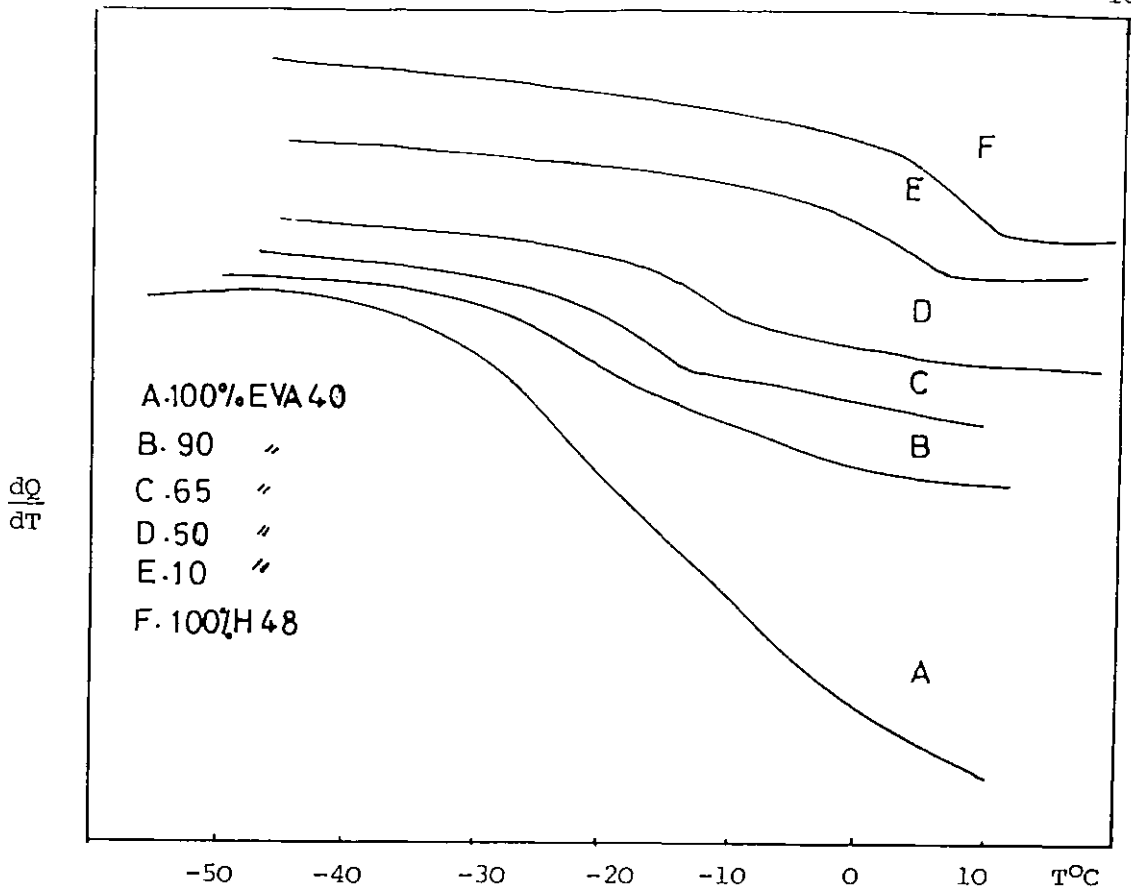
FIG. 4.10. The differential scanning calorimetry traces of EVA40, H48 and their mixtures。

A·100% EVA 40
B· 90 ″
C·65 ″
D·50 ″
E·10 ″
F·100% H 48
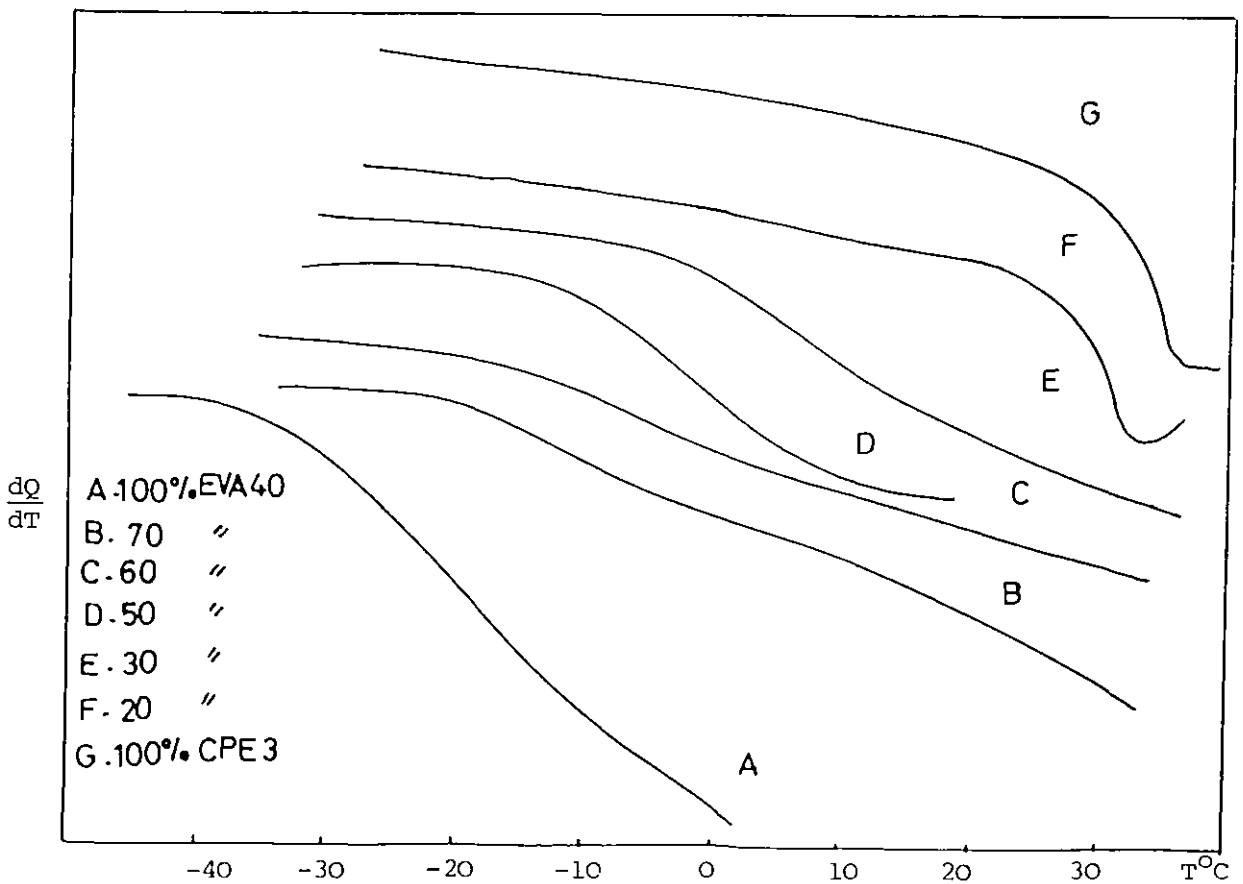
FIG. 4.11. The differential scanning calorimetry traces of EVA40, CPE3 and their mixtures.

A·100% EVA 40
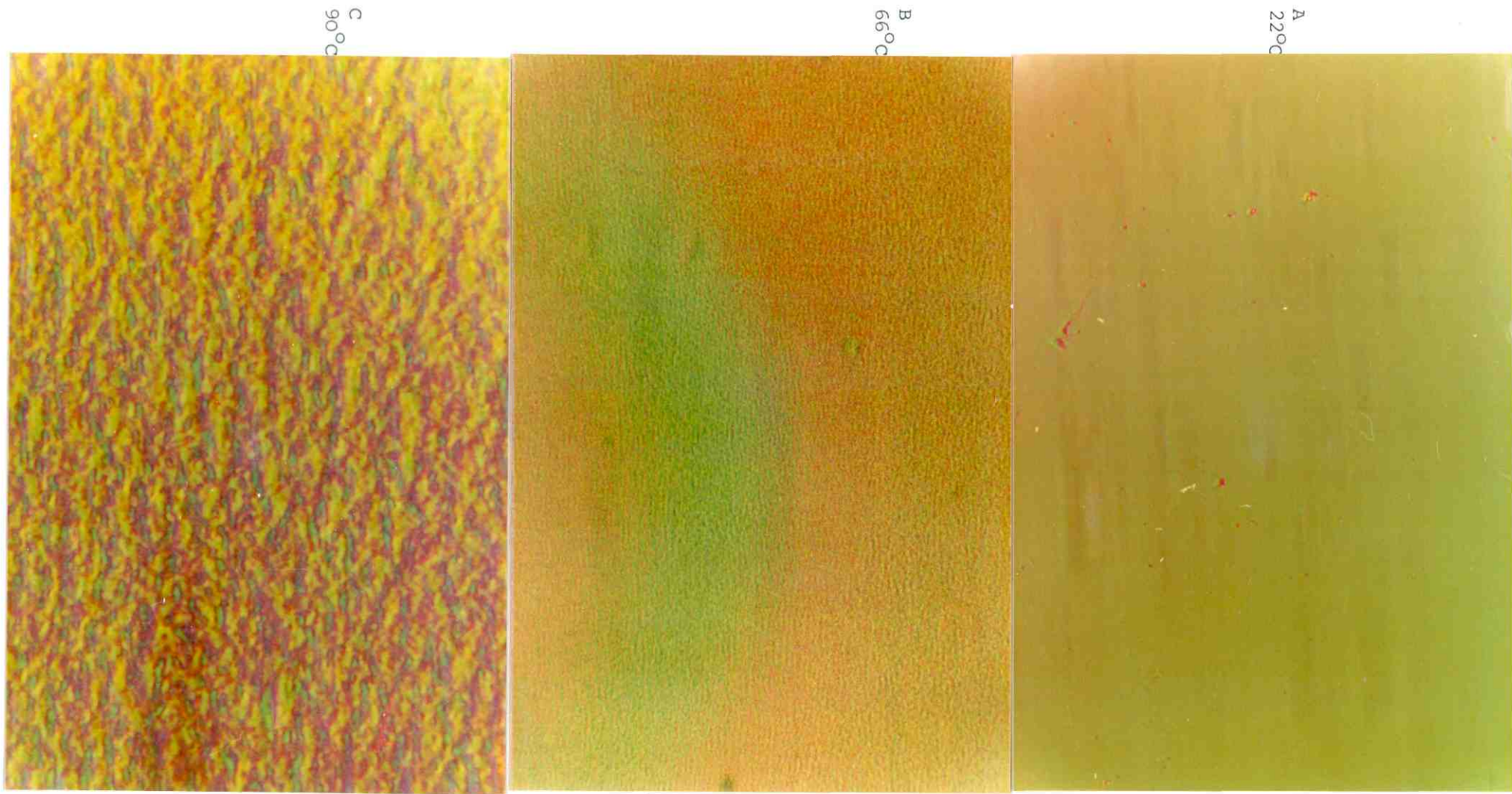B·70 ″
C·60 ″
D·50 ″
E·30 ″
F·20 ″
G·100% CPE 3

FIG. 4.12. The phase contrast microscopy of EVA40-H48 =40 -60 blend at different temperatures

1 cm

11 μm

4.1.4   Phase Contrast and Electron Microscopy

The morphological features of a blend of 60 w% EVA40 in H48,

examined by interference microscopy, are shown in Figure 4.12. In the

first frame the specimen is at room temperature and no structure or

colour differences can be seen (except for dust left on the sample

to ease focussing). In the second picture the specimen was kept at

66°C for one hour and then quenched down to below ambient temperature.

Faint two phase structures can be seen. The same treatment was used

for the picture C at 90°C. A two phase structure is clearly seen.

The separated domain size is of the order of one micron or less. This

was confirmed when morphological features of the blends were observed

under the electron microscope. Electron micrographs of a 50/50 w/w% blend

of EVA45-CPE3 are shown in Figure 4.13. 'A' is at room temperature and

appears homogeneous. Blends B, C and D were heat treated at 100°C for

10, 30 and 300 minutes respectively. The size of the phase separated

domains which are at equilibrium in picture D varies between 0.2 to

0.6 μm.

Similar results for a 60 w% of EVA40 in CPE3 at room

temperature and after heating at 90°C are given in E and F of Figure

4.14 respectively. This figure also contains pictures of 50/50 w%

of EVA45 in H40 at room temperature (G) and after heating at 75°C (H).

A

1 cm
←→
0.208 μm

B

1 cm
←→
0.556 μm

C

1 cm
←→
0.666 μm

D
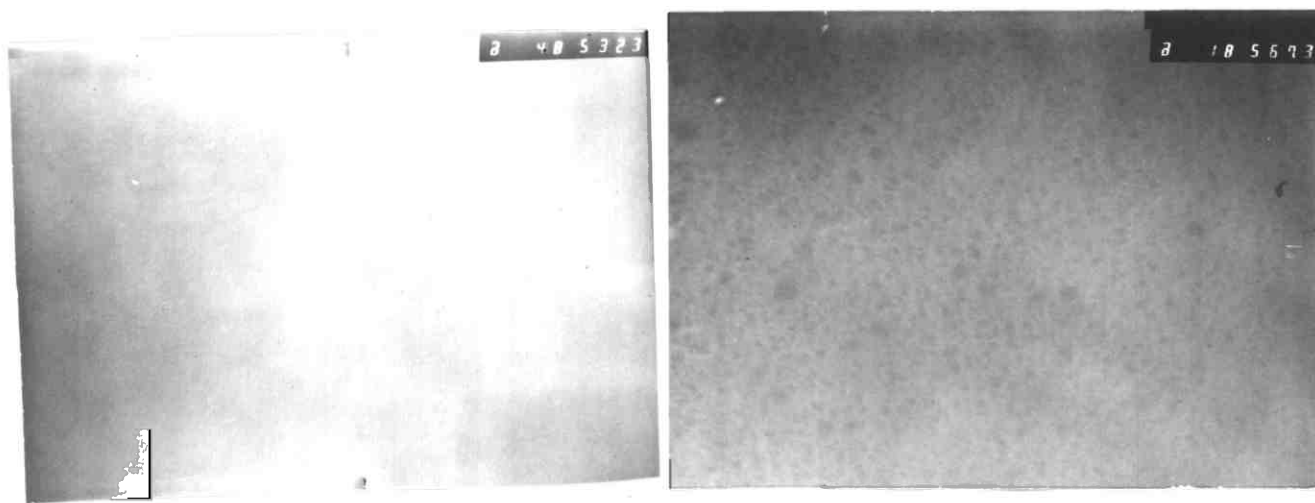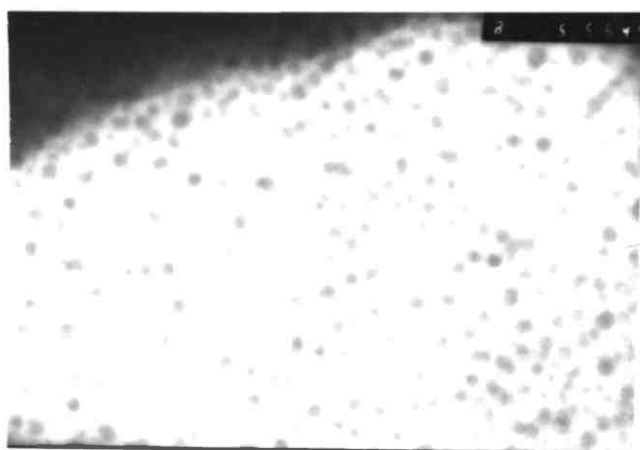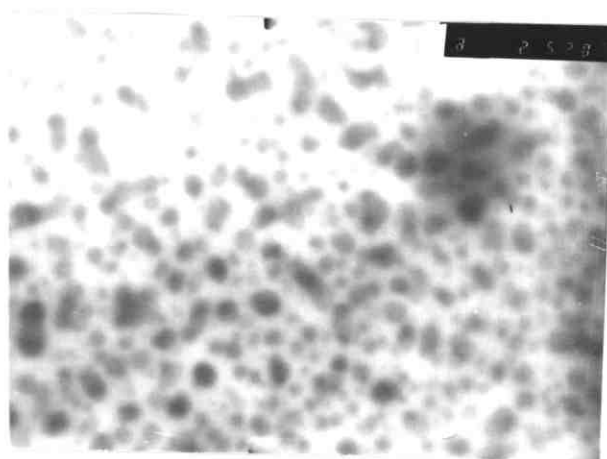
1 cm
←→
0.833 μm

FIG. 4.13.   Transmission electron micrographs of 50/50 mixtures
            of EVA45 and CPE3.
            A.   at room temperature   C.   30 minutes at 100°C
            B.   10 minutes at 100°C   D.   300 minutes at 100°C

E

1 cm

0.333 μm

F

1 cm

0.666 μm

G

1 cm

0.833 μm

H

1 cm
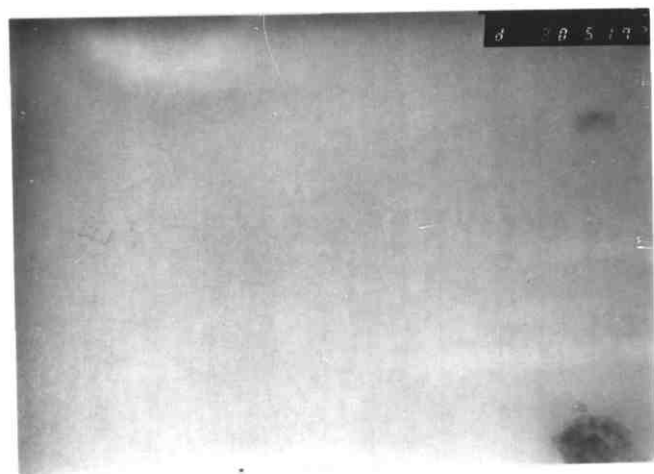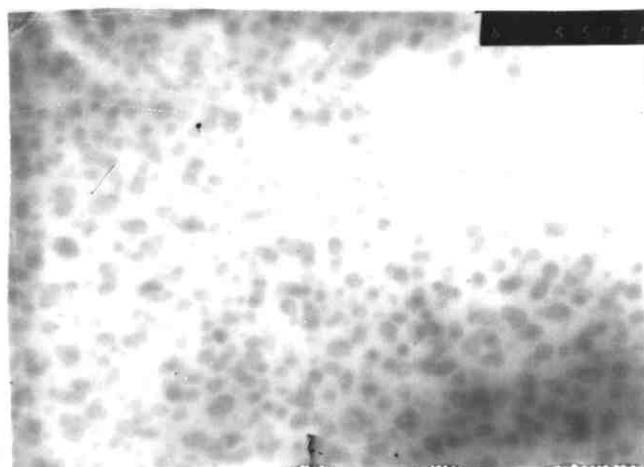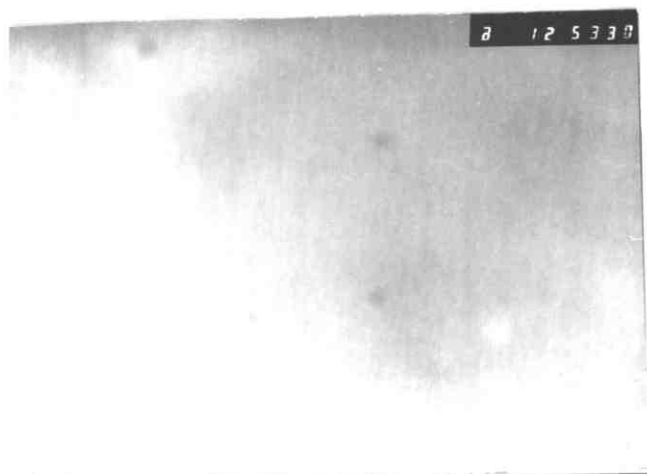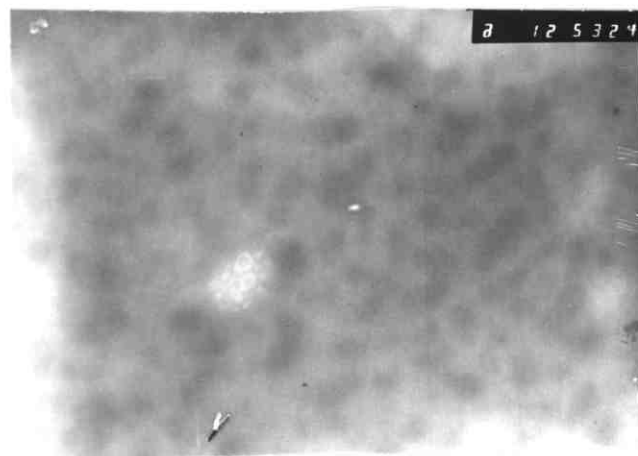
0.833 μm

FIG. 4.14. Transmission electron micrographs of 60 w% EVA40 in CPE3. (E at room temperature, F at 90°C for 300 minutes), and EVA45 in H40 (G at room temperature and H after two hours at 75°C).

4.1.5   Infra-Red Spectroscopy

To estimate the magnitude of the wavelength shifts the scales in the spectrometer were expanded along both axes and the wavelength corresponding to the maximum absorption was accurately measured. This was repeated three times and average values were obtained. The results are summarized in Table 4.1.

TABLE 4.1

Sample	$\mathcal{V}$(C=O) cm^{-1}	$\mathcal{V}$(C-Cl) cm^{-1}	Shift cm^{-1}
EVA45-CPE3			
100-0.0	$1739^{\pm}1.6$		0.0
20-80	$1732.5^{\pm}1.1$		$6.5^{\pm}1.9$
60-40	$1737.7^{\pm}0.6$		$1.3^{\pm}1.7$
0-100		$655.4^{\pm}0.7$	0.0
80-20		$624^{\pm}4.7$	$31.4^{\pm}4.7$
60-40		$647.4^{\pm}1.2$	$8^{\pm}1.4$

These blends were also studied by Professor P.C. Painter of Pennsylvania State University using an FTIR spectrometer. The advantages of the newer instrument are in its higher sensitivity, resolution, the use of signal averaging to enhance the signal to noise ratio, and the ability to manipulate the spectral data by techniques such as spectral subtraction and addition.

The FTIR spectra given for the C=O stretching vibration bond of EVA45 in the presence of 0, 40 and 80 w% of CPE3 at room temperature are shown in Figure 4.15A. The frequency shifts and the ratios of width at half-maximum, WHM, are given in Table 4.2.

TABLE 4.2

Sample	Shift cm^{-1}	WHM
EVA45-CPE3		
100-0	0.0	1
20-80	4	1.41
60-40	2.2	1.27

A weaker interaction for the blend containing less CPE3 is evident from (a) its smaller vibrational shift and (b) less broadening of the C=O absorption peak of EVA45.

These samples were then heated up to 130°C and the tests were repeated. They show the disappearance of the specific interaction at this temperature, see Figure 4.15B. These results confirm the existence of an LCST behaviour in this system as suggested by other methods. To our present knowledge it is the first time an LCST behaviour has been found by infra-red spectroscopy.
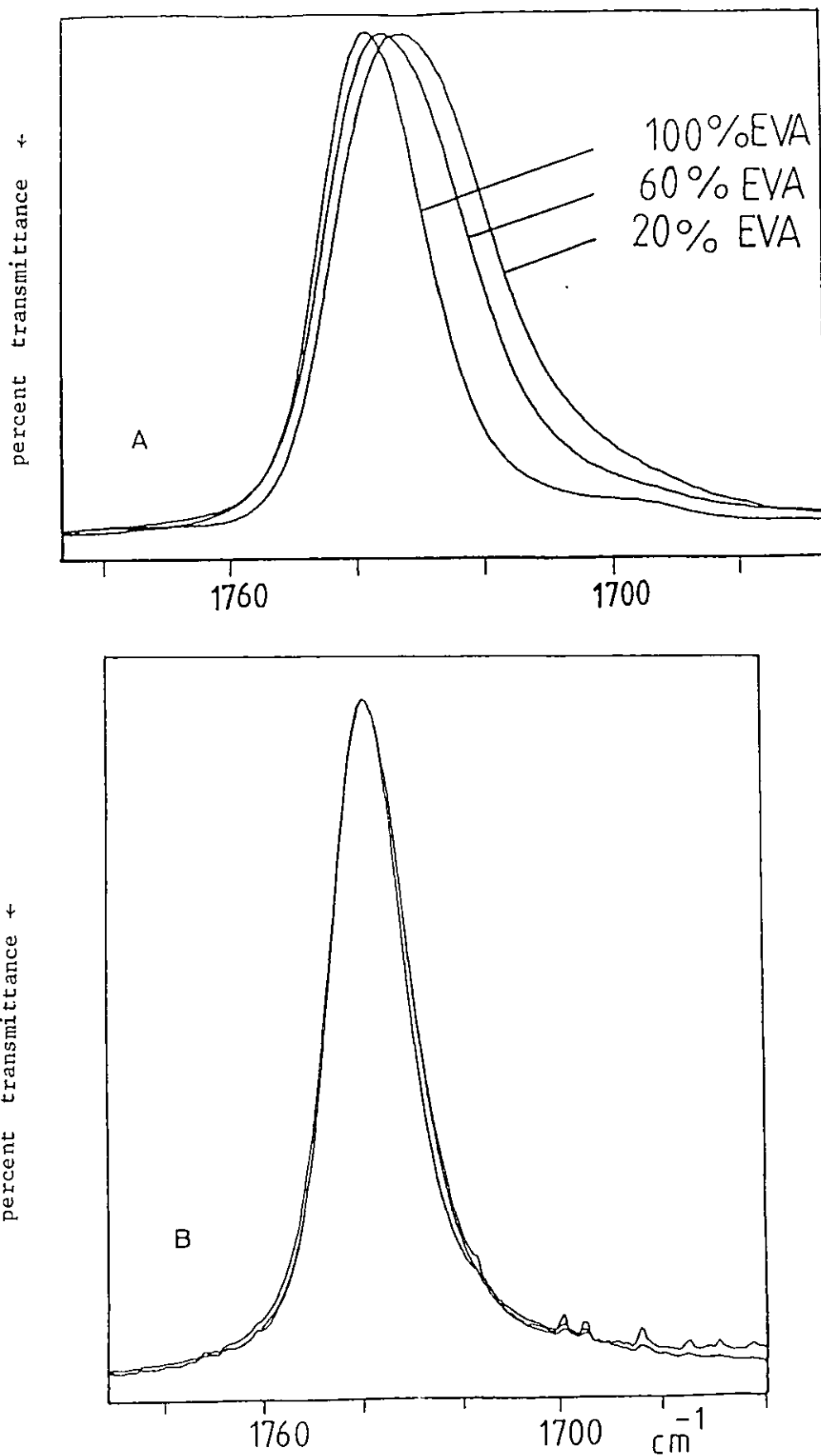
FIG. 4.15. FTIR of EVA45 and its blends with CPE3 (in weight-percent) at; A. room temperature, B. at 130°C.

4.1.6   Light Scattering Turbidimetry

Typical plots of the forwards scattering intensities at an angle of 45° for 50, 60, 70 and 80 w% of EVA40 in CPE3, obtained using the turbidimeter, are shown in Figure 4.16. The temperature was raised at a rate of 0.2^oC min^{-1}. The scale of the scattering axis is arbitrary and the cloud point temperatures correspond to the initial points of increase in the scattering intensities.

The cloud points of the blends may alternatively be obtained by holding the blends at a series of different temperatures for a period of time and recording the intensities of light scattered as before. An example of the results from this method for a 35 w% EVA40 in CPE3 blend is given in Figure 4.17. The right hand side of this figure is the usual scattering intensities versus temperature and the left hand side is the variation of scattered intensities at 72, 79 and 94^oC as a function of time. A similar example for a 50/50 w/w% of EVA40 in H48 kept at 54, 66, 76 and 83^oC is given in Figure 4.18. The results of this procedure have confirmed the cloud point temperature obtained by the usual temperature scanning method.

Repeating these two methods for all the blends of EVA45-CPE3, EVA40-CPE3, EVA45-H48, EVA40-H48, EVA45-H40 and EVA40-H40 gives the cloud point curves of Figures 4.19 to 4.24 respectively.

It was found that increasing the heating rate elevates the apparent cloud point curves. For example, the cloud point of EVA40-CPE3 mixtures for heating rates of 0.2 and 0.5^oC min^{-1} are compared in Figure 4.25. Lower heating rates gives more reliable results.
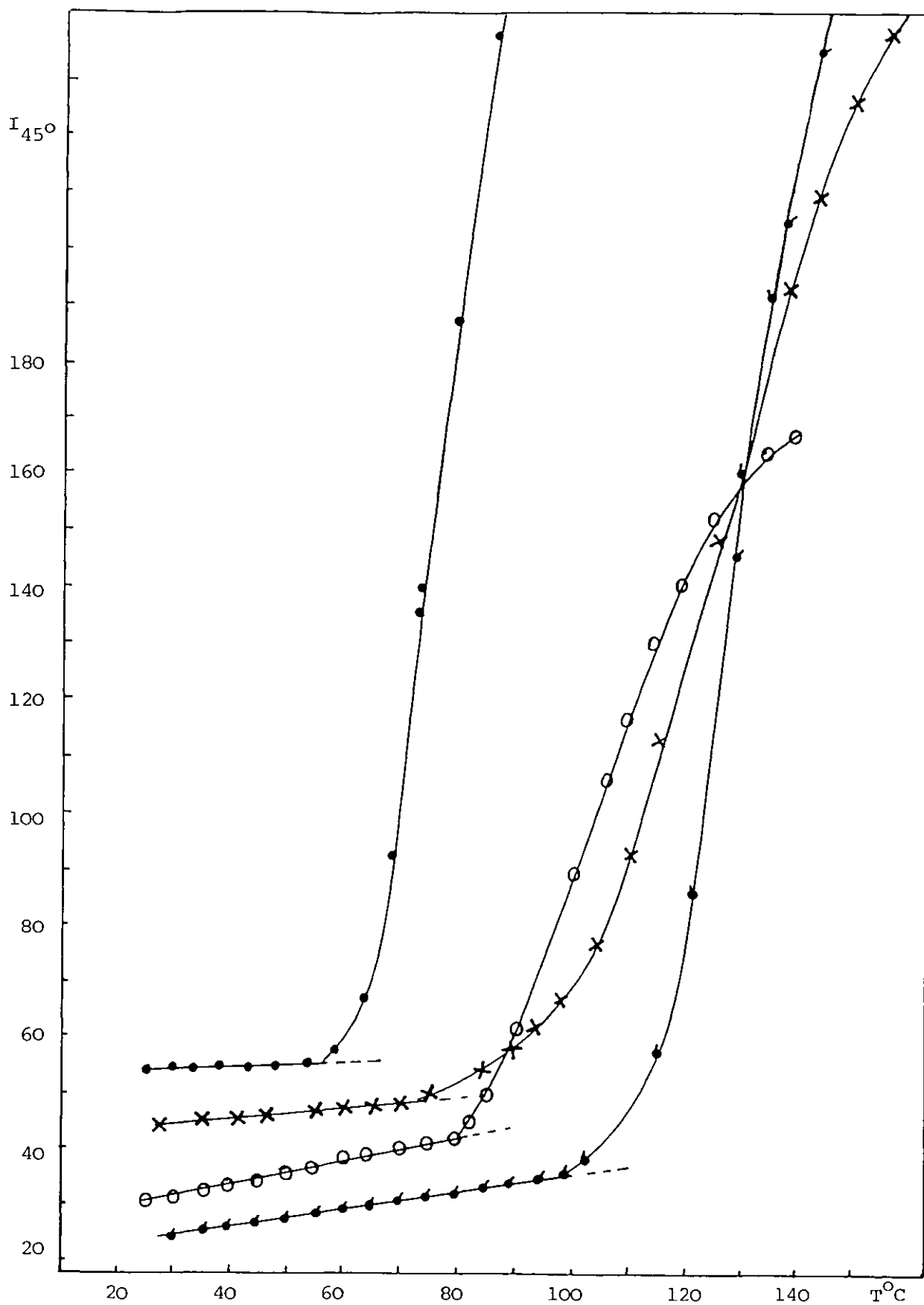
FIG. 4.16. Typical scattering intensities for blends of EVA40-CPE3
as a function of temperature obtained by the turbidimeter.
● 50-50,   ✕ 60-40,   ○ 70-30   and   ♦ 80-20 w/w %
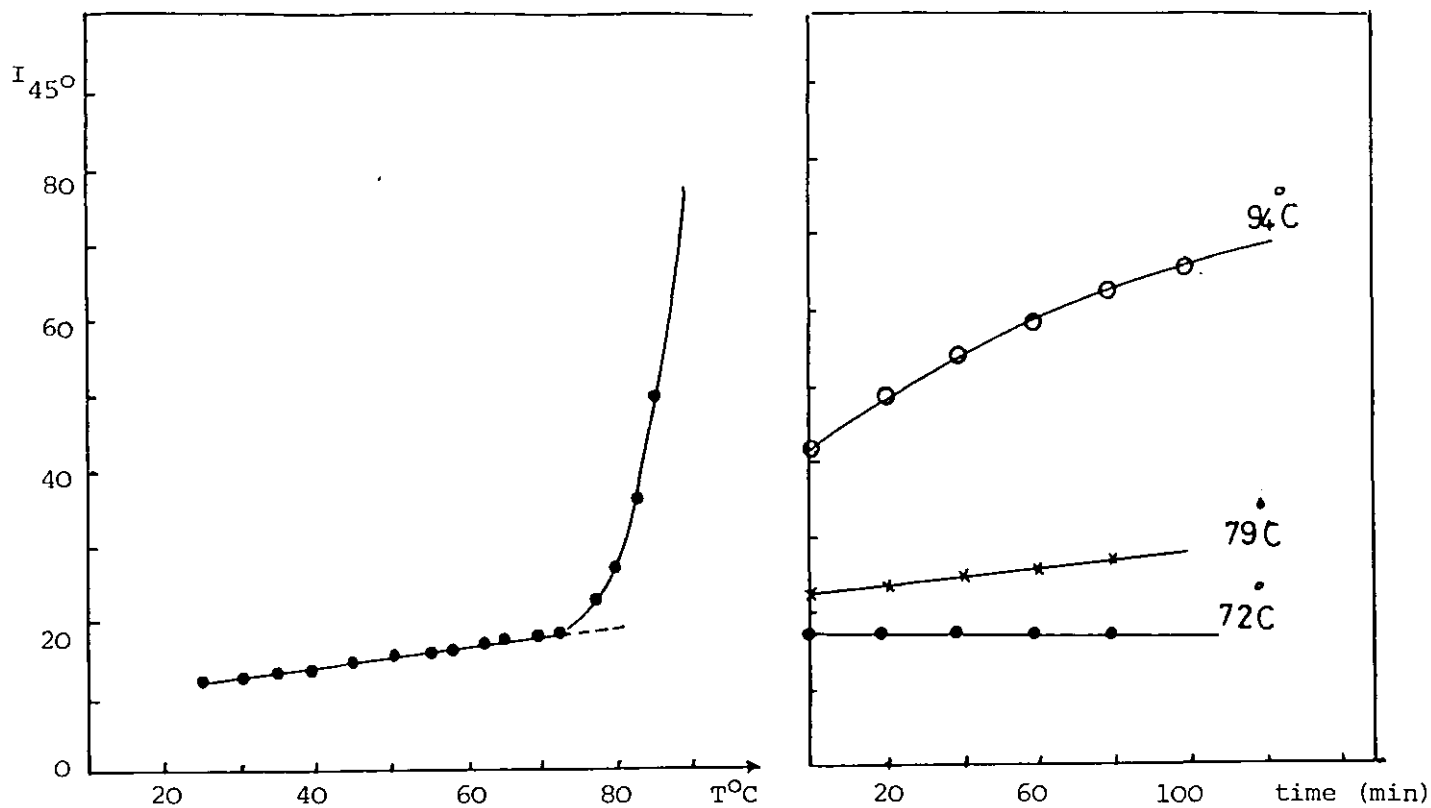
FIG. 4.17. Scattering intensities of EVA40-CPE3 = 35-65 w/w% as a
function of temperature and time.
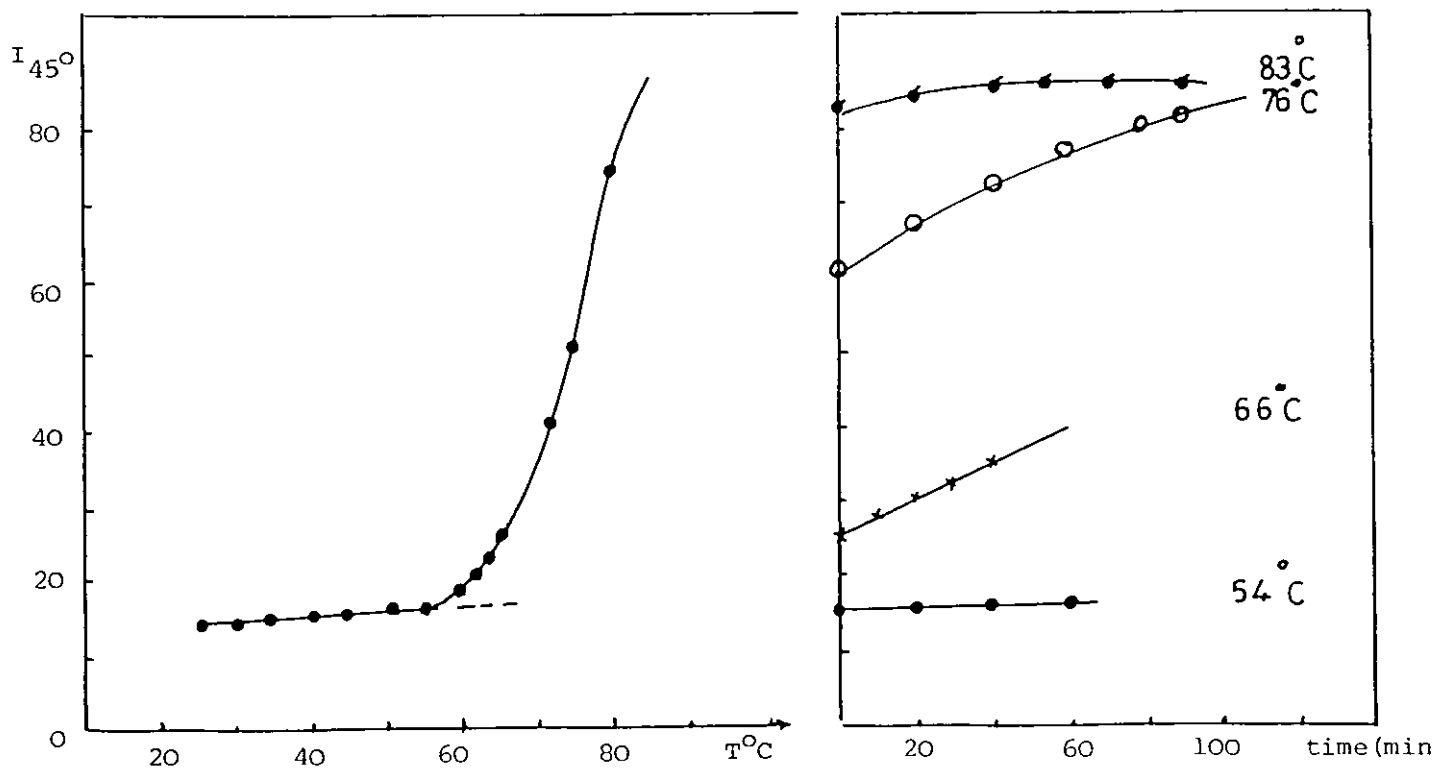
FIG. 4.18. Scattering intensities of EVA40-H48 = 50-50 w/w% as a
function of temperature and time.
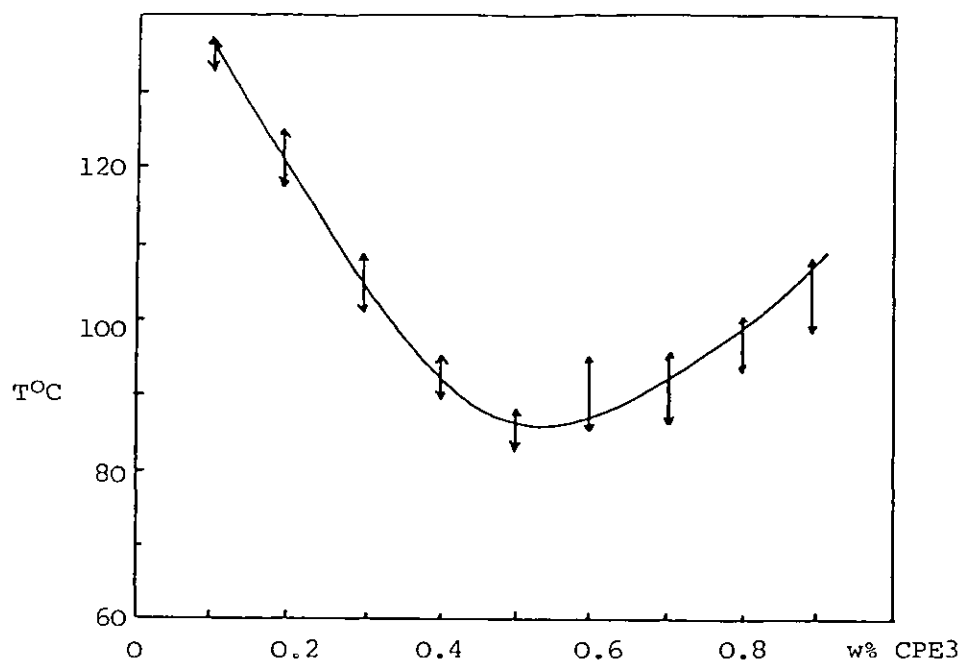
FIG. 4.19. The cloud point curve of the EVA45-CPE3 system.
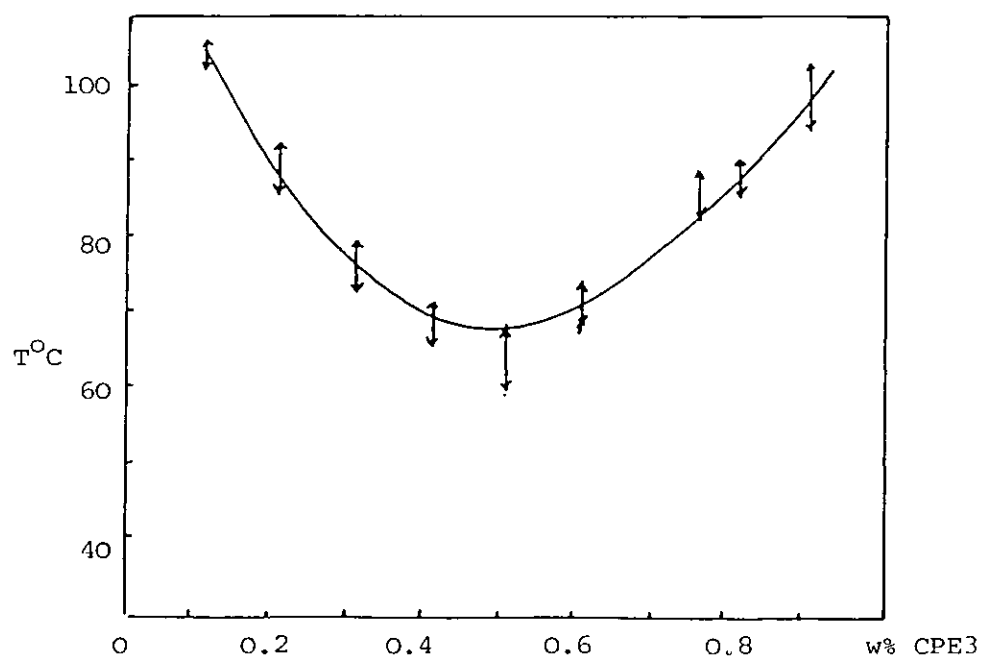
FIG. 4.20. The cloud point curve of the EVA40-CPE3 system.
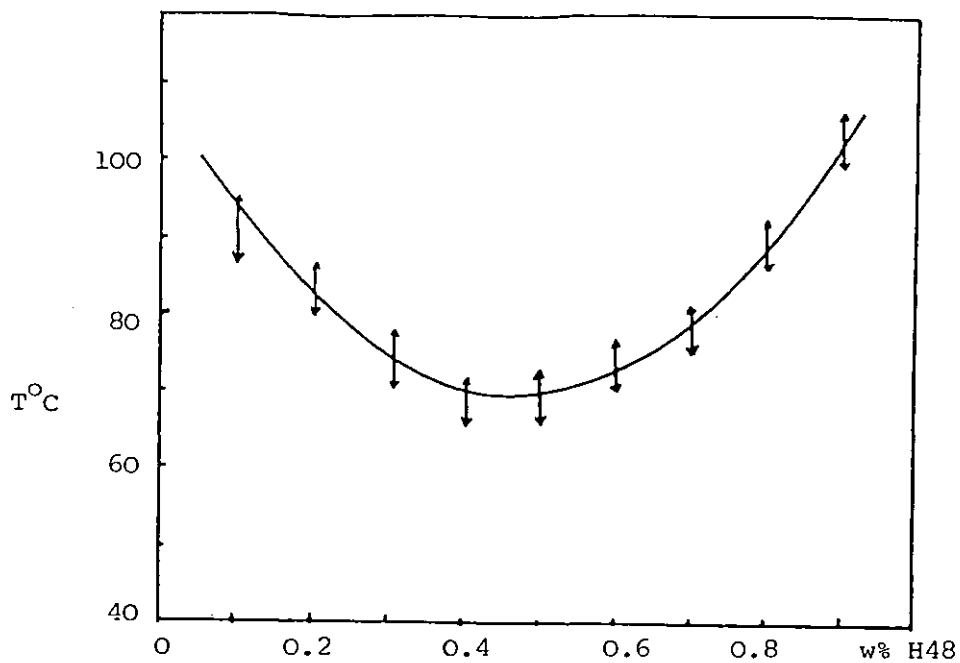
FIG. 4.21. The cloud point curve of the EVA45-H48 system.
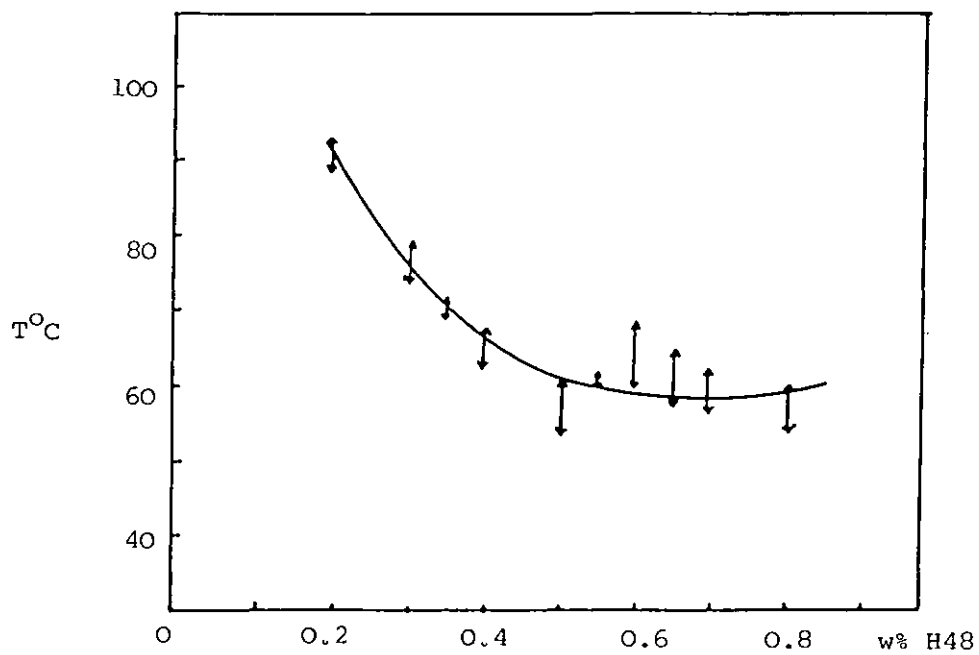
FIG. 4.22. The cloud point curve of the EVA40-H48 system.
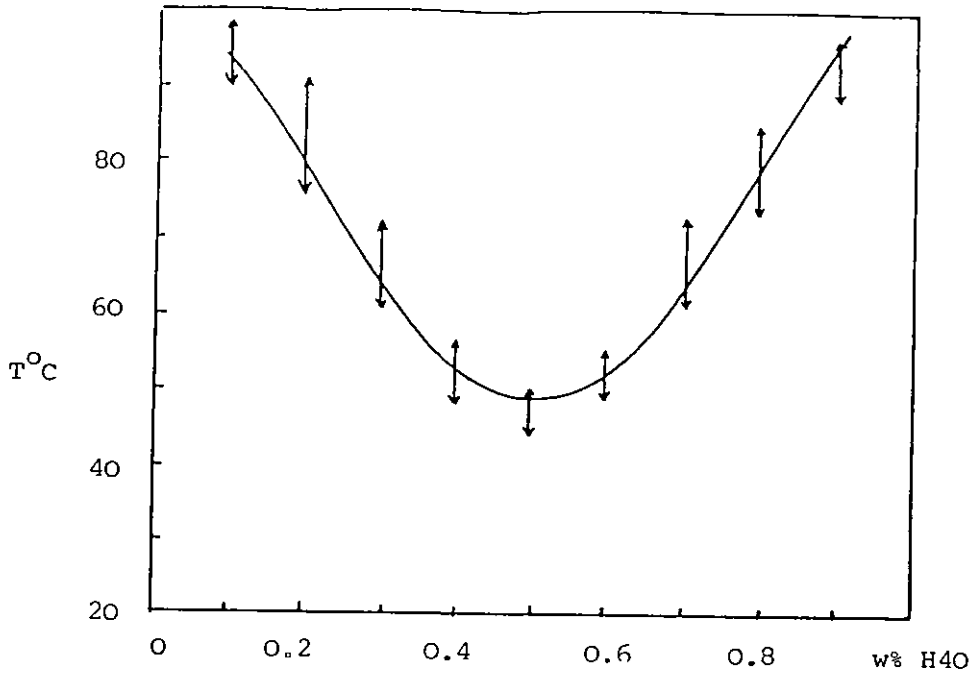
FIG. 4.23. The cloud point curve of the EVA45-H4O system.
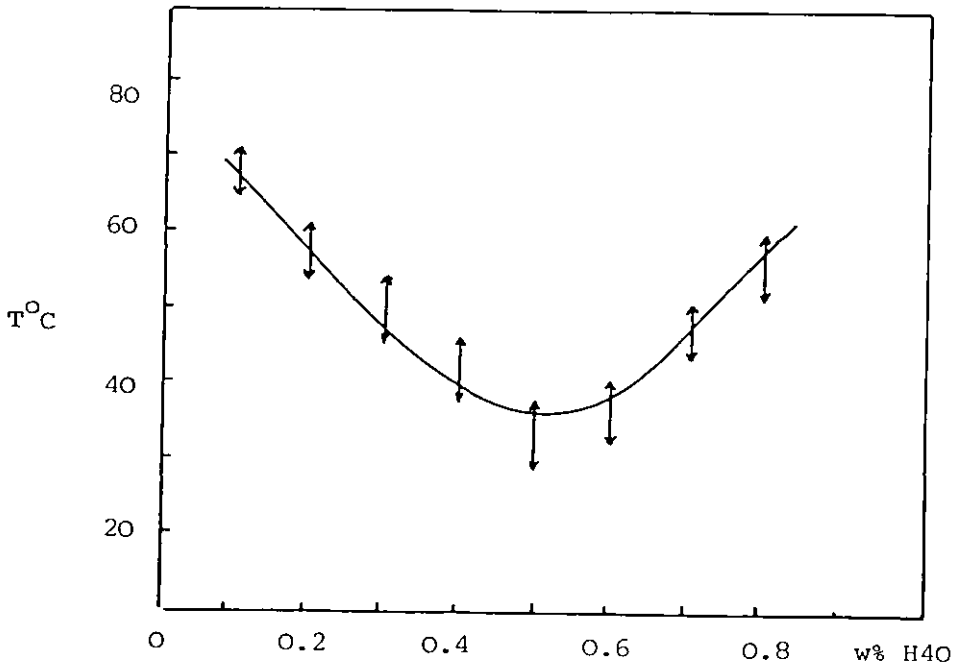
FIG. 4.24. The cloud point curve of the EVA4O-H4O system.

Increasing the degree of chlorination in chlorinated material

and also the amount of acetate in the copolymer increases the

miscibility of the mixtures studied here. This has been summarized

for 50/50 blends in Figure 4.26. This is generally in accordance

with a linear increase in the negative energy of the specific interaction

between chlorinated materials and ester compounds as reported by

Paul (1978). The results of Figure 4.26 indicate that a 1 w% increase

in the chlorine or the acetate raises the cloud point temperature of

the blend by about $2^{\circ}C$. This may not be a general rule for other

compositions as shown in Figure 4.27 for increasing the amount of

acetate and in Figure 4.28 for increasing the degree of chlorination.

All the results presented here are obtained by increasing the

temperature. Reducing the temperature caused the blends to remix when

they were phase separated by a few degrees, ~ 10 $^{\circ}C$, above their cloud

point temperatures. It was found, however, that the blends which were

phase separated at $\sim 50^{\circ}C$ above their cloud point temperatures, did

not remix on cooling within the experimental time scale. This is

presumably due to the reduced mobility of the blends at lower temperature.

4.2   DETERMINATION OF THERMODYNAMIC VARIABLES

4.2.1   Heats of Mixing

The experimental heats of mixing $(J.g^{-1})$ for mixtures of sec-

octyl acetate with both ceroclor 45 and 52 at 64.5, 73.08 and $83.5^{\circ}C$ are

given in Figure 4.29.
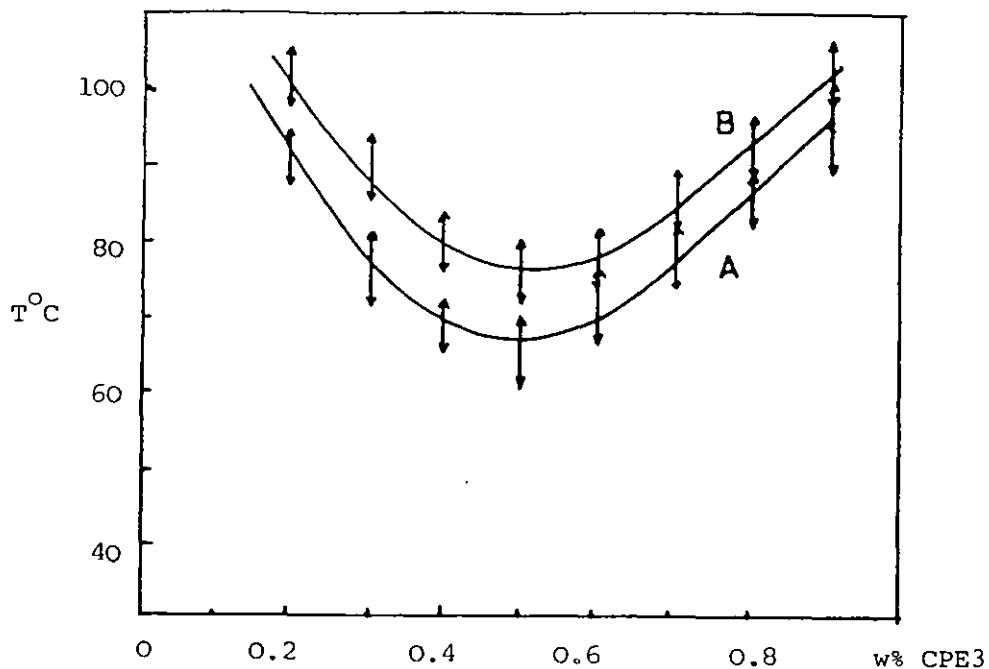
FIG. 4.25. The cloud point curves of the EVA40-CPE3 system for different heating rates.
A. $0.2^{\circ}C.min^{-1}$.   B. $0.5^{\circ}C.min^{-1}$
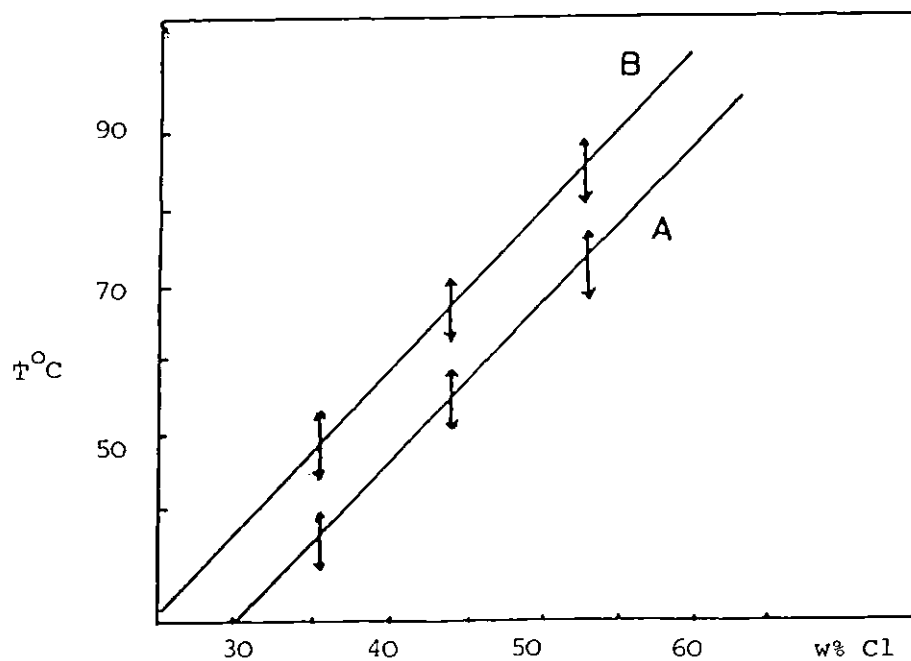
FIG. 4.26. Increases in the cloud point temperature of a 50/50 w/w% blend by increasing the degree of chlorination and the amount of acetate.
A. EVA40   B. EVA45
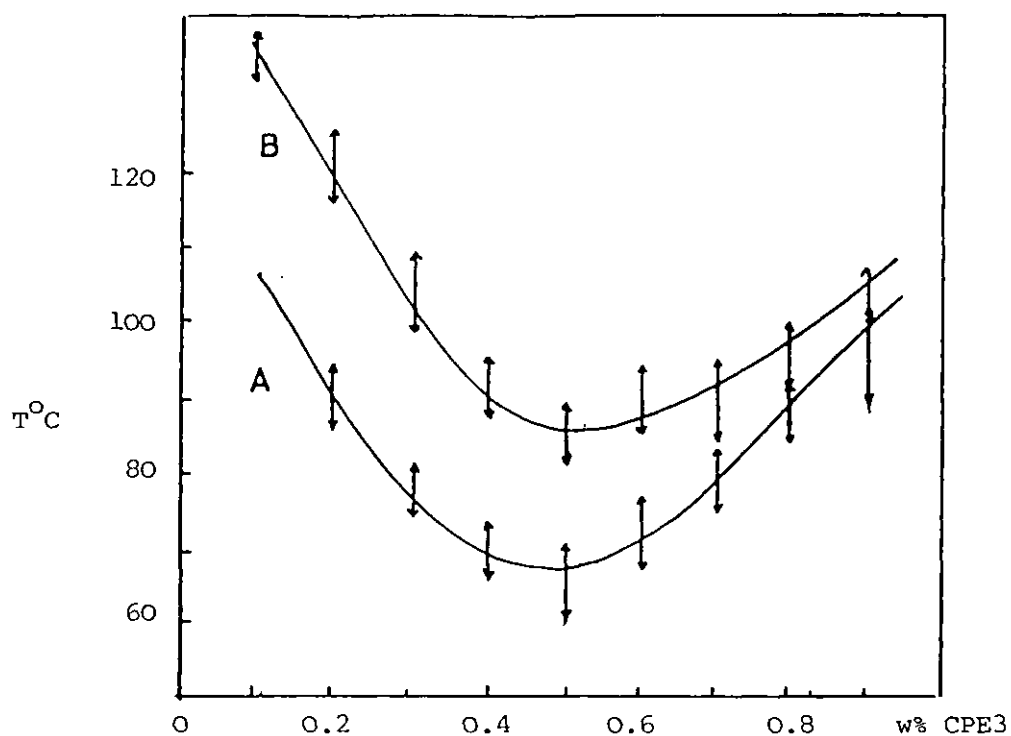
FIG. 4.27. The elevation of the cloud point temperatures by
increasing the amount of acetate. A. EVA40   B.   EVA45
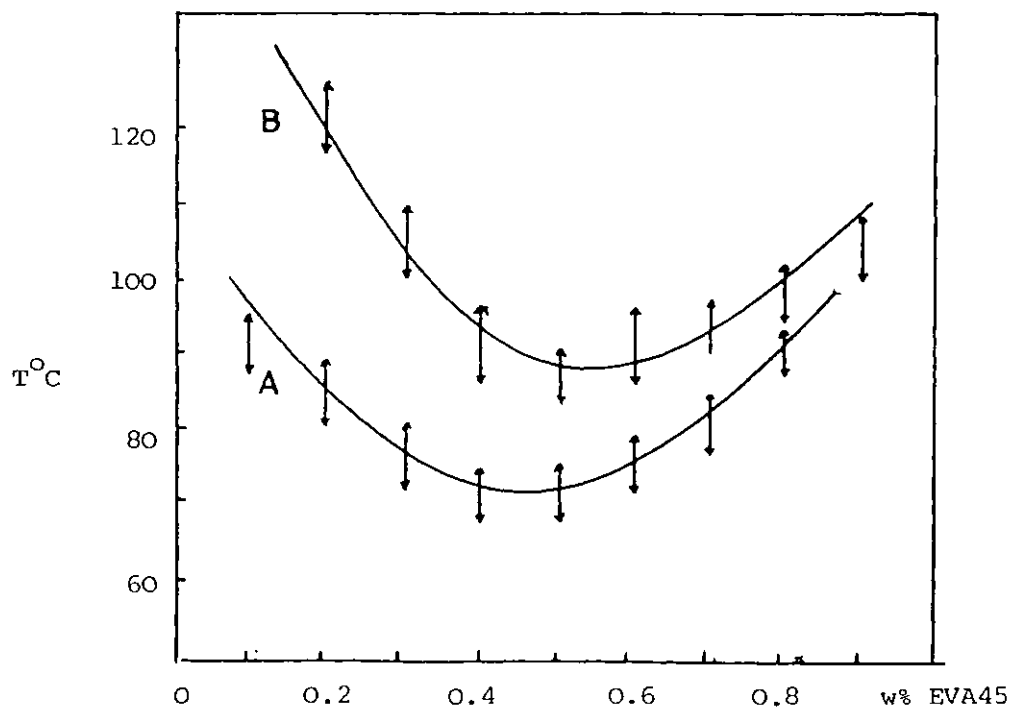
FIG. 4.28. The elevation of the cloud point temperatures by
increasing the degree of chlorination. A. H48,   B.   CPE3

Exothermic heats of mixing were obtained in all cases.

The values are smaller at higher temperatures, but this trend is not

linear with temperature in either case. The mixing of the acetate

with ceroclor 52 is more exothermic than that of ceroclor 45 indicating

a stronger interaction as a result of higher chlorine content. These

results were further used to calculate other thermodynamic parameters

of the mixtures as will be explained in Chapter Five.

4.2.2   Inverse Gas Chromatography

The data, measurements, and the results for the solvent-

polymer interaction parameter for EVA45 and CPE3 for a series of

solvents at 70°C and 100°C, obtained by IGC measurements, are shown

in Tables 4.3 and 4.4 respectively. It can be seen that EVA45 has

the most favourable interaction with an electron acceptor hydrogen-

bonding solvent (chloroform) whereas CPE3 has the most favourable

interactions with electron doner hydrogen-bonding solvents. This

demonstrates the complementary dissimilarity between the two polymers.

Values of Vg_{23}^{o} and the calculated values of $\frac{X_{23}}{V_2}$ for columns

prepared at three different mixture compositions at 70°C and 100°C are

also shown in Tables 4.3 and 4.4 respectively. We have also shown

an average value over all the solvents. The value of $\frac{X_{23}}{V_2}$ should be

independent of solvent probe used but because of effects such as

specific interactions and non-random mixing this is not the case.

The results, however, are similar and show the same general trend with

composition. The estimated error in the measurements of Vg^{o} is between

1.5 to 5%. This translates into an error in X_{12} and X_{13} values

FIG. 4.29. Heats of mixing of sec-octyl acetate and ceroclors at x 64.5, O 73.08 and o 83.5°C. Plotted against weight fraction of ceroclors.

A. Sec-octyl acetate - ceroclor 45
B. Sec-octyl acetate - ceroclor 52

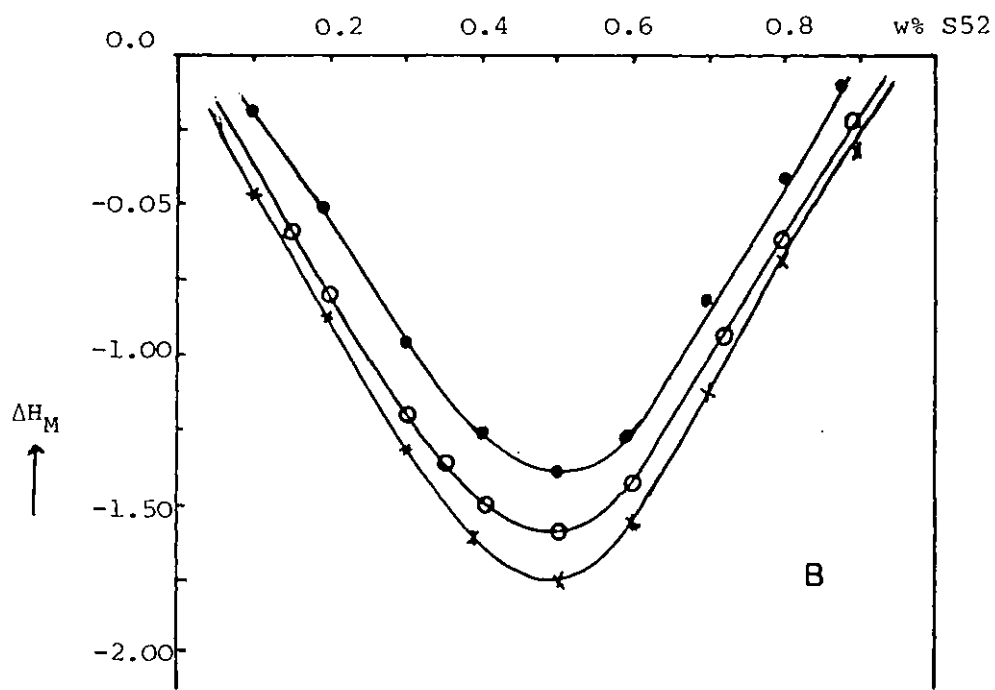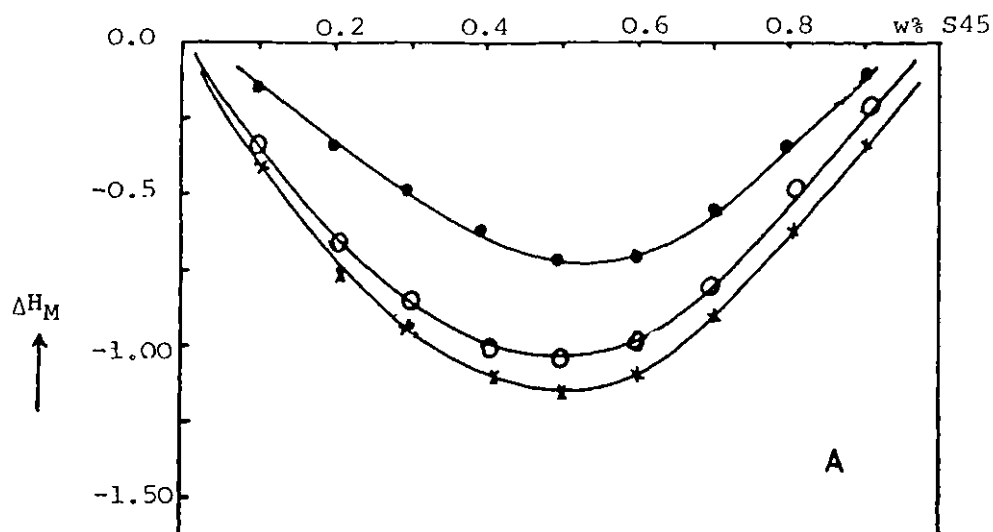| Solvent	P^o_1 (atm)	V_1 *	B_{11} *	EVA 45 $V^o_g(2)$ (cm³/g)	χ_{12}	CPE 3 $V^o_g(3)$ (cm³/g)	χ_{13}	25% w/w CPE 3 $V^o_g(23)$ (cm³/g)	$\frac{\chi_{23}}{V_2}$	50% w/w CPE 3 $V^o_g(23)$ (cm³/g)	$\frac{\chi_{23}}{V_2}$	75% w/w CPE 3 $V^o_g(23)$ (cm³/g)	$\frac{\chi_{23}}{V_2}$
Acetone	1.578	79.204	-1200	16.00	1.548	15.05	1.329	14.56	-.0060	15.00	-.0015	15.64	.0011
Methanol	1.208	42.920	-950	10.01	2.867	5.23	3.236	9.02	.0049	6.00	-.0211	5.973	-.0070
Ethyl acetate	0.785	104.886	-1300	37.37	1.083	23.55	1.265	30.147	-.0063	26.00	-.0060	26.55	-.0010
Tetrahydrofuran	1.145	84.936	-1005	43.25	0.776	34.02	0.737	36.26	-.0089	32.1	-.0089	32.99	-.0058
Diethyl ether	3.032	113.450	-768	10.28	1.000	3.66	1.752	7.58	-.0049	7.2	-.00353	5.878	.0066
Chloroform	1.336	47.625	-860	72.75	0.677	24.34	1.493	52.71	-.0124	37.00	-.0166	32.42	-.0046
n-Pentane	2.788	125.020	-830	8.00	1.237	1.96	2.362	6.07	.0006	4.00	-.0025	4.02	.0107
2-Butanone	.689	95.621	-1508	41.38	1.204	38.20	0.822	35.2	-.0097	30.00	-.0118	32.42	-.0093
Dichloromethane	1.909	40.021	-558	33.37	1.273	13.74	1.881	27.00	-.0355	15.90	-.0356	15.17	-.0201
Average									-.0119		-.0142		-.0079
χ (from ΔH)									-.0022		-.0024		-.0015

Table 4.3 The polymer-solvent interaction parameters and polymer-polymer interaction parameters for

EVA 45, CPE 3 and three of their blends at 70°C.

Solvent	P^o_1 (atm)	V_1 *	B_{11} *	EVA 45 $V^o_g(2)$ (cm³/g)	χ_{12}	CPE 3 $V^o_g(3)$ (cm³/g)	χ_{13}	25% w/w CPE 3 $V^o_g(23)$ (cm³/g)	$\frac{\chi_{23}}{V_2}$	50% w/w CPE 3 $V^o_g(23)$ (cm³/g)	$\frac{\chi_{23}}{V_2}$	75% w/w CPE 3 $V^o_g(23)$ (cm³/g)	$\frac{\chi_{23}}{V_2}$
Acetone	3.606	82.820	-790	8.00	1.7383	6.00	1.7549	8.85	0.0123	6.00	0.0207	4.74	-0.0180
Methanol	3.615	44.820	-543	3.86	3.0889	1.30	3.9060	4.80	0.0610	2.70	0.4982	2.21	0.0294
Ethyl acetate	1.996	110.386	-1030	11.10	1.6865	8.25	1.712	17.00	0.0275	9.00	0.0012	11.50	0.0107
Tetrahydrofuran	2.183	87.209	-780	13.01	1.6607	11.76	1.4906	22.00	0.0391	13.50	0.0042	15.20	0.0126
Diethyl ether	6.388	121.212	-607	3.64	1.6218	1.63	2.1541	5.50	0.0296	3.00	0.0055	2.30	0.0042
Chloroform	3.124	48.946	-690	21.4	1.3960	8.30	2.072	25.70	0.0480	11.90	0.0446	15.00	0.0300
n-Pentane	5.803	133.904	-700	3.00	1.8175	1.00	2.6450	4.00	0.0238	1.90	0.0024	2.01	0.0131
2-Butanone	1.661	98.754	-1100	11.90	1.9023	12.00	1.6228	18.02	0.0262	12.00	0.0006	14.00	0.0078
Dichloromethane	3.190	41.395	-467	9.60	2.3222	4.85	2.7339	11.5	0.0420	6.9	0.0117	10.20	0.0004
Average									.0344		.0108		.0135

Table 4.4 The polymer-solvent interaction parameters and polymer-polymer interaction parameters for

EVA 45, CPE 3 and three of their blends at 100°C. * in cm³ . mol⁻¹

of 1.6 to 6.6%, depending on the total value of Vg^o. This gives an error in $\frac{\chi_{23}}{V_2}$ ranging from $\pm$ 0.001 to $\pm$ 0.005. Values of $\frac{\chi_{23}}{V_2}$ derived from solvent probes such as pentane, methanol and diethyl ether, which give lower retention volumes, are much less reliable.

The results also show less favourable interaction parameters for measurements at higher temperatures as would be expected from the LCST behaviour of the system. A similar temperature dependence of interaction parameter for PS and PVME was observed by Robard and Paterson (1977).

Useful information can be obtained by calculating weight fraction activity coefficients of the solute in the presence of the polymers using Equation 3.28. Such results for EVA45 and CPE3 at 70^oC are given in Table 4.5.

TABLE 4.5

Solvent	EVA45		CPE3	
	$(\frac{a_1}{w_1})^\infty$	$\Delta\bar{H}_1^\infty$ Kcal mol^{-1}	$(\frac{a_1}{w_1})^\infty$	$\Delta\bar{H}_1^\infty$ Kcal mol^{-1}
Acetone	14.85	–	19.80	-1.05
Methanol	56.22	+2.43	166.95	+0.44
Ethyl acetate	12.38	-0.54	16.66	-0.05
Tetrahydrofuran	11.66	-2.97	12.90	-4.09
Diethyl ether	15.16	–	33.99	–
Chloroform	5.44	–	14.02	–
n-Pentane	20.94	+0.11	62.82	+0.92
2-Butanone	16.80	+0.54	16.68	-3.61
Dichloromethane	15.59	–	30.87	+0.54

The calculated values show that the activity coefficients
for solvent-polymer mixtures where no hydrogen-bonds are formed are
generally higher than those of polar solvents, indicating very weak
interaction with the polymers. The solvents, which are proton donors,
have low activity coefficients due to the negative contribution to the
enthalpy of mixing of hydrogen-bond formation. Acetone and butanone
give moderate activity coefficients and the difference in their values
are probably due to difference in molecular shapes. Methanol has
a higher activity coefficient in the presence of these polymers,
because of self association to form dimers. This outweighs the effect
of solvation by hydrogen-bonding.

Another useful quantity is the partial molar heat of mixing
of a probe at infinite dilution in the polymers. This quantity as
defined by Baranyi and Guillet (1977) is

$$\Delta \bar{H}_1 = R \; \delta \ln \; (\; a_1 / \; W_1)^{\infty} / \; \delta(1/T) \qquad\qquad 4.1$$

$\Delta \bar{H}_1^{\infty}$ values obtained from the slopes of the best possible straight
lines through plots of the logarithm of the activity coefficient
versus the reciprocal of the temperature in the range of 70 to 120°C
are also given in Table 4.5. According to these results an
exothermic heat of mixing indicates a strong polymer-solute interaction
whereas an endothermic value indicates repulsive forces between them.
The results also show that EVA45 is insoluble in butanone which was
proved to be correct experimentally.

4.2.3 Volume Change on Mixing

4.2.3.1 Density Measurements of Oligomers

The values of $\dfrac{\Delta V_M}{V^o}$ calculated from the density measurements of

sec-Octyl acetate in ceroclor 52 and ceroclor 45 mixtures, along

with their errors, are given in Figure 4.30. The errors obtained on

repeating the measurements are greater in the regions richer in

ceroclors due to the viscosity and problems of trapped air. The

results show a larger volume reduction for the mixtures containing

ceroclor with higher chlorine content.

The theoretical value of $\dfrac{\Delta V_M}{V^o}$ for sec-octyl acetate in

ceroclor 52 and ceroclor 45, obtained from Equation 2.80, are given

in Appendix C-I. The theoretical value of $\dfrac{\Delta V_M}{V^o}$ for a 50/50 w%

mixture of Oc.Ac-S52 at 64.5°C is -5.30 $\times 10^{-3}$ and that for the same

composition measured experimentally at 25°C is -8.4 $\times 10^{-3}$. For Oc.Ac-S45,

the theoretical value at 64.5°C and experimental value at 25°C are

-4.06 $\times 10^{-3}$ and -5.5 $\times 10^{-3}$ respectively. The agreement here between

experimental and theoretical values is remarkable, provided an allowance

is made for temperature differences.

4.2.3.2 The Results of Cloud Point Measurements Under Pressure

The cloud points obtained for the 50/50 w/w% of EVA45 in

CPE3 investigated under pressure are listed below:
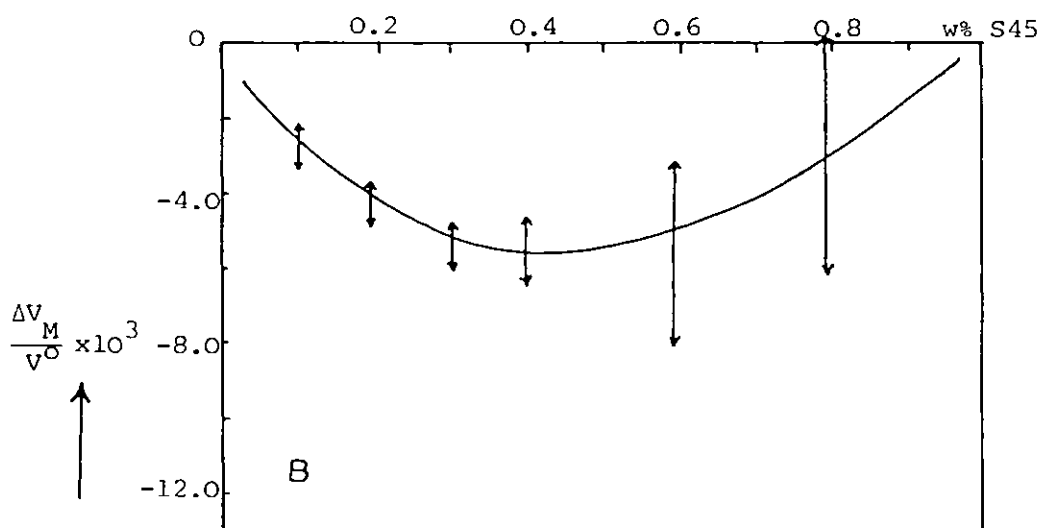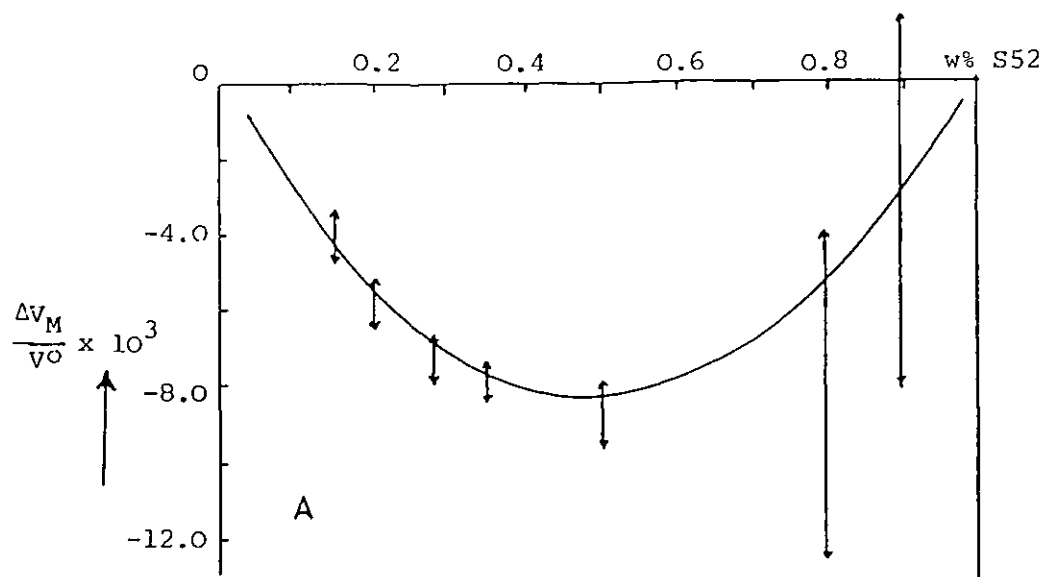
FIG. 4.30. The volume change on mixing for
A. Sec-octyl acetate - S52
B. Sec-octyl acetate - S45
at 25°C.

TABLE 4.6

Pressure atm	Cloud point $^{\circ}C$
1	82.0
300	86.0
450	89.0
550	91.5
750	96.0

The slope of the best fitting line, obtained by a linear regression program, through these points was taken as $(\frac{dT}{dp})_C$, and was found to be 0.0187 deg atm^{-1}. Using the ΔH_M value of the analogue material at 83.5°C (ΔH_M = -1.355 J·cm^{-3} = -13.371 atm) the value of ΔV_M according to Equation 3.35 is ΔV_M = -7.02 x 10^{-4}. This is comparable with the theoretical value of -10 x 10^{-4} at 83.5°C as derived in Section 5.2.4.

Operational difficulties of the pressure apparatus have limited our cloud point investigations to this one system. According to the results of Tripathi (1979) and Saeki et al. (1975, 1976) the pressure will not change the shape of the cloud point curve appreciably, but only shift it to higher or lower temperatures.

CHAPTER FIVE

SIMULATION OF PHASE BOUNDARIES

5.1.1   Application of a Modified Lattice Model

Thermodynamic definitions of the spinodal, binodal and critical conditions were given in Chapter Two. The spinodal and binodal curves and also the critical point of a system can be either (a) defined mathematically as by McMaster (1973) and in the present work, or (b) obtained from the direct iterative construction of double tangents to the ΔG_M curves, as shown in Figure 2.1 and described by Koningsveld et al. (1974A, B). Both these procedures have been used by several workers to simulate the phase boundaries of mixtures. For example, Olabisi (1975) and ten Brinke et al. (1981) have used McMaster's derivations, while Koningsveld and collaborators (1970, 1974 A, B, 1977) have used the iteration method by varying the g function.

Koningsveld et al. (1974B) analysed the spinodal, binodal and phase separation data of polystyrene in cyclohexane using a modification of his previous theory (Koningsveld et al. 1974A). In this extensive treatment, the authors modified the concentration dependence of g for the two extreme cases of dilute and concentrated solutions. Other modified verisions of the g function were used by Kleintjens et al. (1976), Irvine and Gordon (1980) and also in the present work.

One must remember that the treatment of the phase boundaries

of a mixture by this procedure, is based on a specific g function

which contains some approximations. The exact expressions for the

spinodal, binodal and the critical condition of a binary mixture, on

this basis are very complicated due to the variable nature of the g

function. Recently, however, Fujita and Teramoto (1982) have derived

new expressions based on the g function of Koningsveld for phase

boundaries of a ternary mixture. They treated g as concentration,

pressure and temperature dependent, but no numerical applications of

their derivations are given. It is, therefore, difficult to see how

well their treatment fits with experimental observations.

The expressions of Koningsveld et al. for the spinodal,

binodal and critical point are given in several of their papers

(1970, 1971, 1974 A, B). Simpler equations on the same basis are

derived here.

The molecular weight distributions of the polymers are neglected

and the temperature dependence of g is restricted to the first two

terms of Equation 1.5.

$$g = g_1 + g_2/T \qquad\qquad 5.1$$

This is comparable with the assumption about the form of $X = A + \dfrac{B}{RT}$

made by McMaster (1975) and van Aartsen (1970).

In this case the temperature variation of g depends on the

sign of g_2 and hence on the nature of the mixture. When g takes this

form either LCST or UCST behaviour may be predicted, depending upon the

value of g. This equation will not be adequate if both types of

partial miscibility occur simultaneously. In that case the linear

temperature dependence of g becomes predominant (i.e. the third term

of Equation 1.5). Here, we assume no concentration dependance

in the g function and define a critical temperature for a blend

at infinite molecular weight as:

$$T_{c\infty} = -\, g_2 /\, g_1 \ , \ g_2 = T(g - g_1) \qquad\qquad 5.2$$

The other approximation used here is that the ΔG_M relation

will be limited to Equation 2.29. The simplest approach, therefore,

is starting from the spinodal curve as defined by relation 2.31.

Application of this condition to Equation 2.29 gives:

$$\frac{\partial^2}{\partial \phi_2^{\,2}} \left(\frac{\Delta G_M}{RT} \right) = \left(\frac{1}{m_1\phi_1} + \frac{1}{m_2\phi_2} \right) - 2g = 0$$

$$= \left(\frac{1}{m_1\phi_1} + \frac{1}{m_2\phi_2} \right)_{SP} - 2 \left(g_1 + \frac{g_2}{T_{SP}} \right) \doteq 0 \qquad 5.3$$

where the subscript SP stands for spinodal. The rearrangement of this

equation for T_{SP} when g_2 is substituted from Equation 5.2 gives:

$$\frac{1}{T_{SP}} = \frac{1}{T_{c\infty}} \left\{ 1 - \frac{1}{2g_1} \left(\frac{1}{\phi_1 m_1} + \frac{1}{\phi_2 m_2} \right)_{SP} \right\} \qquad 5.4$$

where the terms have their normal meaning as given before. The $T_{c\infty}$

and consolute temperature, T_c, of a mixture may also be related by

application of the critical condition to Equation 2.29, where

$$\frac{\partial^3}{\partial \phi_2^{\,3}} \left(\frac{\Delta G_M}{RT} \right) = \left(\frac{1}{m_1\phi_1^{\,2}} - \frac{1}{m_2\phi_2^{\,2}} \right)_c = 0 \qquad\qquad 5.5$$

or

$$\phi_{2,c} = \frac{1}{1+\left(\dfrac{m_2}{m_1} \right)^{1/2}} \ , \ \phi_{1,c} = \frac{1}{1+\left(\dfrac{m_1}{m_2} \right)^{1/2}} \qquad 5.6$$

Substitution of $\phi_{1,c}$ and $\phi_{2,c}$ in Equation 5.4 gives:

$$\frac{1}{T_c} = \frac{1}{T_{c\infty}} \{ 1 - \frac{1}{2g_1} \ (m_1^{-\frac{1}{2}} + m_2^{-\frac{1}{2}})_c^2 \ \} \qquad 5.7$$

From these considerations the magnitude of g at the critical condition is:

$$g_c = \frac{1}{2} \ (m_1^{-\frac{1}{2}} + m_2^{-\frac{1}{2}})_c^2 \qquad 5.8$$

the position of which is given by Equation 5.6. In the present treatment as in the Flory-Huggins lattice model, the position of the critical point depends on $|m_2 - m_1|$. For $m_2 = m_1$, $\phi_{2,c} = 0.5$ and for $m_2 > m_1$, $\phi_{2,c}$ will be less than 0.5 and vice versa. In the extreme case of a solvent-polymer mixture, $\phi_{2,c}$ tends to zero as m_2 goes to infinity.

At the binodal condition the phases are separated but still in equilibrium. To work out the binodal temperature and composition, the chemical potential difference between each species in the mixture and their standard chemical potential will be set equal in each phase. At the equilibrium boundaries

$$(\mu_1 - \mu_1^{\ O})_A = (\mu_1' - \mu_1'^{\ O})_B \qquad 5.9$$

and

$$(\mu_2 - \mu_2^{\ O})_A = (\mu_2' - \mu_2'^{\ O})_B \qquad 5.10$$

where the subscripts A and B refer to thermodynamically homogeneous and inhomogeneous phases respectively. The chemical potential of species one in the mixture is given by:

$$\frac{\Delta \mu_1}{RT} = \ln\phi_1 + (1 - \frac{m_1}{m_2}) \ \phi_2 + m_1 g \phi_2^2 \qquad 5.11$$

Application of the relation 5.9 to the chemical potential of species

one in both phases gives:

$$\ln \frac{\phi_1}{\phi_2} + (1 - \frac{m_1}{m_2}) \cdot (\phi_2 - \phi'_2) = m_1 g (\phi'_2{}^2 - \phi_2{}^2) \qquad 5.12$$

A similar procedure for species two gives:

$$\ln \frac{\phi_1}{\phi_2} + (1 - \frac{m_1}{m_2}) (\phi_1 - \phi'_1) = m_2 g (\phi'_1{}^2 - \phi_1{}^2) \qquad 5.13$$

Equation 5.12 is multiplied by $1/m_1$ and Equation 5.13 is multiplied by

$1/m_2$. Subtracting these two   equations from each other gives:

$$\frac{1}{m_2} \ln \frac{\phi_2}{\phi'_2} - \frac{1}{m_1} \ln \frac{\phi_1}{\phi'_1} = 2g (\phi_2 - \phi'_2) \qquad 5.14$$

where $\phi_1 + \phi_2 = 1$ and $\phi'_1 + \phi'_2 = 1$. Introducing $T_{c\infty}$ in Equation 5.2

and rearranging for the binodal temperature, T_{bn}, gives

$$\frac{1}{T_{bn}} = \frac{1}{T_{c\infty}} \{ (1 - \frac{1}{2g_1} \cdot \frac{1}{(\phi_2 - \phi'_2)}) (\frac{1}{m_2} \ln \frac{\phi_2}{\phi'_2} - \frac{1}{m_1} \ln \frac{\phi_1}{\phi'_1}) \}$$

$$5.15$$

In numerical applications of these equations the g function can

be obtained (a) from the conditions of Equations 5.12 or 5.13 where

ϕ_1, ϕ_2, ϕ'_1 and ϕ'_2 are known from the cloud point curve of the mixture.

(b) From different experimental measurements such as, I.G.C., vapour

pressures of absorbed solvents, etc. An alternative way of finding g

is by plotting $\frac{1}{T_c}$ versus $(\frac{1}{m_1^{1/2}} + \frac{1}{m_2^{1/2}})_c^2$ for a series of molecular

weights. The slope of the plot provides g_1 and g_2 may be estimated

from the energy of interaction between the pairs. The ratio between

m_1 and m_2 is important although their precise values are not critical.

The values used in this work are 600 and 650 respectively. The g value

for a 50/50 w% blend of EVA45-CPE3 at 86°C was obtained by a

linear interpolation of the I.G.C. results at 70 and 100°C as given

in Tables 4.3 and 4.4. This was found to give g = +0.000207 which was

used without any alteration for other compositions of the mixture. The

simulated spinodal and binodal for EVA45-CPE3 blends using the equations

derived above, are shown in Figure 5.1A. The critical point is also

shown on the graph.

The overall agreement between the calculated spinodal, binodal

and critical point and the experimental cloud point is satisfactory,

but, the metastable region between spinodal and the binodal is

narrower than expected and the simulated curves are more symmetrical

than the experimental cloud point curves. Decreasing g_1 from 0.5 to

a lower value shifts the phase boundaries to a higher temperature.

This is shown in Figure 5.1B for g_1 = 0.1. Multiplying m_1 and m_2 by

a factor of two, lowers the phase boundaries by about 2 degrees.

Altering g, however, can change the position and the shapes of

phase boundaries considerably.

The value of g obtained by fitting Equations 5.12 and 5.13 to

the experimental cloud point curve given in Figure 4.19 was also used

to simulate the spinodal and the binodal curves and to compute T_c and

ϕ_{2c}. This is a simpler way to find the position and the shape of the

spinodal relative to the binodal curve. Examples of the results

obtained by this procedure for g_1 = 0.5 and g_1 = 0.1 are given in

Figures 5.2A and B. The main disadvantage of the latter method is in

attributing a value obtained from the cloud point to g which means that

the other mathematical equations   follow the experimental cloud

point curve.

FIG. 5.1. Theoretical x spinodal, o binodal and critical point calculated for EVA45-CPE3 mixtures according to a modified lattice model given in the text , Plotted against volume fraction of CPE3. g is taken from I.G.C. results.

A. $g = +0.000207$ $g_1 = 0.5$ $\phi_{2,c} = 0.4899$ $T_c = 358.1^{\circ}K$
B. $g = +0.000207$ $g_1 = 0.1$ $\phi_{2,c} = 0.4899$ $T_c = 370.4^{\circ}K$

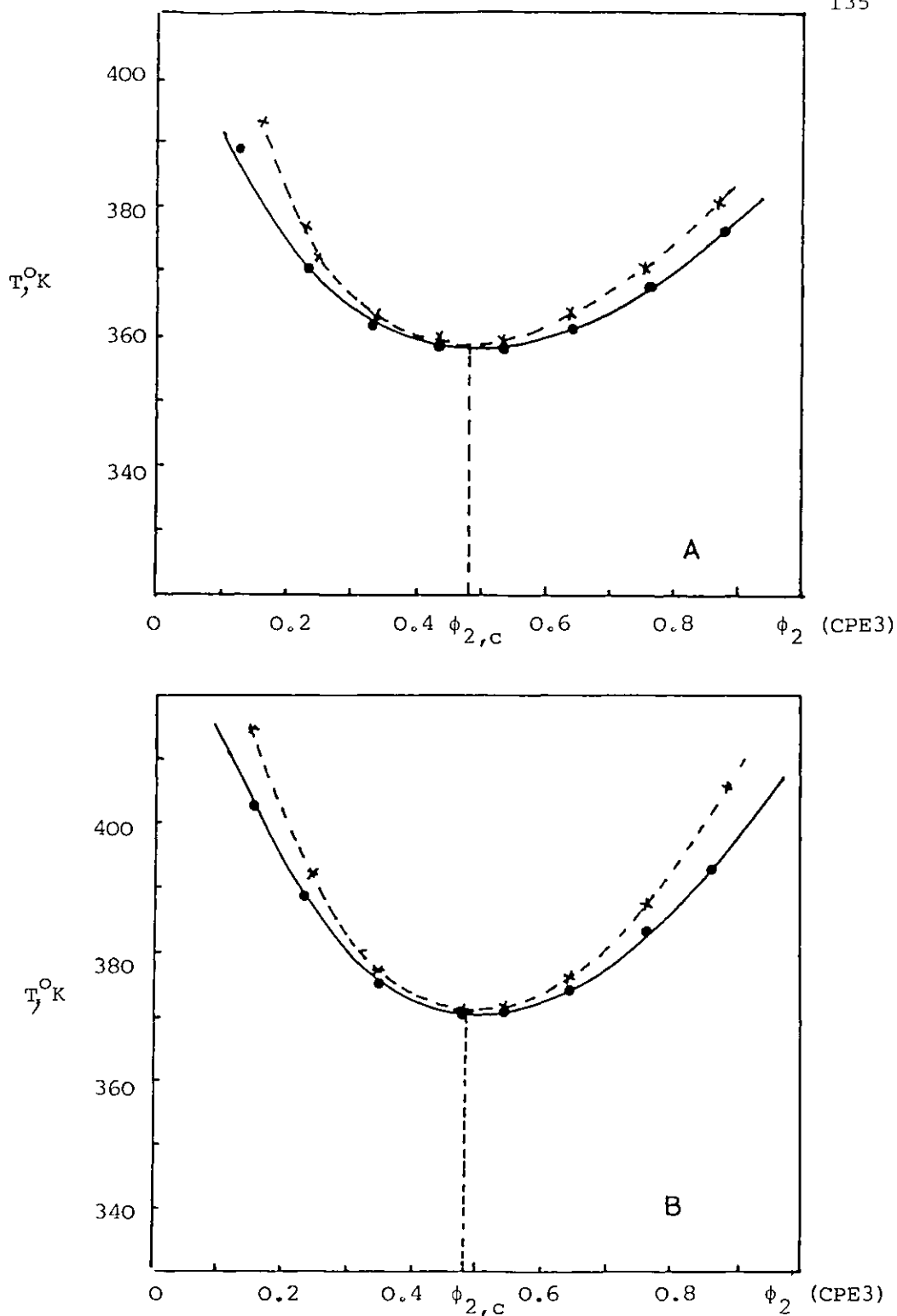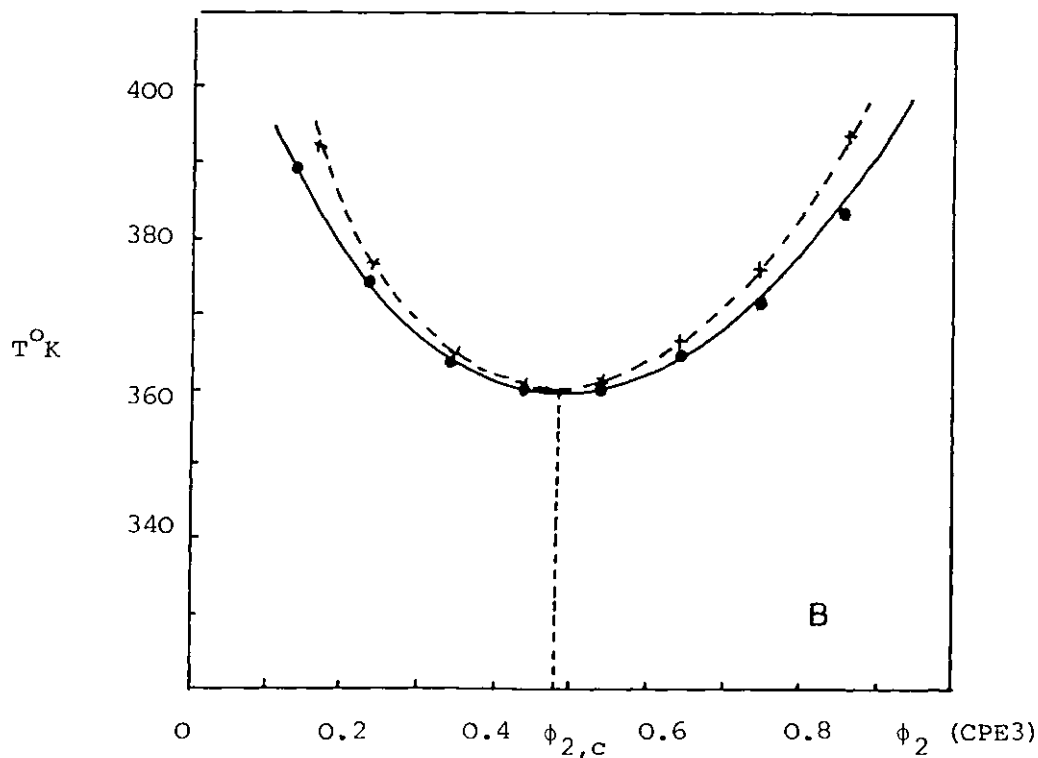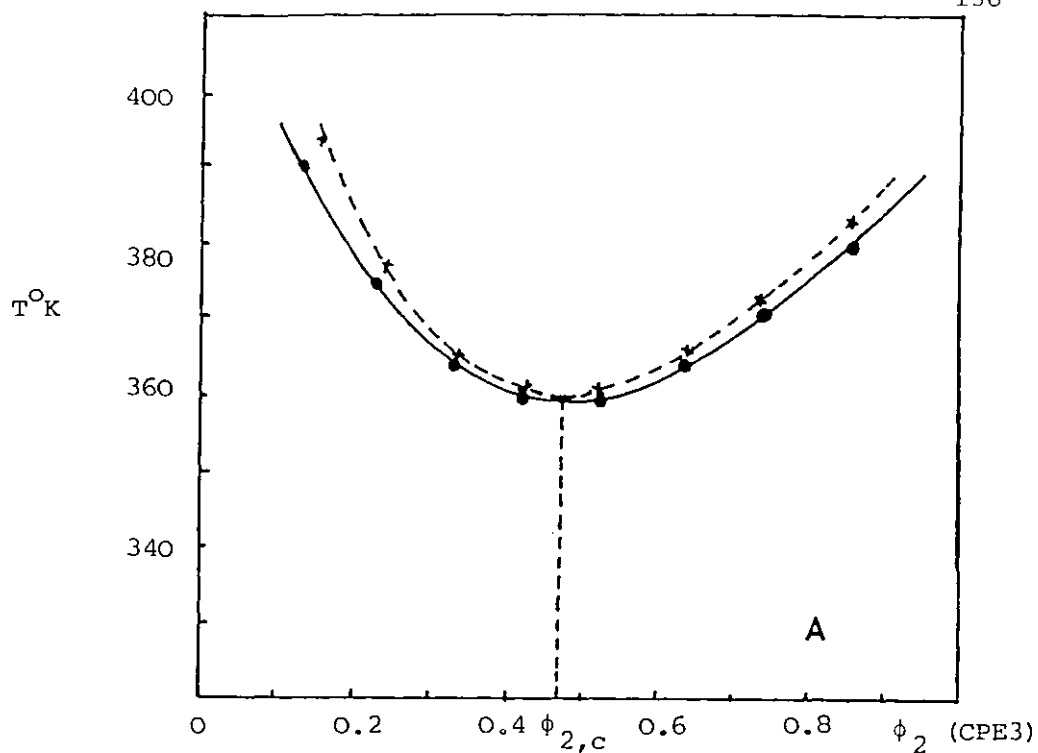FIG. 5.2. Theoretical x spinodal, o binodal and critical point
calculated for EVA45-CPE3 mixtures according to a modified
lattice model described in the text. Plotted against
volume fraction of CPE3. The g values were calculated
from $\Delta\mu_{1A} = \Delta\mu_{2B}$ condition.

A. $g_1 = 0.5$ $\phi_{2,c} = 0.4899$ $T_c = 359.2$

B. $g_1 = 0.1$ $\phi_{2,c} = 0.4899$ $T_c = 359.2$

These simple equations, however, can be used if the equation

of state parameters of a system are not known.

5.1.2   The Koningsveld Interaction Parameter

Scott in 1949, and Tompa in 1956 formulated the Flory-

Huggins free energy expression for ternary systems in order to take

into account the polydispersity of polymers. This formulation was

slightly modified by Koningsveld et al. (1974A) who introduced a semi-

empirical correction term, Γ, in order to quantify the interactions

in a binary mixture. Assuming no chain branching, for blends of two

homopolymers, the free energy equation of Koningsveld et al. can be

written as:

$$\frac{\Delta G_M}{RT} = \Sigma \frac{\phi_{1,i}}{m_{1,i}} \ln \phi_{1,i} + \Sigma \frac{\phi_{2,i}}{m_{2,J}} \ln \phi_{2,j} + \Gamma(\phi_2, T, P) \qquad 5.16$$

where ΔG_M is the Gibbs free energy change on mixing per mole of lattice

sites, $\phi_{1,i}$ and $\phi_{2,J}$ are the volume fractions of molecular species i in

polymer one and J that in polymer two, and $m_{1,i}$ and $m_{2,J}$ their

respective chain lengths expressed as the number of lattice sites they

occupy. RT has the usual meaning, P stands for pressure. The semi-

empirical correction term as a function of an interaction term may be

written as:

$$\Gamma = g(\phi_2, T, P)\phi_1\phi_2 \qquad 5.17$$

where ϕ_1 and ϕ_2 are the volume fractions of the polymers. The

concentration, temperature, and pressure dependence of g is given by:

$$g = \sum_{k=0}^{n} g_k \phi^k \qquad 5.18$$

$$\{g = g_{k,1} + g_{k,2}/T + g_{k,3}T + g_{k,4}\ln T \qquad 1.5\}$$

$$\{\partial \, (\Delta G_M/RT)/\partial P\}_T \;\; = \;\; \Delta V_M \;\; = \;\; \phi_1 \phi_2 \, (\partial g/\partial P)_T \qquad\qquad 5.19$$

For further calculations, it is convenient to retain the first two terms of Equation 1.5, where increasing the temperature causes g to decrease or increase depending on the sign of $g_{k,2}$. The results do not lose their general qualitative validity by this limitation, which considerably facilitates calculation of the g parameters. Introducing these assumptions in Equation 5.16, for monodisperse polymers yields:

$$\{\frac{\Delta G_M}{RT} = \frac{\phi_1}{m_1} \ln \Phi_1 \; + \frac{\phi_2}{m_2} \ln \Phi_2 + g \, \phi_1 \phi_2 \qquad\qquad 2.29\}$$

This is the simplest equation frequently used by Koningsveld et al. to estimate the stability of binary mixtures (e.g. see Koningsveld et al. 1980 and Kleintjens et al., 1980). It is worth noting that g will be equal to g_{12} when there are no vacancies in the lattice, i.e. g_{01} etc. are zero.

$$g\phi_1\phi_2 = \phi_O \ln \phi_o + g_{01} \, \phi_O \, \phi_1 + g_{02}\phi_O \, \phi_2 + g_{12} \, \phi_1 \, \phi_2 \qquad\qquad 5.20$$

where ϕ_O is the volume fraction of vacancies and g_{01}, g_{02} and g_{12} are the interaction terms for the ternary system.

A value for g_{12} can be estimated from the molar heat of mixing of oligomeric analogues using Equation 5.21.

$$\frac{\Delta H_M \, (J.mol^{-1})}{RT \; (J.mol^{-1})} \;\; = g_{12}\Phi_1 \; \Phi_2 \qquad\qquad 5.21$$

In order to facilitate calculations of g_{12} and ΔG_M the heats of mixing of oligomeric materials reported in Section 4.2.1 were normalized per mole of sec-octyl acetate. The g_{12} values thus obtained for the mixtures of the acetate and ceroclor 52 and 45 at temperatures

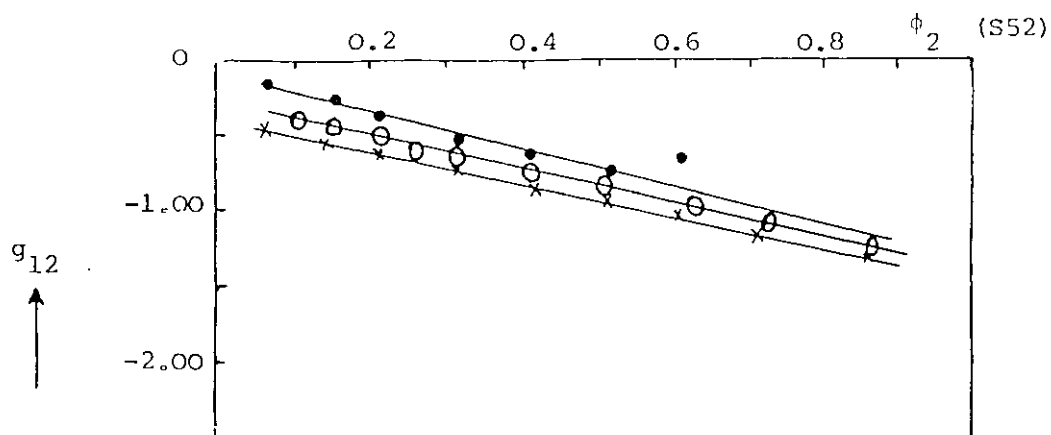FIG. 5.3. The Koningsveld g_{12} function calculated from the heat of mixing of sec-octyl acetate in S52 plotted against volume fraction of S52 at temperatures, x 64.5, o 73.08 and •83.5°C.
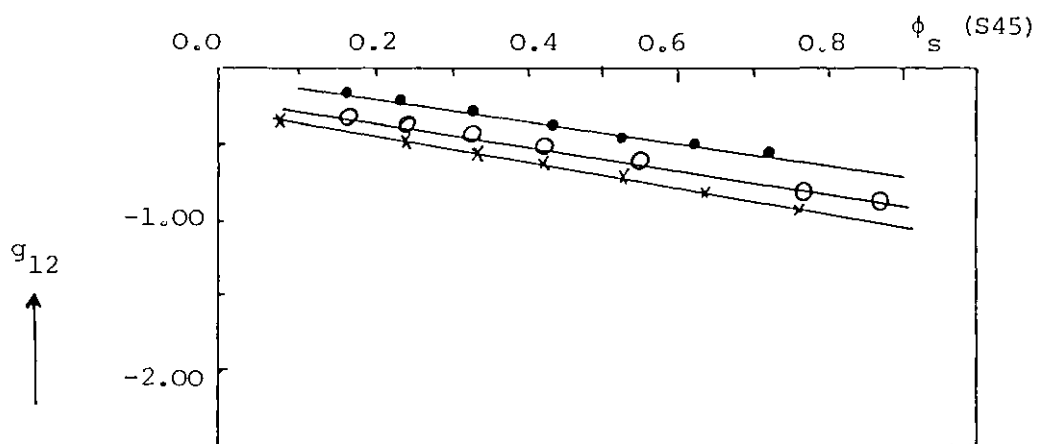

FIG. 5.4. The Koningsveld g_{12} function calculated from the heat of mixing of sec-octyl acetate in S45 plotted against volume fraction of S45 at temperatures, x 64.5, o 73.08 and •83.5°C.

of 64.5, 73.08 and 83.5°C are presented in Figures 5.3 and 5.4

respectively. It is important to note that the g_{12} function is negative

and decreases in size as temperature increases and increases in size as the

concentration of ceroclor increases. This implies that the existing

specific interaction between these two points is weaker at higher temp-

eratures and lower concentrations of chlorinated materials. The linear

concentration dependence of g_{12} has also been observed by Koningsveld

(1970) for mixtures of polystyrene with cyclohexane.

The values of $\dfrac{\Delta G_M}{RT}$ may be calculated from the g_{12} function

given in Figures 5.3 and 5.4 by using Equation 2.29 for the mixtures

at given temperatures. In this calculation m_1 is assumed to be 172

for sec-octyl acetate and m_2 to be 437 or 395 for S52 or S45 respect-

ively. The Gibbs free energies of these mixtures calculated in this

manner are presented in Figures 5.5 and 5.6. These figures show that

the free energy change on mixing of these mixtures decreases as the

temperature increases and furthermore that no region of instability is

observed by this treatment.

In order to estimate the thermodynamic quantities of the

EVA45-CPE3 blends the above procedures have been extended to cover

the temperature behaviour of this mixture. The g function was obtained

(a) from the I.G.C. results as presented in Section 4.2.2, (b) from

fitting the theoretical binodal equation into the cloud point curve

of the mixture as explained in Section 5.1.1. Calculated values of

$\dfrac{\Delta G_M}{RT}$ at 70°C for EVA45-CPE3, where m_1 = 600 and m_2 = 650 and g values

from I.G.C. are shown in Figures 5.7. The values of m_1 and m_2 are

assumed to be equivalent to the number of lattice sites which the

polymer chains occupy. The $\dfrac{\Delta \mu_1}{RT}$ values of this mixture calculated from

Equation 5.11 are presented in Figure 5.8.
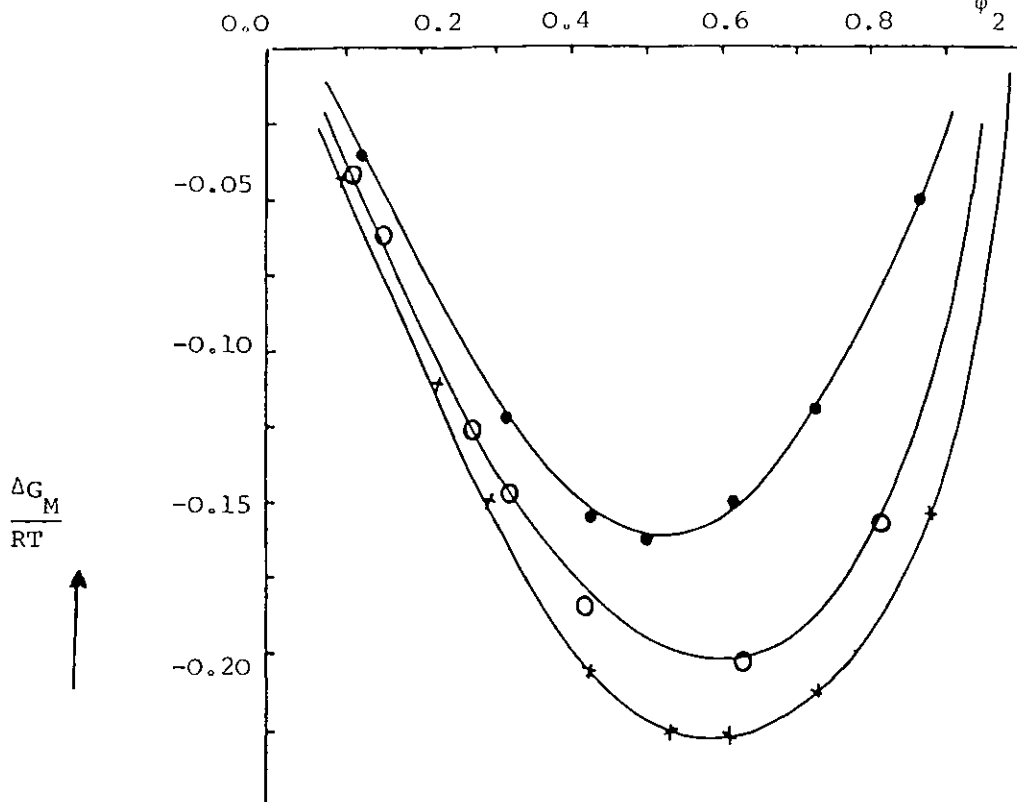
FIG. 5.5. The Gibbs free energy of sec-octyl acetate and S52 mixtures plotted against volume fraction of S52 at temperatures of x 64.5, o 73.08 and ● 83.5°C.
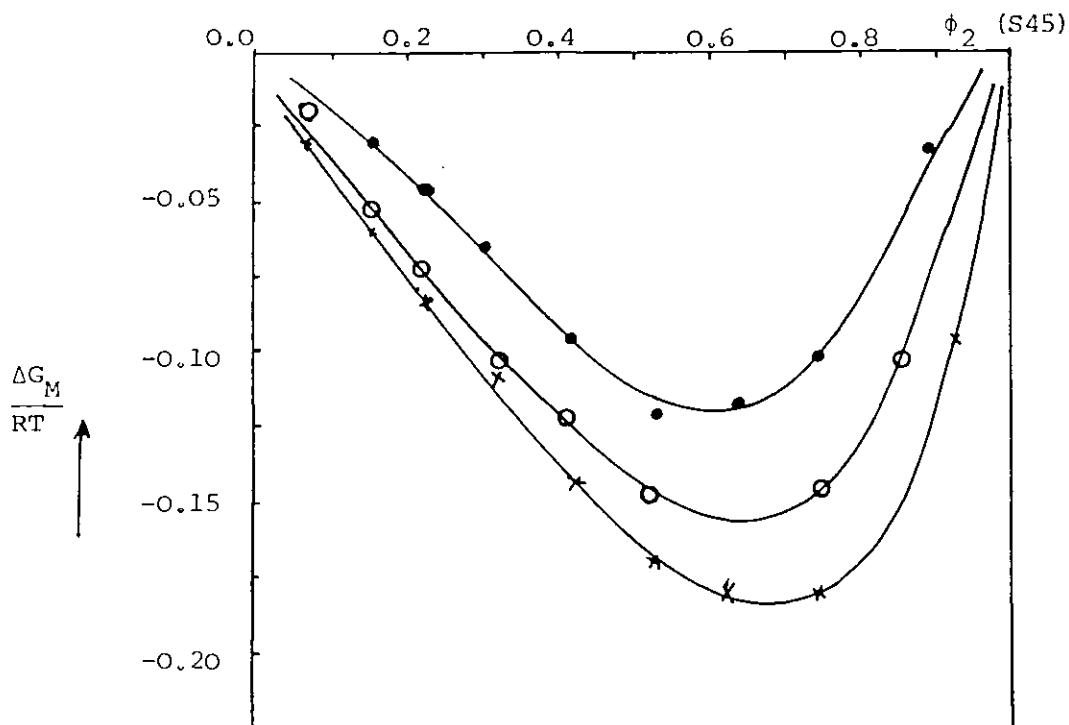
FIG. 5.6. The Gibbs free energy of sec-octyl acetate and S45 mixtures plotted against volume fraction of S45 at temperatures of x 64.5, o 73.08 and ● 83.5°C.
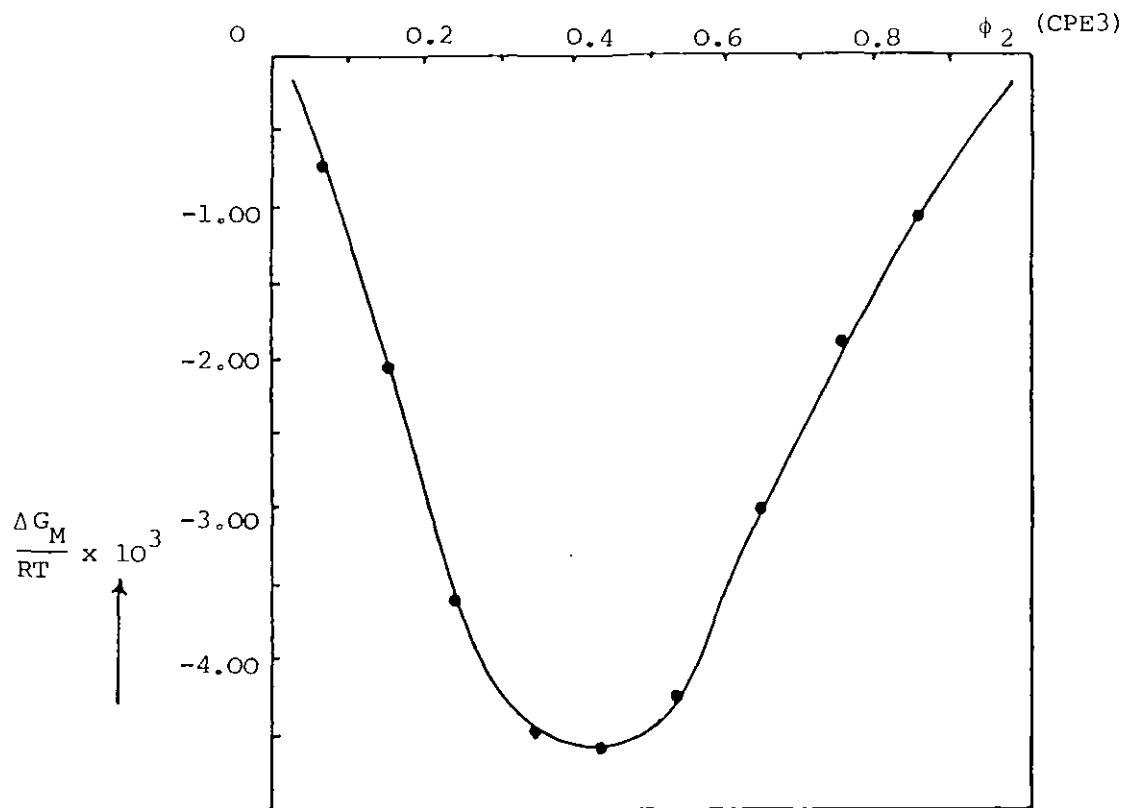
FIG. 5.7. The Gibbs free energy of the EVA45-CPE3 system at $70^{\circ}C$ plotted against volume fraction of CPE3. The g value was taken from the IGC results.

FIG. 5.8. The chemical potential of EVA45 in the mixtures of EVA45-CPE3 at $70^{\circ}C$. Plotted against volume fraction of CPE3. The g value was taken from the IGC results.

No region of instability is observed at this temperature

in either case. This is in agreement with experimental results,

whereas at $100^{\circ}C$, both $\dfrac{\Delta G_M}{RT}$ and $\dfrac{\Delta \mu_1}{RT}$ show an unstable region between

$0.3 \leqslant \phi_2 \leqslant 0.8$ as shown in Figures 5.9 and 5.10. Here the value of

g(+0.0033) was obtained by equating the chemical potential of the

constituents at $100^{\circ}C$ on the cloud point curve.

These calculations, however, are only qualitatively important

and provide only an estimate of the thermodynamic states of the

mixture due to the inherent simplifications of the Flory-Huggins

model.

5.2   APPLICATION OF FLORY'S EQUATION OF STATE THEORY

5.2.1   The Equation of State Parameters of the Pure Components

In this theory the properties of the blends are defined in

terms of the state parameters of the pure components. The theory

accounts properly for the differing nature of the components as well

as for the interactions between neighbouring molecules. The work

of Biroz et al. (1971), who compared solubility parameter theory with

Prigogine's corresponding equation of state theory and also of

Patterson and Delmas (1970) who compared Prigogine's and Flory's

theories, favoured Flory's theory. The application of this theory

in explaining the entropy and enthalpy contributions to the residual

free energy of mixing have been studied by Eichinger and Flory (1968),

Booth and Pickles (1973), Shih and Flory (1972), Chalal et al. (1973),

and presently in this work.
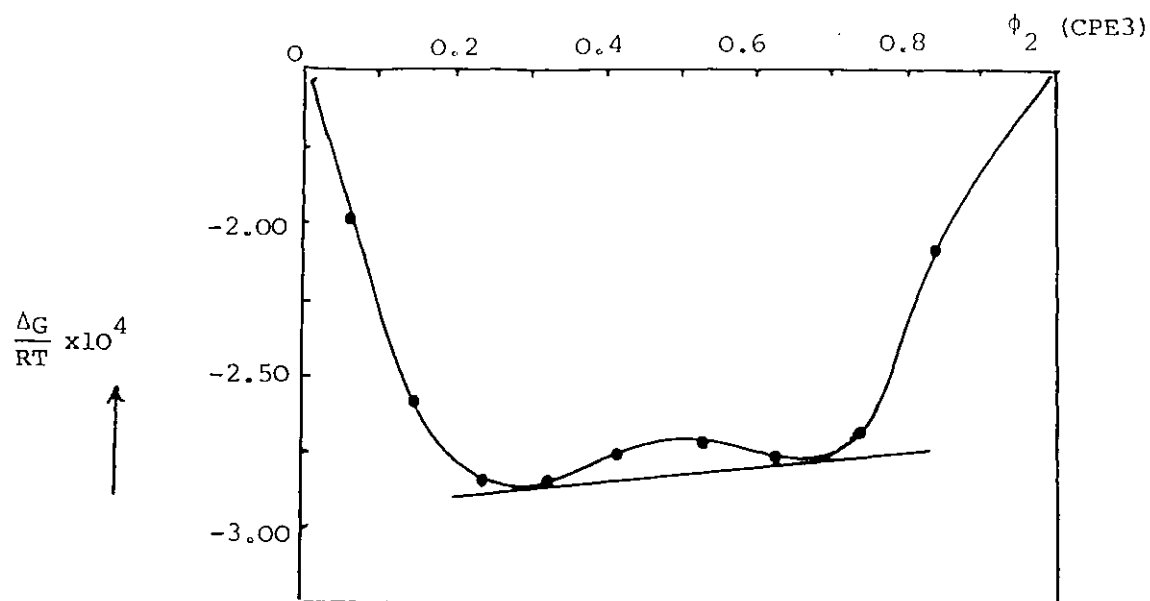
FIG. 5.9. The Gibbs free energy change on mixing of EVA45-CPE3 mixtures at 100°C plotted against volumes fraction of CPE3. $g_{12} = +0.0033$.

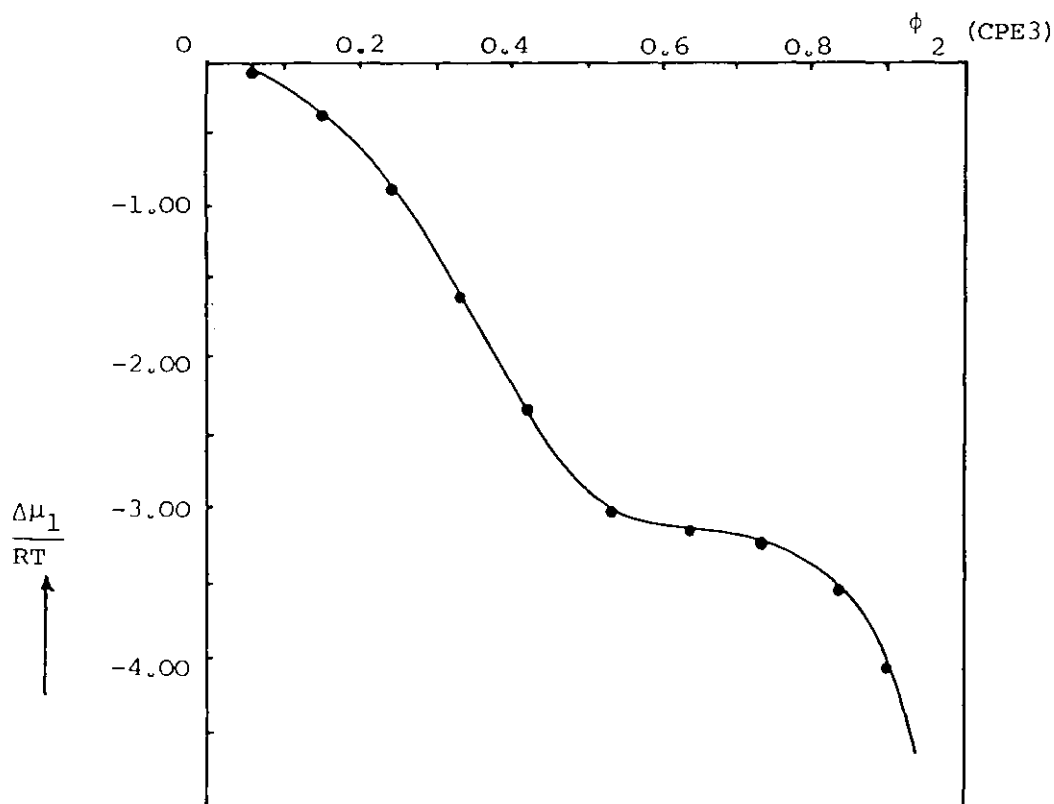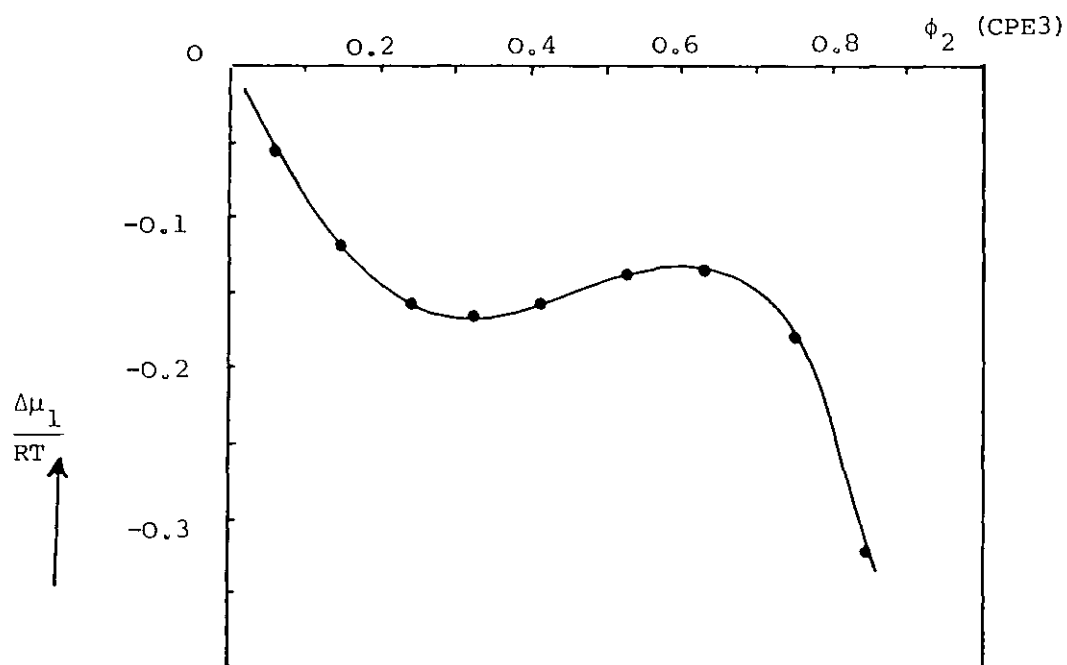Fig. 5.10. The chemical potential of EVA45 in the mixtures of EVA45-CPE3 at 100°C plotted against volume fraction of CPE3. $g_{12} = +0.0033$.

In the view of these workers, the modified Flory equation
of state theory is an improvement but not completely satisfactory in
explaining the thermodynamic states of polymeric mixtures, governed
by dispersion (or attraction) forces. The application of this theory
to a binary mixture requires the following state parameters of the
pure components:

a.   The specific volume, v_{SP}.

b.   The surface area per unit of core volume ratio, S_1 / S_2

c.   The thermal expansion coefficient, $\alpha = \frac{1}{v} \cdot \frac{dv}{dt}$

d.   The thermal pressure coefficient, $\gamma = (\frac{dP}{dT})_V$

e.   The interaction term, X_{12}.

a. The specific volume of the components

These are obtainable from the densities ($v_{SP} = \frac{1}{d}$) at a
particular temperature. The densities of several polymers are given
by van Krevelen (1972) and Brandrup and Imergut (1975). In general,
densities can be measured by pycnometry, equal density titration and
other methods.

The temperature dependence of the specific volume is given
by $v_{SP} = v_{SP}{}^{O} e^{\alpha \Delta T}$ which for a small ΔT gives:

$$v_{SP} \simeq v_{SP}{}^{O} (1 + \alpha \Delta T)$$ 5.22

b. The surface area per unit core volume ratio

This ratio can be calculated (i) by using the tabulation of
group surface areas and volumes given by Bondi (1964) who listed the
volume of molecules impenetrable to thermal collision, the so-called
van der Waals volumes, and the corresponding area per molecule, or

(ii) as Flory and co-workers have often done, by casting shadows of
molecules for various orientations, where an average area for the
monomer unit is estimated from the area of the projections (Eichinger
and Flory, 1968 and Shih and Flory, 1972). These workers normally
assume a spherical shape for small molecules and a cylindrical shape
for polymers. (iii) The other alternative is the use of the Abe and
Flory (1965) equations:

$$\frac{s_1}{s_2} = \left(\frac{V_1{}^*}{V_2{}^*} \right)^{-1/3} = \left(\frac{r_1}{r_2} \right)^{-1/3} \qquad 5.23$$

where V^* is the product of $v_{SP}{}^*$ and the molecular weight of the
corresponding component. None of these methods, however, gives a
precise value for $\frac{s_1}{s_2}$ and the agreement between the different methods
is usually poor. For example, the estimated ratio of $\frac{s_1}{s_2}$ for benzene-
poly (dimethyl siloxane), from Bondi's group contribution, is 1.14
and that of the sphere-cylindrical method is 1.67 (Shih and Flory,
1972). For methyl ethyl ketone-poly (styrene) the value given by
Bondi is 1.2 compared with the value of 2.1 given by the sphere-
cylindrical approximation (Flory and Höcker, 1971). The intermediate
value of $\frac{s_1}{s_2}$ is normally taken by these authors for further calculations.

The ratio of $\frac{s_1}{s_2}$ is close to unity when two polymers or two
solvents are mixed, unless there is a strong specific interaction
within the molecules of one of the components. It will be shown later
that this ratio plays a role in determining the polymer-polymer
miscibility and also the shape of the phase boundaries. The $\frac{s_1}{s_2}$
ratios, calculated from Bondi's approximation, for the systems
investigated here, are presented in Table 5.1. In this calculation
the intermolecular interactions of the two components were not considered.
The ratios calculated from Equation 5.23, for some of the blends, are

TABLE 5.1

RATIOS ACCORDING TO (a) BONDI (1964) AND (b) EQUATION 5.23.

No	Blends	$\frac{s_1}{s_2}$ a	$\frac{s_1}{s_2}$ b
1	OC.AC-S52	1.064	1.2054
2	OC.AC-S45	1.059	1.2055
3	EVA45-CPE3	1.025	0.9246
4	EVA45-H48	1.021	1.0184
5	EVA45-H40	1.018	
6	EVA40-CPE3	1.019	
7	EVA40-H48	1.016	
8	EVA40-H40	1.013	

c. The coefficient of thermal expansion

This coefficient plays an important role in the miscibility of polymer blends and is obtainable either from densities or dilatometric measurements of the samples. The latter provides more accurate values for α at various temperatures. The former gives slightly higher corresponding values due to the trapped air in the oligomeric materials or in the interfaces between the solid polymers and liquid media.

In order to measure the thermal expansion coefficients of a series of n-alkenes, Orwoll and Flory (1967) designed a special dilatometer, a different version of which is given by Rabek (1980) and

employed here to measure the thermal expansion coefficients of solid and liquid materials.

The temperature and pressure dependence of α can be calculated from theoretical considerations when it is written in terms of the reduced variables and provided its value is known at one particular temperature and pressure:

$$\alpha = \frac{1}{v} \cdot \frac{\partial v}{\partial T} = \frac{\tilde{T}}{T\tilde{v}} \cdot (\frac{\partial \tilde{v}}{\partial \tilde{T}})_{\tilde{P}}$$
5.24

$$d\alpha(T,P) = (\frac{\partial \alpha}{\partial T})_P dT + (\frac{\partial \alpha}{\partial P})_T dP$$
5.25

where

$$(\frac{\partial \alpha}{\partial T})_{P=0} = (7 + 4\alpha T) \cdot \alpha^2/3$$
5.26

and

$$(\frac{\partial \alpha}{\partial P})_T = -T\alpha/\gamma \{1 + 13\alpha T/3 + 4(\alpha T)^2/3\}$$
5.27

Neglecting the pressure dependence of α at atmospheric pressure gives:

$$\alpha = \alpha_0 + \alpha_0^2 (7 + 4\alpha_0 T) \Delta T/3$$
5.28

This equation was used to calculate α at the required temperatures.

The thermal expansion coefficient of the pure components obtained by dilatometry at 83.5°C are given in Table 5.2.

TABLE 5.2

No	Material	$\alpha \times 10^4$ (deg.$^{-1}$)
1	(OC.AC)*	8.850
2	S45	6.575
3	S52	6.625
4	EVA45	4.5103
5	H48	4.4199
6	CPE3	3.6546

* sec-octyl acetate

d.   The thermal pressure coefficient

Reliable values for the thermal pressure coefficients of polymeric materials, solids or liquids, are not generally available. This is mainly due to the practical difficulties of measuring this quantity.

Allen et al. (1960B), however, designed a pressure bomb to measure the thermal pressure coefficients of polymeric materials. A slightly modified version of it was used by Orwoll and Flory (1967) to measure this quantity for n-alkenes. Application of this method to solid polymeric materials is difficult and time-consuming. The thermal pressure coefficient, however, does not have a significant effect on the treatment of polymer-polymer miscibility by Flory's equation of state theory, i.e. the equation of state is not sensitive to the γ coefficients and a good estimation of these is sufficient.

One way to estimate this coefficient is through the solubility parameter (δ) of the component which itself is related to the cohesive energy density (C.E.D.) and therefore to the strength of internal pressure of the structural molecules. According to Allen et al. (1960B), the internal pressure, and consequently the thermal pressure coefficient, can be computed from the thermal expansion coefficient, α, and the isothermal compressibility, β_T, at any temperature by using the following relation:

$$P_i \equiv \left(\frac{\partial U}{\partial V} \right)_T = T\left(\frac{\partial P}{\partial T} \right)_V - P \qquad \text{5.29}$$

where U is the internal energy. This equation at low pressures can be written as

$$P_i = T \left(\frac{\alpha}{\beta_T} \right) \cong T\gamma \qquad \text{5.30}$$

These authors, and also Olabisi and Simha (1977) have used the following relation for calculating P_i from the C.E.D.:

$$P_i = m.(C.E.D.) = m\,\delta^2 \qquad \text{5.31}$$

or $\quad m\,\delta^2 \cong T\,\gamma$ $\qquad\qquad$ 5.32

where m for most polymers is close to one. Thus, knowing the

solubility parameter of the component theoretically or experimentally,

γ at any temperature, can be estimated. The best way to calculate the

solubility parameters is from group contributions using Small's

theory (1953). According to Small, δ is a linear function of an

additive structural constant, f_i, called the "molar attraction constant":

$$\delta = \frac{d}{M}\,\Sigma f_i \quad (cal.cm^{-3})^{\frac{1}{2}} \qquad\qquad 5.33$$

where d is the density and M is the molecular weight of the repeating

units in the polymer. Small calculated the molar attraction constants

of different groups from vapour pressures and heats of vaporization

data. His values were recently improved and updated by Hoy (1970) and

van Krevelen (1972). Askadskii et al. (1977) have modified this

method by considering all possible configurations, orientations and

specific interactions of molecules. They have computed the solubility

parameters of a large number of solvents and polymers which show a

remarkable agreement with experimental results. These calculations

normally give δ and γ at 25°C, where the temperature dependence of γ

at atmospheric pressures is given by:

$$\frac{\partial \gamma}{\partial T} = -\gamma(1 + 2\,\alpha T)/T \qquad\qquad 5.34$$

or

$$\gamma = \gamma_o - \gamma_o\,(1 + 2\,\alpha_o T)\,\Delta T/T \qquad\qquad 5.35$$

The solubility parameters and the thermal pressure coefficients of

the pure materials at 25°C calculated according to Equations 5.32 and

5.33 are presented in Table 5.3. The f_i values were taken from Hoy's

(1970) data. Intramolecular interactions of the pure components were

neglected. .

TABLE 5.3

No	Material	**δ $(cal.cm^{-3})^{\frac{1}{2}}$	χ $(cal.cm^{-3}.deg^{-1})$
1	(OC.AC.)*	7.092	0.1670
2	S45	8.558	0.2456
3	S52	8.986	0.2708
4	EVA40	8.487	0.2415
5	EVA45	8.540	0.2446
6	H40	8.690	0.2532
7	H48	9.208	0.2843
8	CPE3	9.273	0.2884

* sec-octyl acetate   ** $1\ cal.cm^{-3} = 4.18\ J.cm^{-3}$

e. The interaction term, X_{12}

The simplest approach in calculating X_{12} is the use of experimental heats of mixing of model compounds, given in Figure 4.29, as recommended by Eichinger and Flory (1968). The results of applying Equation 2.74 and 2.77 to the model compounds in this work are given in Table 5.4.

TABLE 5.4

Mixture	X_{12} $(J.cm^{-3})$			
	$64.5^{O}C$	$73.08^{O}C$	$83.5^{O}C$	s_2/s_1
OC.AC-S45	-5.00	-4.20	-2.63	0.883
OC.AC-S52	-7.50	-6.50	-4.90	0.881

The values thus determined can be used to calculate partial molar residual quantities of the mixtures. The temperature dependence of X_{12} is not mathematically understood. Therefore, any interpolation or extrapolation of it was avoided, where possible.

Knowing the aforementioned parameters, the other equation of state quantities for pure and binary mixtures can be computed as follows:

(i) The Pure Component Parameters

The thermal expansion coefficient gives $\tilde{v}$ according to Equation 2.51. Knowing $\tilde{v}$ Equation 2.48 provides $\tilde{T}$ and hence T* and $v_{SP}*$ ($v_{SP}* = v_{SP}/\tilde{v}$) which can be obtained from Equation 2.39. The thermal pressure coefficient is related to P* by Equation 2.52 where $\tilde{P} = P/P*$. The value of v* can be obtained from Equation 2.40, for infinite chain length assuming $3C \simeq 2(3Cr = 2r + 1)$. Results of these calculations for sec-octyl acetate, ceroclors 45 and 52, EVA45, H48 and CPE3 at $83.5^{\circ}C$ are given in Table 5.5.

TABLE 5.5

THE STATE PARAMETERS FOR THE PURE MATERIALS AT $83.5^{\circ}C$

Material	$\alpha \times 10^4$ deg^{-1}	γ $J.cm^{-3}.$ deg^{-1}	v_{SP} $cm^3.g^{-1}$	$v_{SP}*$ $cm^3.g^{-1}$	$\tilde{v}$	$T*$ $^{\circ}K$	$P*$ $J.cm^{-3}$[†]
OC.AC	8.850	0.4893	1.2442	0.9877	1.2596	6067.21	276.930
S45	6.575	0.6708	0.9025	0.7506	1.2022	7200.98	345.854
S52	6.625	0.7360	0.8306	0.6901	1.2036	7167.45	380.305
EVA45	4.5103	0.8043	1.0636	0.9288	1.14509	9250.29	376.182
H48	4.4199	0.9544	0.81506	0.7134	1.1424	9384.51	444.342
CPE3	3.6546	0.9592	0.8089	0.7223	1.1198	10790.13	429.477

† 1 atm = 0.1013 $J.cm^{-3}$ = 0.02422 $cal.cm^{-3}$

(ii)   Binary Mixture Parameters

The ϕ_2 and θ_2 values are given by Equations 2.59 and 2.66

respectively. P* and T* are given by Equations 2.69 and 2.72 where

$\tilde{P}$ and $\tilde{T}$ are defined as before. The values of $\tilde{v}$ are obtainable from

either Equation 5.36 or 5.37 by iterative means.

$$\tilde{v} = (\frac{\tilde{T}\tilde{v}^{1/3}}{\tilde{v}^{1/3}-1} - \tilde{P}\tilde{v})^{-1} \qquad\qquad 5.36$$

$$\tilde{v} = (1 - \tilde{T}\tilde{v})^{-3} \qquad\qquad 5.37$$

v* of a binary mixture can be similarly obtained as described for

pure components, but the number of external degrees of freedom per

molecule of mixture is

$$C = \phi_1 C_1 + \phi_2 C_2 - \phi_1 \phi_2 C_{12} \qquad\qquad 5.38$$

This is the shortest and simplest approach in obtaining all

the state parameters required for pure components and their blends at

any temperature and composition.

5.2.2   Simulation of Phase Boundaries by Applying Flory's

Equation of State Theory

Using the general version of Flory's equation of state

theory, McMaster (1973) examined the contribution of the state parameters

to the miscibility of hypothetical polymer-polymer mixtures, by

allowing variations in the values of these parameters. He observed

that the theory is capable of predicting both LCST and UCST behaviours

individually or simultaneously, the shape and position of which depend

upon the equation of state parameters.

Olabisi (1975) has applied McMaster's treatments to a real system consisting of a poly(caprolactone) and poly(vinyl chloride) mixture. His spinodal simulation shows that for a constant negative value of X_{12} as the $\dfrac{S_1}{S_2}$ ratio increases the spinodal curve tends to show more obvious bimodality.

The asymmetrical phase boundary has recently been attributed by ten Brinke et al. (1980) to the following condition:

$$Q_{12} = 0.0, \quad X_{12} < 0, \quad \frac{s_1}{s_2} < 1, \quad \frac{r_1}{r_2} < 1 \text{ and } C_{12} > 0$$

The equation for the spinodal, based purely on the chemical potential of Flory's equation of state theory is derived in the present work. In this derivation the pressure effect on the phase boundary is considered, whereas the effect of polydispersity and the C_{12} factor are neglected.

The addition of the combinatorial chemical potential of component one and the effect of the pressure term into Equation 2.102 gives:

$$\frac{\Delta\mu_1}{RT} = \ln \phi_1 + (1 - \frac{r_1}{r_2})\phi_2 + \frac{P_1{}^*V_1{}^*}{RT} \quad \{3 \frac{T}{T_1{}^*} \ln \frac{\tilde{v}_1{}^{1/3} - 1}{\tilde{v}^{1/3} - 1} + \frac{1}{\tilde{v}_1} - \frac{1}{\tilde{v}}$$

$$+ \tilde{P}_1(\tilde{v}-\tilde{v}_1)\} + \frac{V_1{}^*X_{12}}{RT} \cdot \frac{\theta_2{}^2}{\tilde{v}} - \frac{V_1{}^*Q_{12}}{R} \theta_2{}^2 \qquad\qquad 5.39$$

The spinodal condition is $\dfrac{\delta}{\delta\phi_1}(\dfrac{\Delta\mu_1}{RT}) = \dfrac{\partial}{\partial\phi_2}(\dfrac{\Delta\mu_1}{RT}) = 0.$

Differentiating Equation 5.39 with respect to ϕ_2 gives:

$$- \frac{1}{\phi_1} + (1 - \frac{r_1}{r_2}) - \frac{P_1^* V_1^*}{RT_1^*} \cdot \frac{A}{\tilde{v} - \tilde{v}^{2/3}} + \frac{P_1^* V_1^*}{RT_{SP}} (\frac{1}{\tilde{v}^2} + \tilde{P}_1) A$$

$$+ \frac{V_1^* X_{12}}{RT_{SP}} \cdot (\frac{2\theta_2}{\tilde{v}} \cdot \frac{\theta_1 \theta_2}{\phi_1 \phi_2}) - \frac{V_1^* X_{12}}{RT_{SP}} \circ \frac{\theta_2^2}{\tilde{v}^2} \cdot A - \frac{V_1^* Q_{12}}{R} (2\theta_2 \cdot$$

$$\frac{\theta_1 \theta_2}{\phi_1 \phi_2}) = 0 \qquad\qquad 5.40$$

where $A = \dfrac{\partial \tilde{v}}{\partial \phi_2} = - \dfrac{\partial \tilde{v}}{\partial \phi_1}$ or,

$$\frac{\partial \tilde{v}}{\partial \phi_2} = \frac{B - C (\frac{\tilde{P}}{\tilde{T}} + \frac{1}{\tilde{T} \tilde{v}^2})}{\frac{2}{\tilde{v}^3} - \frac{\tilde{T}}{3\tilde{v}^{5/3}} \cdot \frac{(3\tilde{v}^{1/3} - 2)}{(\tilde{v}^{1/3} - 1)^2}} \qquad\qquad 5.41$$

and

$$B = \frac{\partial \tilde{P}}{\partial \phi_2} = \frac{\tilde{P}}{\tilde{P}^*} \{P_1^* - P_2^* - \theta_2 X_{12} (1 - \frac{\theta_1}{\phi_2})\} \qquad\qquad 5.42$$

$$C = \frac{\partial \tilde{T}}{\partial \phi_2} = \frac{\tilde{T}}{\tilde{P}} \cdot B + \frac{T}{P^*} (\frac{P_2^*}{T_2^*} - \frac{P_1^*}{T_1^*}) \qquad\qquad 5.43$$

Using Equations 5.40 to 5.43 a number of spinodal curves at various

conditions have been simulated. The results are generally in agreement

with the finding of McMaster (1973) and ten Brinke et al. (1980).

One example is the spinodal curves simulated for EVA45-CPE3 when

$Q_{12} = -0.010 \ J.cm^{-3}.deg^{-1}$. This is shown in Figure 5.11. The shape of

the curve for $Q_{12} = 0$ is similar to that of Olabisi (1975) and ten Brinke

et al. (1980) and occurs in a higher temperature range. The negative

value of Q_{12} reduces the interaction term, which in turn reduces the

miscibility. The other state parameters of this simulation are shown

in the Figure caption. The simulated spinodal is more symmetrical than

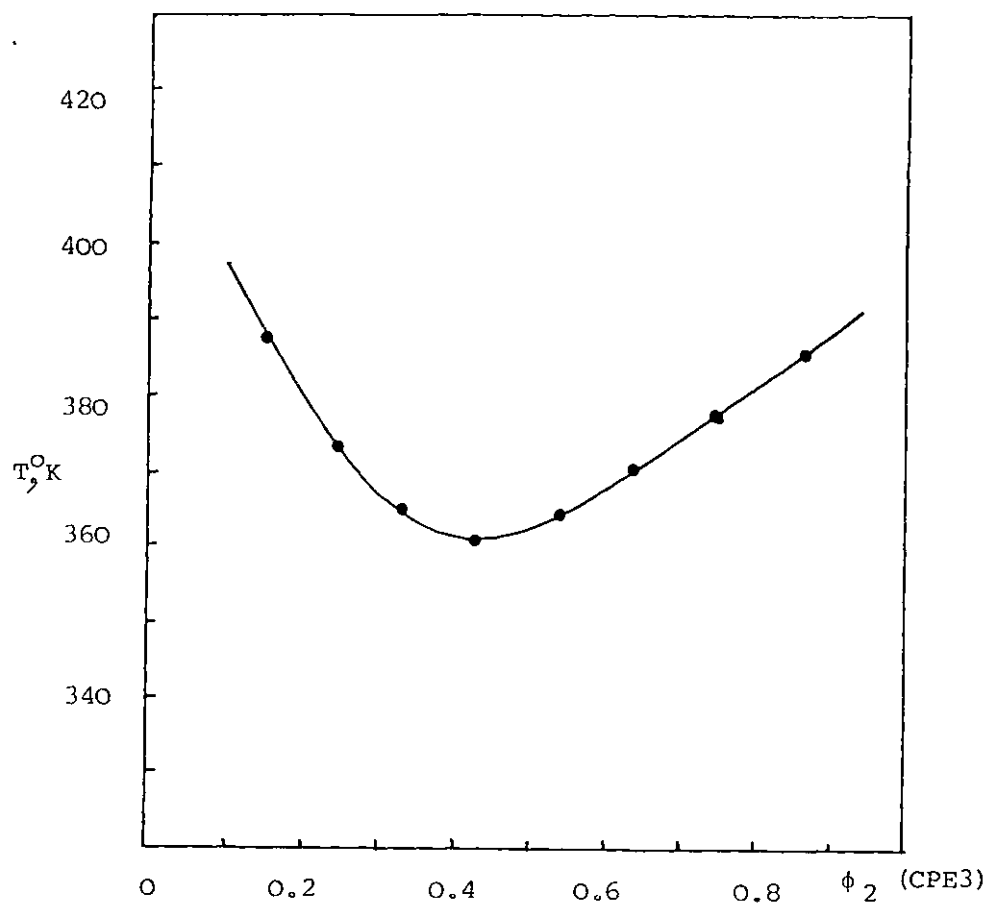the experimental cloud point curve given in Figure 4.19. The reason

FIG. 5.11. Simulated spinodal curve for the EVA45-CPE3 mixtures, using Flory's equation of state theory at the following condition:

$$X_{12} = -4.9 \quad J.cm^{-3}, \qquad Q_{12} = -0.010 \quad J.cm^{-3}, deg^{-1}$$

$$\frac{s_1}{s_2} = 1.03, \quad \frac{r_2}{r_1} = 1.336 \quad \text{and} \quad v_1{}^* = 2 \times 10^5$$

for an asymmetry in the cloud point curve may be a strong intramolecular interaction in CPE which tends to become significant in the region with higher CPE content. The effect of this factor was neglected in Flory's equation of state theory.

The spinodal equation is sensitively dependent on $\tilde{v}$ and the Q_{12} factor. On the other hand, it is not very sensitive to small variations of $\dfrac{s_2}{s_1}$ or V_1^*. Decreasing $\dfrac{s_2}{s_1}$ ratio from 1.03 to 0.98 lowers the T_{SP} by about 2 degrees and increasing V_1^* by a factor of 5 lowers it by about 4 degrees.

Similarly simulated spinodal curves for EVA45-H48 mixtures at quoted conditions are presented in Figure 5.12. The simulated spinodal curves in Figure 5.12A, B, are flatter than the experimental cloud point curves given in Figure 4.20. This is due to large negative values of X_{12} given by the heat of mixing of the analogue compounds at 73.08 and 83.5°C. A similar effect of X_{12} on the spinodal curve was observed by McMaster (1973). Reducing the value of X_{12} to a value of -0.17 J.cm^{-3} will improve the shape of the spinodal curve as shown in Figure 5.12C.

The simulated results are generally in agreement with the proposal of McMaster (1973) that a negative Q_{12} decreases the miscibility by reducing the contact energy. They also conform to the condition set up by ten Brinke et al. (1980) for an asymmetrical spinodal curve. They also show that a smaller negative value of X_{12} improves the shape of the spinodal curve due to the temperature dependence of the interaction term as given in Table 5.4.
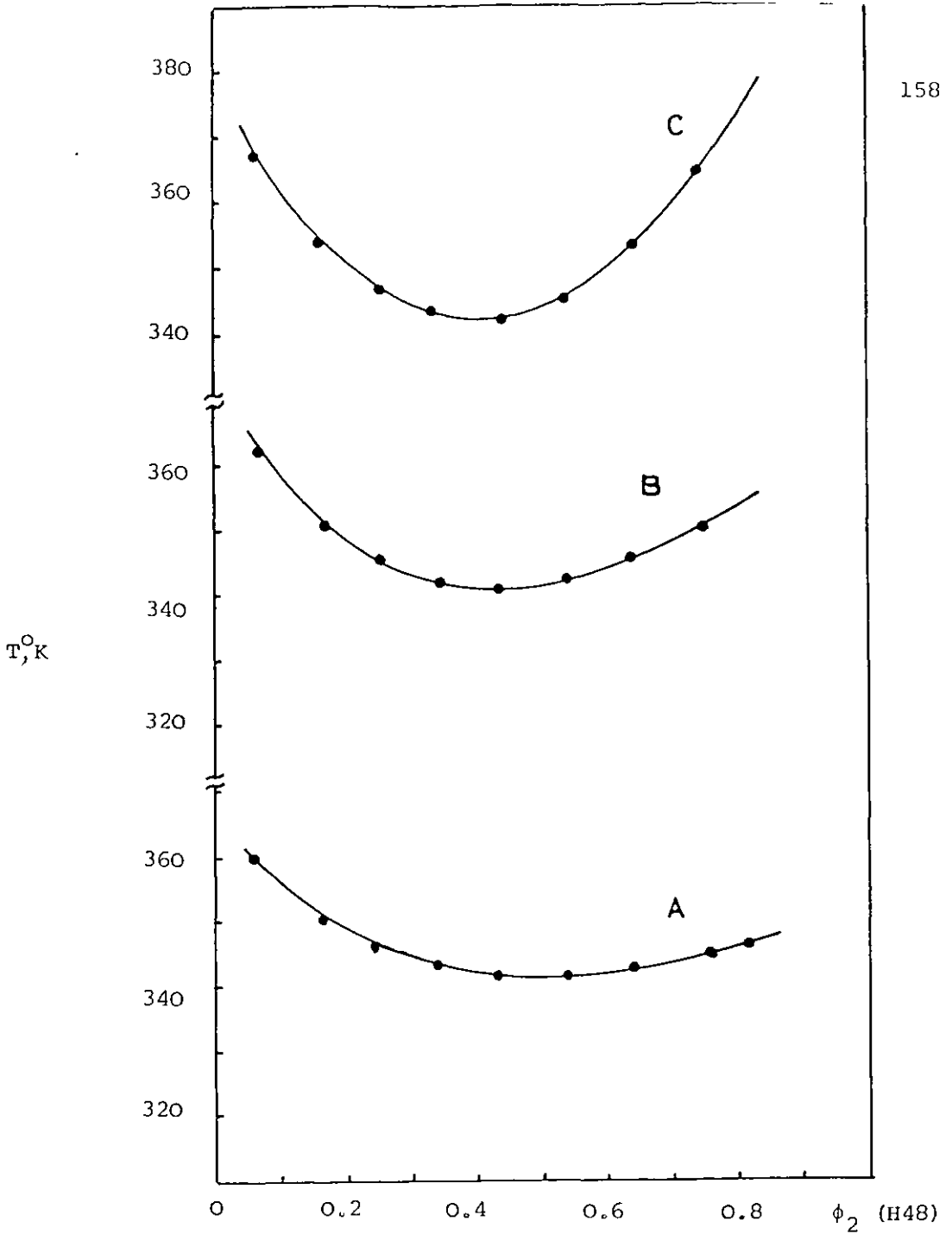
FIG. 5.12. Simulated spinodal curves for EVA45-H48 mixtures, using Flory's equation of state theory at following conditions. Plotted against H48 segmental fraction.

A. $X_{12} = -4.2$ J.cm^{-3} $Q_{12} = -0.108$ J.cm^{-3}.deg^{-1}

B. $X_{12} = -2.63$ J.cm^{-3} $Q_{12} = -0.00678$ J.cm^{-3}.deg^{-1}

C. $X_{12} = -0.17$ J.cm^{-3} $Q_{12} = -0.00048$ J.cm^{-3}.deg^{-1}

$$\frac{s_2}{s_1} = 0.98 \qquad \frac{r_2}{r_1} = 1.68 \quad \text{and} \quad V_1^* = 2 \times 10^5$$

5.2.3   The Interaction Parameters

To calculate χ_H, Equations 2.82 and 2.51 were used where the thermal expansion coefficients of the mixtures were continuously computed from the $\tilde{v}$ values of the mixtures. The entropy interaction parameter, χ_s, was calculated from Equation 2.91 and χ_t from Equation 2.92 or 2.93. In these calculations the entropy correction factor, Q_{12}, was introduced in Equation 2.91 in the same manner as in Equation 2.102. The Q_{12} values were taken from the spinodal simulation of the corresponding mixture. These calculations were carried out for atmospheric pressure. Results obtained for EVA45-H48 and EVA45-CPE3 mixtures at $83.5^{o}C$ are given in Figures 5.13 and 5.14 respectively. Other specifications of these computations are given in the figure captions.

In order to obtain χ_H, χ_s and χ_t at infinite dilution, $(\chi_H^{\infty}$, χ_S^{∞} and $\chi_t^{\infty})$ Eichinger and Flory (1968) have expanded Equations 2.82, 2.91 and 2.92 in series to infinite dilution of component two. In doing so, they neglected the contribution of Q_{12} to the X_{12} parameter. Whereas here we correct for this contribution, knowing that X_{12} contains a contribution from the entropy of the interaction between unlike neighbouring segments in a similar way to the enthalpy term. To include this correction, we substitute X_{12} from Equation 2.101 into the series expansions giving:

$$\chi_t^{\infty} = \frac{P_1^* V_1^*}{RT\tilde{v}_1} \left\{ \frac{X_{12} - T\tilde{v}Q_{12}}{P_1^*} \cdot (\frac{s_2}{s_1})^2 + \frac{1}{2} \alpha_1 TA^2 \right\} + O(\phi_2^3) \qquad 5.44$$

$$\chi_S^{\infty} = -\frac{P_1^* V_1^*}{RT\tilde{v}_1} \left\{ \frac{X_{12}}{P_1^*} \cdot (\frac{s_2}{s_1})^2 \alpha_1 T + \frac{T\tilde{v}Q_{12}}{P_1^*} \cdot (\frac{s_2}{s_1})^2 - \frac{\alpha_1 TA^2}{2} (\right.$$

$$\left. 1 + \frac{4}{3} \alpha_1 T + \frac{4}{3}\alpha_1^2 T^2) \right\} + O(\phi_2^3) \qquad 5.45$$

FIG. 5.13. The interaction parameters for EVA45-H48 mixtures at 83.5°C calculated according to Flory's equation of state theory. Plotted against segmental fraction of H48 $X_{12} = -2.63$ J.cm^{-3} and $Q_{12} = -0.00678$ J.cm^{-3}.deg^{-1}.

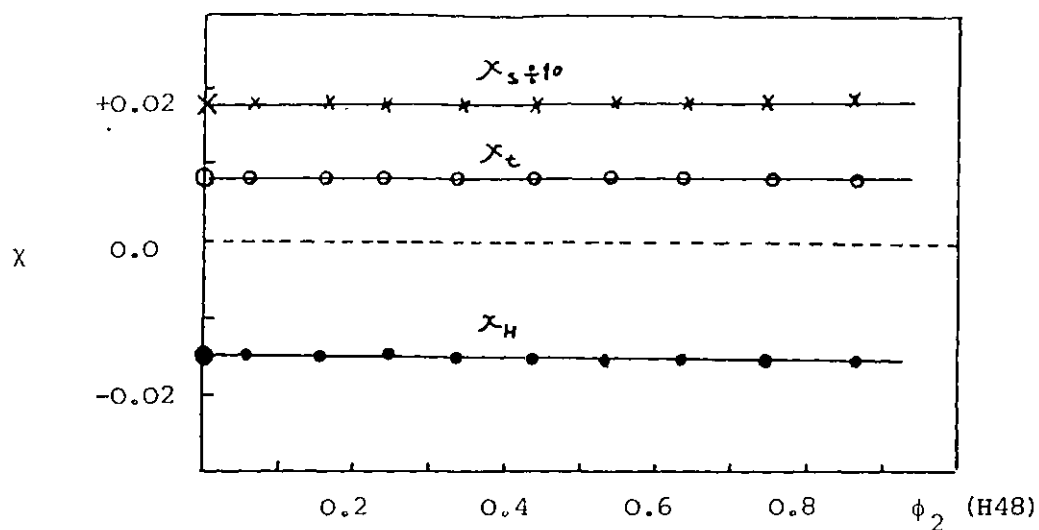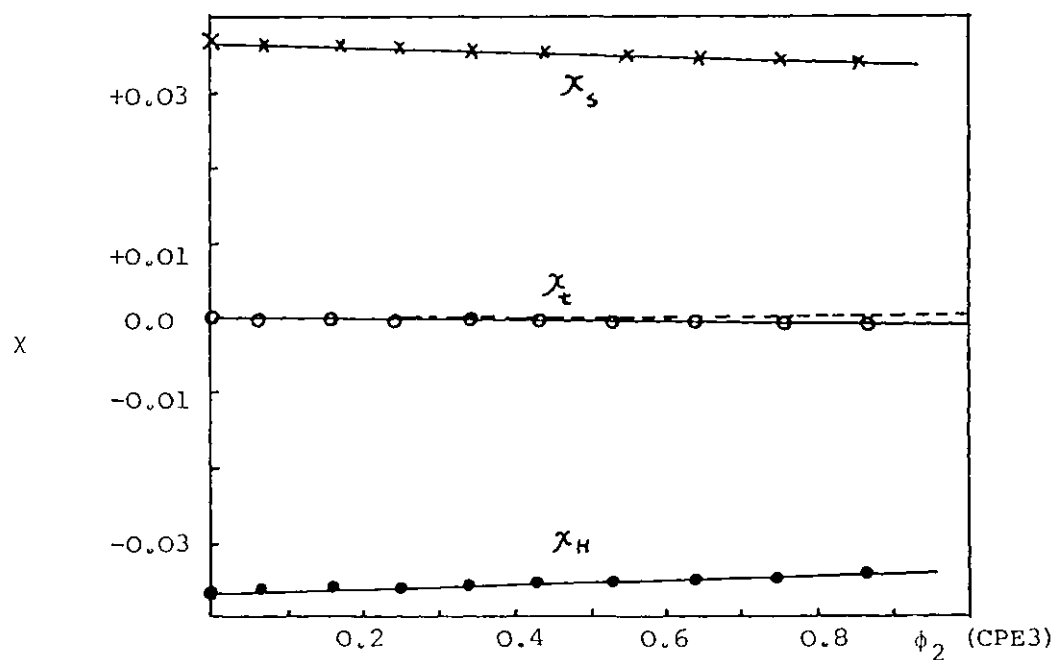
FIG. 5.14. The interaction parameters for EVA45-CPE3 mixtures at 83.5°C calculated according to Flory's equation of state theory. Plotted against segmental fraction of CPE3. $X_{12} = -4.9$ J.cm^{-3} and $Q_{12} = -0.010$ J.cm^{-3}.deg^{-1}

χ_H^∞ can be obtained by subtraction of Equation 5.45 from 5.44 or,
by series expansion of its corresponding equation:

$$\chi_H^\infty = \frac{P_1^* V_1^*}{RT\tilde{v}_1} \left\{ \frac{X_{12}}{P_1^*} \cdot \left(\frac{s_2}{s_1} \right)^2 - \frac{2}{3} (A\alpha_1 T)^2 \right\} (1+\alpha_1 T) + O(\phi_2^3) \qquad 5.46$$

In these expressions A is given by:

$$A = \left(1 - \frac{T_1^*}{T_2^*} \right) \left(\frac{P_2^*}{P_1^*} \right) - \left(\frac{s_2}{s_1} \right) \left(\frac{X_{12}}{P_1^*} \right) \qquad 5.47$$

The term $O(\phi_2^3)$ is given in Flory's paper (1965) and as in the
calculation of Shih and Flory (1972) was neglected in this work, due to
its minor effect on the reduced partial molar residual quantities
at infinite dilution. The calculated values of χ_t^∞, χ_s^∞ and χ_H^∞ are also
given in Figures 5.13 and 5.14 at $\phi_2 = 0$.

The significance of these treatments are in the "exchange"
entropy and energy contribution to the χ_H^∞ and χ_s^∞. These exchange
quantities are the purely energetic and entropic parts (excluding the
equation of state terms) of the χ_H^∞ and χ_s^∞ respectively and given by:

$$\chi_{H:1} \text{ (exchange)} = \frac{V_1^* X_{12}}{RT\tilde{v}_1} \cdot \left(\frac{s_2}{s_1} \right)^2 \qquad 5.48$$

$$\chi_{S:1} \text{ (exchange)} = -\frac{V_1^* Q_{12}}{R} \left(\frac{s_2}{s_1} \right)^2 \qquad 5.49$$

The calculated values of $\chi_{H:1}$ (exchange) and χ_H^∞ and also $\chi_{S:1}$
(exchange) and χ_s^∞ at $83.5^\circ C$ for EVA45-H48 and EVA45-CPE3 mixtures
are given in Table 5.6.

TABLE 5.6

Mixture	χ_H^∞	$\chi_{H:1}^\infty$ (exch)	χ_S^∞	$\chi_{S:1}^\infty$ (exch)
EVA45-H48	-0.1729	-0.1487	+0.1815	+0.1566
EVA45-CPE3	-0.3692	-0.3062	+0.3730	+0.2552

5.2.4   The Excess Volume, Enthalpy and Free Energy Change on Mixing

The volume changes on mixing were calculated for EVA45-H48

and EVA45-CPE3 mixtures at temperatures at which the heat of mixing

of their model compounds were measured. The values of X_{12} for Oc.Ac-S45

and Oc.Ac-S52 were assumed to be equivalent to those of EVA45-H48

and EVA45-CPE3 respectively, at the same temperatures. This assumption

may not be completely correct, but it is the practical way of finding

X_{12} for the solid polymer mixtures.

The $\dfrac{\Delta V_M}{V^o}$ calculated using Equation 2.80 on the aforementioned

basis is presented in Figure 5.15. The $\tilde{v}$ used in these calculations

were obtained from Equation 2.47. It is evident that the volume

changes on mixing of EVA45-CPE3 mixtures are larger in size than those

of EVA45-H48 mixtures, and also both values become smaller at higher

temperatures. The theoretical value of $\dfrac{\Delta V_M}{V^o}$ for a 50/50 w% blend of

EVA45-CPE3 at 83.5°C is -13.8×10^{-4}, in comparison with its experimental

value of -7.2×10^{-4} obtained by measuring $\left(\dfrac{dT}{dP} \right)_c$ over the temperature

range of 82-96°C. This is based on the assumption of Eichinger and

Flory that the volume should be less dependent upon entropy than the

energy. Reducing the entropy contribution of the energy term using

Equation 2.80 reduces the value of $\dfrac{\Delta V_M}{V^o}$ for the same blend at the same
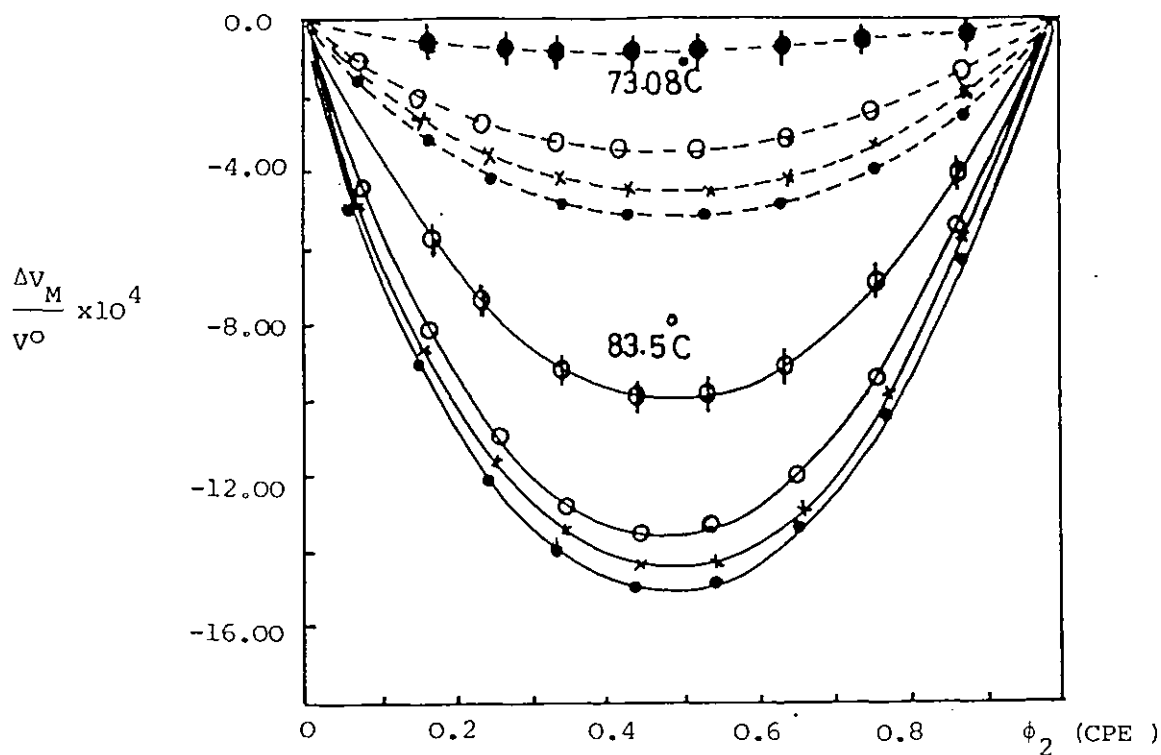
FIG. 5.15. $\frac{\Delta V_M}{V^O}$ theoretically calculated, as described in the

text, for EVA45-H48 (---), EVA45-CPE3 (———) mixtures
at ● 64.5, x 73.08 and o 83.5°C. Their values are
plotted against segmental fraction of CPE.

The values corresponding to the curve marked by ϕ are
obtained from the EVA45-CPE3 data at 83.5°C after correcting
for the entropy dependence of the interaction term. The
curve marked by ◆ is obtained in the same way from data as
73.08°C for the EVA45-H48 system.

temperature to $-10.\times 10^{-4}$. The theory also, after entropy correction, predicts a very small negative volume change on mixing for EVA45-H48 at $73.08^{\circ}C$ which is just above the phase boundary. This can only be explained by the fact that the reduced volume of the mixture, $\tilde{v}$, just above the phase boundary will not exceed the additivity volume of the mixture. The values of $\frac{\Delta V_M}{v^O}$ for EVA45-H48 mixtures at $83.5^{\circ}C$, after entropy correction, approach zero as may be expected from the simulated spinodal.

A small variation of the $\frac{s_1}{s_2}$ ratio has no significant effect on the magnitude of this quantity. The only important factor here is the reduced volume of the mixture, $\tilde{v}$, which can change the sign and magnitude of $\frac{\Delta V_M}{v^O}$. $\tilde{v}$ in turn is related to the strength of the $\bar{X}_{12}$ quantity in as much as a strong specific interaction can outweigh the variational effects of $\frac{s_1}{s_2}$ and other related parameters. For a large negative or positive enthalpy of mixing, $\frac{\Delta V_M}{v^O}$ is necessarily of the same sign.

In addition to the interaction parameters and volume changes on mixing already described, Flory's equation of state theory is capable of giving the residual Gibbs free energy change on mixing of a mixture. This will provide more information about the stability of the mixture at any given temperature as described by Flory et al. (1968). In order to calculate this quantity the enthalpy change on mixing was computed from Equation 2.74 or 2.75 where:

$$\bar{r}Nv^* = v_{SP}^* = m_1 v_{1,SP}^* + m_2 v_{2,SP}^* \qquad\qquad 5.50$$

and v_{SP}^* is the hard core volume of one gram of mixture. Other

terms of this equation were defined in Chapter Two.

The residual enthalpy changes on mixing, per gram of mixture,

which were calculated for EVA45-H48 and EVA45-CPE3 mixtures are of the

same order of magnitude as shown in Figures 4.29A, B. The calculations,

similarly give a reduction in the residual enthalpy change on mixing

as the temperature increases for both mixtures.

The residual entropy changes on mixing were similarly

calculated using Equation 2.90, while the residual Gibbs free energy

changes on mixing were computed from:

$$G^R_M = \Delta H^R_M - TS^R_M \qquad\qquad 5.51$$

The residual free energy changes on mixing at 73.08 and

$83.5^\circ C$ for EVA45-H48 mixtures obtained in this manner are presented

in Figure 5.16A. The theory predicts a reduction in the free energy

changes of the mixtures at higher temperatures. The predicted trend

of this quantity is in agreement with the theoretical phase boundary

of the mixture when the Q_{12} is zero. Introducing the entropy correction

term, derived as $- v_{SP}^* TQ_{12}\phi_1\theta_2$, in Equation 5.51 gives a

positive values of G^R for the mixture at 73.08 and $83.5^\circ C$ as shown

in Figure 5.16B. This is in accordance with the simulated spinodal

and experimental cloud point curves of the mixture. The latter

calculations correctly predict more instability in the mixture as the

temperature increases.
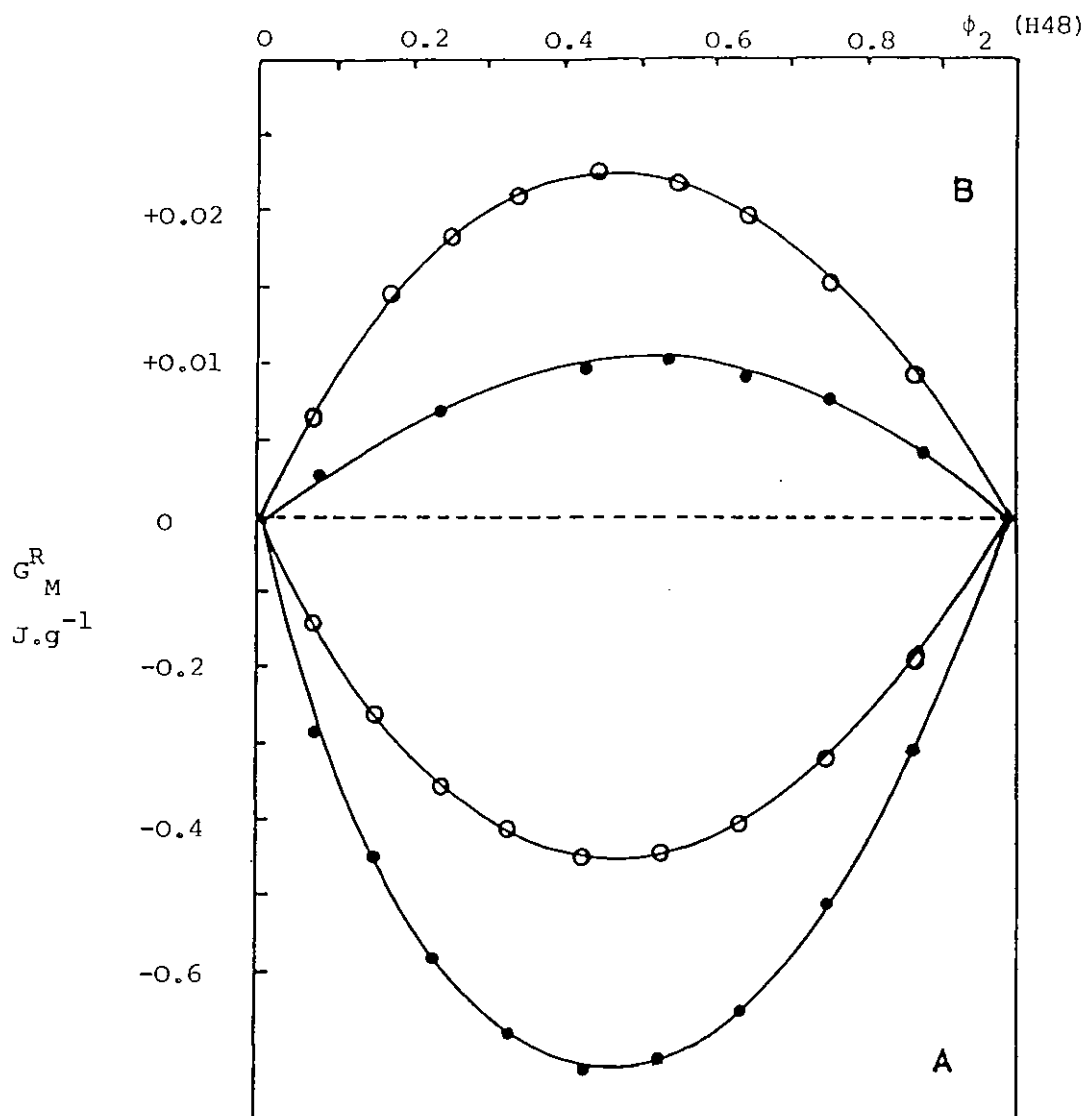
FIG. 5.16. Theoretical residual free energy change of mixing of EVA45-H48 at ● 73.08 and o 83.5°C calculated from Flory's equation of state theory. Plotted against segmental fraction of H48.

A. X_{12} (73.08°C) = -4.2 J.cm^{-3} Q_{12} = 0.0   J.cm^{-3}.deg^{-1}

   X_{12} (83.5°C) = -2.62 J.cm^{-3} Q_{12} = 0.0   J.cm^{-3}.deg^{-1}

B. X_{12} (73.08°C) = -4.2 J.cm^{-3} Q_{12} = -0.0108 J.cm^{-3}.deg^{-1}

   X_{12} (83.5°C) = -2.62 J.cm^{-3} Q_{12} = -0.00678 J.cm^{-3}.deg^{-1}

Similar calculations of G_M^R for EVA45-CPE3 at 83.5^oC

correctly give a homogeneous mixture in both cases (i.e. $Q_{12} = 0.0$

and $Q_{12} = -0.01$ $J.cm^{-3}.deg^{-1}$) as shown in Figure 5.17. The entropy

correction term reduces the value of G_M^R considerably at this

temperature.

The calculations referred to in this text so far, were

carried out in respect of component one which gave X_{12}, Q_{12}, X_{12} etc.

One may consider the possibility of performing similar calculations

in connection with the component two in which case $X_{12} \neq X_{21}$
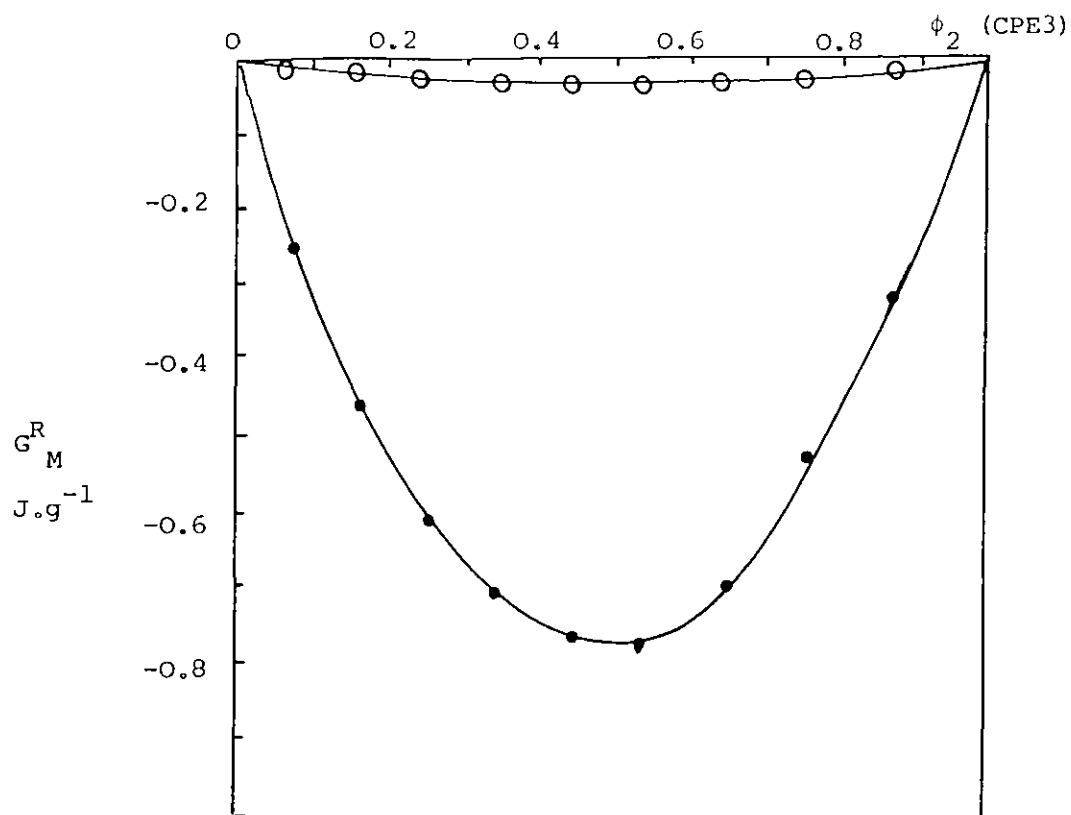
and $Q_{12} \neq Q_{21}$.

FIG. 5.17. Theoretical residual free energy change on mixing of
EVA45-CPE3 at $83.5^{\circ}C$ calculated from Flory's equation
of state theory at following conditions:

● $X_{12} = -4.9$ $J.cm^{-3}$ and $Q_{12} = 0.0$ $J.cm^{-3}.deg^{-1}$

o $X_{12} = -4.9$ $J.cm^{-3}$ and $Q_{12} = -0.010$ $J.cm^{-3}.deg^{-1}$

5.2.5   A Review of Flory's Equation of State Theory

This theory was used to explain the experimental findings.
It   proved to be reasonably successful in interpreting the excess
properties of the mixtures when the entropy correction factor, Q_{12},
was used.   It is more comprehensive than any other existing theory for
polymer miscibility, but the theory is not fully able to interpret
the volume change on mixing.   The excess volumes observed by Shih
and Flory (1972) for C_6H_6-PDMS mixtures are considerably different
from those predicted by the theory and this cannot be resolved by any
reasonable adjustable parameter.   The Q_{12} factor, at least as
introduced at present, does not give a completely satisfactory
explanation of the volume change on mixing.   The Q_{12} takes into account
the volume dependence of the residual quantities as explained in
Sections 5.2.3 and 5.2.4, but it has no effect on the combinatorial
part as shown in Figure 5.18 for the combinatorial and residual entropy
of mixing of EVA45-CPE3 at $83.5^{\circ}C$.   The volume dependence of the
combinatorial part, which was   neglected by Flory in his early
derivations, can be significant if there is a large densification on
mixing.   A consistent correction for the volume dependence of Flory's
equation of state theory, has to start from a completely new form of
the partition function.

Furthermore, there are three adjustable or semi-adjustable
parameters in Flory's equation of state theory, $\frac{s_1}{s_2}$, X_{12} and Q_{12}.
We believe that the semi-adjustable parameter, $\frac{s_1}{s_2}$, must not be used
as a binary adjustable parameter, since s_1 (or s_2) for any polymer is
independent of the other polymer in a mixture.   Thus two binary inter-
related adjustable parameters will remain, X_{12} and Q_{12}.   There is a
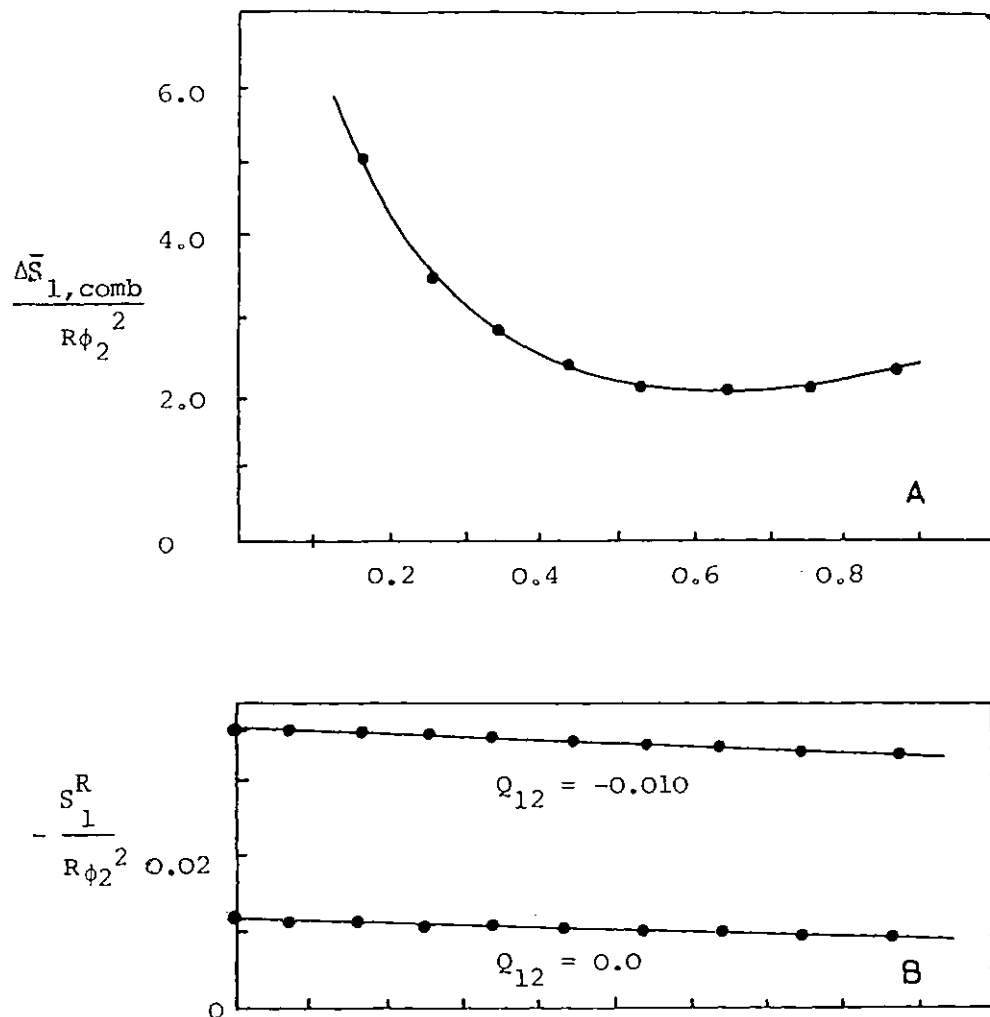limited range of variation for the X_{12} parameter if we follow the

FIG. 5.18. A. The combinatorial entropy change on mixing of
EVA45-CPE3 at 83.5°C.

B. The effect of Q_{12} on the reduced partial molar
residual entropy change of mixing of EVA45-CPE3
at 83.5°C.

Flory random mixing assumption. X_{12} therefore should be treated as a constant depending upon the functional groups comprising the molecules of the components and specifying a binary mixture at a particular pressure, temperature and composition. Introduction of the Q_{12} as an empirical parameter, however, limits the usefulness of the theory.

5.2.6   Recent Improvements Over Flory's Equation of State Theory

Renuncio and Prausnitz (1976) have questioned the complete randomness assumption used by Flory in his derivations. They correctly believe that a polymer segment has selective rules on choosing its closest neighbour. By plotting X_{12} against the $\frac{s_2}{s_1}$ ratio, for three binary systems, they show that it is not possible to fix one set of parameters $(X_{12}$ and $\frac{s_2}{2_1})$ which simultaneously fit the experimental excess enthalpy and volume change on mixing. To improve the randomness assumption in the mixtures, they introduced two fraction sites between segment i and J as θ_{iJ} and θ_{Ji} where $\theta_{iJ} \neq \theta_{Ji}$ and $\theta_{iJ} + \theta_{JJ} = 1$, $\theta_{ii} + \theta_{Ji} = 1$. One can immediately deduce that for $\theta_{Ji} > \theta_{JJ}$, i-J contact is favourable whereas for $\theta_{Ji} < \theta_{JJ}$ it is unfavourable for mixing. θ_{JJ} can be related to the overall site fractions as given by Renuncio and Prausnitz (1976).

Barandani (1979) has introduced a non-random mixing concept into the partition function, by using a two-fluid theory coupled with the non-randomness assumption. He used two adjustable parameters, ν_{12} and ν_{21}, limited in two elliptical regions to fit the theory to the experimental results of poly (iso-butene), PIB in benzene, heptane, cyclohexane and acetone with a constant $\dfrac{s_1}{s_2}$. The improvement over Flory's values for these systems, given by Eichinger and Flory (1968) is very small.

Canovas et al. (1982) have derived the following equation of state by using a similar concept to Barandani.

$$\frac{\tilde{P}\tilde{v}}{\tilde{T}} = \frac{\tilde{v}^{1/3}}{\tilde{v}^{1/3}-1} - \frac{1}{\tilde{T}\tilde{v}} + \frac{A}{\tilde{T}^2\tilde{v}^2} + \frac{C}{\tilde{T}\tilde{v}} \qquad\qquad 5.52$$

The values of A and C which are volume dependent are given in their paper. This equation of state will reduce to Equation 2.47 for A = C = 0. The third term on the right hand side of Equation 5.52 arises due to the volume dependence of the local composition. The fourth term is a consequence of the volume dependence of the combinatorial contribution. The value of $\tilde{v}$ resulting from suppressing the A and C terms of Equation 5.52 differ from the one calculated from Equation 2.47. This is shown by Canovas et al. (1982) for a mixture of PIB in benzene at 25°C. Unfortunately, the non-randomness assumption, even by correcting the equation of state for combinatorial and non-combinatorial factors is unlikely to be a great improvement over the Flory equation of state theory. It assumes $v_1^* = v_2^* = v^*$ and neglects the effect of internal degrees of freedom, whereas Hamada et al. (1980) have shown that Flory's theory can be largely improved by use of C_{12} and v_{12}^*. The predicted values of

ΔH_M and $\dfrac{\tilde{v}^E}{\tilde{v}^o}$ have shown a marked agreement with experimental results.

Introduction of these corrections to the non-randomness assumption will undoubtedly give further improvement over the Flory theory.

CHAPTER SIX

CONCLUSIONS

The object of this work was to study experimentally and theoretically the miscibilities of high molecular weight polymers. Several miscible pairs of chlorinated polyethylenes with ethylene-vinyl acetate copolymers have been found. Phase boundaries of an LCST type were found for all the mixtures by light scattering turbidimetry. The region of miscibility is increased by increasing the degree of chlorination in the chlorinated material and the amount of vinyl acetate in the copolymers for the mixtures studied in this work.

Negative interaction parameters between their analogues compounds were deduced from microcalorimetry. Inverse gas chromatography has also given a negative interaction parameter for the polymeric blends below their phase transition temperatures. Fourier transform infra-red spectroscopy at room temperature has detected a lower stretching frequency for the carbonyl group in the presence of chlorinated material.

Different techniques have been shown to be useful in polymer-polymer miscibility studies, when a single glass transition is used as a criteria for miscibility. A combination of interference and electron microscopy has provided information about the morphological behaviour of the blends as a function of temperature.

The contractions of the liquid model compounds were quantified by a densimeter and that of a solid blend by the effect of pressure on the cloud point. The value of $\frac{\Delta V_M}{V^O}$ in the temperature range of 82 to 92^OC was -7.2×10^{-4} for a 50/50 w/w% blend of EVA45 in CPE3 according to the latter method. Pressure also caused the region of miscibility to increase which is a characteristic phenomena of LCST behaviour with negative interaction terms.

In the thermodynamic consideration of the blends a modified Flory-Huggins lattice model and Flory's equation of state theory were used. The Flory-Huggins, χ parameters were replaced by the g function of Koningsveld. This modification could approximate the interaction between the polymers and also could predict the phase boundary of the mixtures. To utilize Flory's equation of state theory, the thermal expansion coefficients of the constituents were measured and a method developed to estimate the thermal pressure coefficients of the pure components. The energy parameter of the mixture, X_{12}, was calculated from the heats of mixing of model compounds. It was demonstrated that Flory's equation of state theory can predict the excess quantities such as excess volume, enthalpy and free energy change on mixing and also the spinodal phase boundary of the mixture when the entropy correction factor, Q_{12}, was used. This factor was quantified by fitting the spinodal equation to the experimental cloud point curve of the mixture. The volume change on mixing for the blend mentioned above at 83.5^OC was calculated to be $-10. \times 10^{-4}$ by this theory.

Finally, we conclude that a theory able to predict the experimental findings would be more complicated than Flory's equation of state theory and would probably start with a new partition function which would contain an entropy correction factor.

APPENDIX

Appendix A

A-I. Derivation of Partition Function, Ω

To obtain Ω , we consider a one-dimensional system of N

impenetrable,non-interacting particles on a line of length L. If 1^* is

the hard-core length of a particle and $1=L/N$ then $1-1^*$ is the free

length available to each particle and Ω is given by:

$$\Omega = \{ (1-1^*) \, e \}^N \qquad\qquad A.I$$

This equation originated in modelling a liquid in a disordered

cell of free volume V. e^N is an entropy function and the partition

function is defined as follows:

$$\Omega_{liquid} = (2\pi\, mkT/h^2)^{3N/2} \cdot V^N/N! \qquad\qquad A.2$$

This partition function for an ordered solid becomes

$$\Omega_{crystal} = (2\pi\, mkT/h^2)^{3N/2} \cdot V^N/N^N \qquad\qquad A.3$$

N! appears in equation A.2 because the molecules in a fluid are

indistiguishable . The entropy change from crystalline to liquid

state is:

$$\Delta S_{c\rightarrow l} = k.\ln\frac{\Omega_{liquid}}{\Omega_{crystal}} = k.\ln\frac{N^N}{N!} \qquad\qquad A.4$$

Appling Stirling's theorem, $\ln N!=N\ln N-N$, to equation A.4 gives:

$$\Delta S_{c\rightarrow l} = kN= k.\ln e^N \qquad\qquad A.5$$

or ,

$$\Omega_{liquid} = \Omega_{crystal} \times \cdot e^N \qquad\qquad A.6$$

Equation A.1 then follows from our realisation that,

$$\Omega_{crystal} \equiv (1-1^*)^N \qquad\qquad A.7$$

and

$$\Omega_{liquid} \equiv \{(1-1^*)e\}^N = \{ \gamma^{1/3}(v^{1/3}-v^{*1/3}) \ e\}^N \qquad\qquad A.8$$

A.11 . Thermal Expansion Coefficient

$$\alpha=(1/v).(\delta v/\delta T)_P \qquad\qquad 2.49$$

Substituting $v=\tilde{v}.v^*$ and $T=\tilde{T}.T^*$ in above equation yields:

$$\alpha T= (\tilde{T}/\tilde{v}).(\delta\tilde{v}/\delta\tilde{T})_P \qquad\qquad A.9$$

Using equation 2.48 to evaluate $\tilde{T}/\tilde{v}$ and $(\delta\tilde{T}/\delta\tilde{v})_P$ will change equation A.9 to:

$$\alpha T=(\tilde{v}^{1/3}-1)/\tilde{v}^{7/3} . (\tilde{v}^{8/3}/(4/3\ \tilde{v}^{1/3}-\tilde{v}^{2/3})) \qquad\qquad A.10$$

or

$$\alpha T =3(\tilde{v}^{1/3}-1)/(4-3\tilde{v}^{1/3}) \qquad\qquad A.11$$

and

$$\tilde{v}^{1/3}=1+\{ (\alpha T)/(3+3\alpha T) \} \qquad\qquad 2.51$$

A.111. Thermal Pressure Coefficient
——————————————————————————

$$\gamma = (\delta P/\delta T)_V = (\delta \tilde{P} \cdot P^* / \delta \tilde{T} \cdot T^*)_V$$

$$= P^*/T^* \cdot (\delta \tilde{P}/\delta \tilde{T})_V \qquad\qquad A.12$$

Differentiating equation 2.47 with respect to T at constant v gives:

$$\delta \tilde{P}/\delta \tilde{T} = \tilde{v}^{-2/3}/(\tilde{v}^{1/3} - 1) \qquad\qquad A.13$$

Combining it with equation A.12,

$$P^* = (\gamma T/\tilde{T}) \cdot (\tilde{v}^{1/3} - 1)/\tilde{v}^{-2/3} \qquad\qquad A.14$$

From equation 2.48 it follows that

$$\tilde{T}\,\tilde{v}^{2} = (\tilde{v}^{1/3} - 1)/\tilde{v}^{-2/3} \qquad\qquad 2.48$$

therefore:

$$P^* = \gamma T \tilde{v}^{2} \qquad\qquad 2.52$$

Appendix B

B.1   Partial Molar Heat of mixing for Binary Mixtures

Differentiating equation 2.76 with respect to N_1 gives:

$$(\delta H_M / \delta N_1)_{T,P,N_2} = P_1^* V_1^* (\tilde{v}_1^{-1} - \tilde{v}^{-1}) + (P_1^* V_1^* N_1 / \tilde{v}^2) \cdot (\delta \tilde{v}/N_1) + (P_1^* V_1^* N_2 / \tilde{v}^2)$$

$$\cdot (\delta \tilde{v}/\delta N_1) + (V_1^* \Theta_2 X_{12}/\tilde{v}) + (N_1 V_1^* X_{12}/\tilde{v}) \cdot (\delta \Theta_2/\delta N_1) - (N_1 V_1^* \Theta_2 X_{12} / \tilde{v}^2) \cdot (\delta \tilde{v}/\delta N_1)$$

B.1

$\delta \Theta_2/\delta N_1$ and $\delta \tilde{v}/\delta N_1$ were obtained separately as follows:

$$\Theta_2 = S_2 \Phi_2 / (S_2 \Phi_2 + S_1 \Phi_1) = (S_2 r_2 N_2 / (S_2 r_2 N_2 + S_1 r_1 N_1)$$

2.66

$$(\delta \Theta_2 / \delta N_1) = -\Theta_1 \Theta_2 / N_1$$

B.2

Three relationships are needed to evalute $\delta \tilde{v}/\delta N_1$,

$$\delta \tilde{v}/\delta N_1 = (\delta \tilde{v}/\delta T^*) \cdot (\delta T^*/\delta \phi_2) \cdot (\delta \phi_2 /\delta N_1)$$

B.3

a. $$T^*/T = \tilde{v}^{4/3} / (\tilde{v}^{1/3} - 1)$$

2.48

$$1/T \cdot (\delta T^*/\delta \tilde{v}) = \tilde{v}^{1/3} \cdot (3\tilde{v}^{1/3} - 4)/3 \cdot (\tilde{v}^{1/3} - 1)^2 = -\tilde{v}^{1/3} T^{*2} (4 - 3\tilde{v}^{1/3})/$$

$$3T^2 \tilde{v}^{8/3}$$

B.4

or

$$\delta \tilde{v}/\delta T^* = -(T \tilde{v}^{7/3} \cdot 3)/(T^* \cdot (4 - 3\tilde{v}^{1/3}))$$

B.5

b.   To find $\delta T^*/\delta\Phi_2$ equation 2.72 is recalled,

$$(\delta T^*/\delta\Phi_2)_{N_2} = \frac{(\delta P^*/\delta\Phi_2).(\Phi_1 P_1^*/T_1^* + \Phi_2 P_2^*/T_2^*) - P^*(P_2^*/T_2^* - P_1^*/T_1^*)}{(\Phi_1 P_1^*/T_1^* + \Phi_2 P_2^*/T_2^*)^2} \qquad \text{B.6}$$

$$= \frac{(\delta P^*/\delta\Phi_2).(P^*/T^*) - P^*/T^*(P_2^*/T_2^* - P_1^*/T_1^*)\ T^*}{(P^*/T^*)^2}$$

$$= (T^*/P^*).(\delta P^*/\delta\Phi_2 - P_2^*(T/T_2^*) + (P_1^*(T/T_1^*))) \qquad \text{B.7}$$

where

$$P^* = \Phi_1 P_1^* + \Phi_2 P_2^* - \Phi_1 \Theta_2 X_{12} \qquad 2.69$$

$$\delta P^*/\delta\Phi_2 = -P_1^* + P_2^* - X_{12}\{\Phi_1 (\delta\Theta_2/\delta\Phi_2) - \Theta_2\}$$

$$= -P_1^* + P_2^* - X_{12}\{\Phi_1 (\Theta_1 \Theta_2/\Phi_1\Phi_2) - \Theta_2\}$$

$$= -P_1^* + P_2^* - X_{12}(\Theta_2/\Phi_2).(\Phi_1 - \Theta_2) \qquad \text{B.8}$$

Substituting it into equation B.7 and rearranging :

$$(\delta T^*/\delta\Phi_2)_{N_2} = (T^*/P^*)\ \{\ P_2^*(1 - T^*/T_2^*) - P_1(1 - T^*/T_1^*) - (\Phi_1 - \Theta_2)X_{12}$$

$$(\ \Theta_2\ /\ \Phi_2\ )\ \}$$

$$= (T^*/P^* \Phi_2)\ \{\ P_1^*(\tilde{T}_1 - \tilde{T}.)/\tilde{T} + X_{12}\ \Theta_2^2\ \} \qquad \text{B.9}$$

C. The last part of equation B.3 to be evaluated is $(\delta\phi_2/\delta N_1)_{N_2}$

$$\phi_2 = r_2 N_2 / (r_2 N_2 + r_1 N_1)$$

$$(\delta\phi_2/\delta N_1)_{N_2} = -(\phi_1\phi_2/N_1) \qquad\qquad\text{B.10}$$

Substituting equations B.5, B.9 and B.10 into equation B.3 we have:

$$(\delta\tilde{v}/\delta N_1)_{N_2} = \frac{\tilde{T}}{P^*} \cdot \frac{3\tilde{v}^{7/3}}{(4-3\tilde{v}^{1/3})} \cdot \frac{\phi_1}{N_1} \cdot \{P_1^*(\tilde{T}_1 - \tilde{T})/\tilde{T} + X_{12}\theta_2^{\,2}\}$$

$$\text{B.11}$$

Before substituting equation B.11 into equation B.1 a small alteration is required in the latter one as,

$$(\delta\Delta H_M/\delta N_1)_{N_2,\,T,P} = P_1^* V_1^* (\tilde{v}^{-1} - \tilde{v}^{-1}) + (V_1^*\theta_2 X_{12}/\tilde{v}) - (V_1^* X_{12}\theta_2/\tilde{v}) +$$

$$(v^*/\tilde{v}^2).(\delta\tilde{v}/\delta N_1).(P_1^* r_1 N_1 + P_2^* r_2 N_2 - r_1 N_1 \theta_2 X_{12}) \qquad \text{B.12}$$

The term in the last brackets is equal to $\bar{r} N P^*$ (see equations 2.57 and 2.69) and by replacing all $\phi_1 = 1 - \phi_2$ equations B.11 and B.12 will give:

$$(\delta\Delta H_M/\delta N_1)_{T,P,N_2} = P_1^* V_1^* (\tilde{v}_1^{-1} - \tilde{v}^{-1}) + (V_1^*\theta_2 X_{12}/\tilde{v}) + (\tilde{T}\phi_1 \bar{r} N/N_1 .(v^*/\tilde{v}^2)$$

$$.(3\tilde{v}^{7/3}/(4-3\tilde{v}^{1/3})).\{P_1^*(\tilde{T}_1 - \tilde{T})/\tilde{T} + X_{12}\theta_2^{\,2}\} \qquad \text{B.13}$$

We have $\bar{r} N\phi_1 = r_1 N_1$ and $V_1^* = r_1 v^*$ also

$$\alpha = \{3.(\tilde{v}^{1/3} - 1)/(4 - 3\tilde{v}^{1/3})T\} \;,\; \tilde{T} = (\tilde{v}^{1/3} - 1)/(\tilde{v}^{4/3})$$

,therefore equation B.13 will be simpler,i.e.

$$(\delta\Delta H_M/\delta N_1)_{T,P,N_2} = P_1^*v_1^*(\tilde{v}_1^{-1} - \tilde{v}^{-1}) + (v_1^*\Theta_2^2 X_{12}/\tilde{v}) + (P_1^*v_1^* \cdot \alpha T(\tilde{T}_1 - \tilde{T})/\tilde{T}\tilde{v})$$

$$+ X_{12}v_1^*\alpha T\Theta_2^2/\tilde{v}$$

$$= P_1^*v_1^*\{(\tilde{v}_1^{-1} - \tilde{v}^{-1}) + (\alpha T/\tilde{v}) \cdot (\tilde{T}_1 - \tilde{T})/\tilde{T}\} + (v_1^*X_{12}/\tilde{v}) \cdot (1 + \alpha T)\Theta_2^2$$

<div align="right">2.82</div>

B.11 . Free Energy Change on Mixing

$-E_{o_M}/kT$ in equation 2.60 will be substituted by:

$$-Eo_M C/P^*v^*\tilde{T} = \bar{r} N C/\tilde{v}\tilde{T} \qquad\qquad B.14$$

The Helmholtz free energy of a mixture is given by:

$$F_M = -kT \ln Z \qquad\qquad\qquad B.15$$

or $\quad \Delta F_M = F_M - (F_1 + F_2) \qquad\qquad B.16$

where F_1 and F_2 are the free energies of the pure components. Thus,equation 2.60 for condition B.16 gives:

$$\Delta F_M = -kT \ln \frac{Z_{comb.}}{Z_{comb.,1}\, Z_{comb.,2}} \cdot (\gamma v^*)^{\bar{r}NC - r_1 N_1 C_1 - r_2 N_2 C_2}$$

$$+kT \ln \frac{(\tilde{v}_1^{1/3} - 1)^{3r_1 N_1 C_1} \cdot (\tilde{v}_2^{1/3} - 1)^{3 r_2 N_2 C_2}}{(\tilde{v}^{1/3} - 1)^{3 \bar{r}NC}}$$

$$+kT(r_1 N_1 C_1/\tilde{v}_1\tilde{T}_1 - r_2 N_2 C_2/\tilde{v}_2\tilde{T}_2 - \bar{r}NC/\tilde{v}\tilde{T}) \qquad\qquad B.17$$

By using $T = \tilde{T}_i T_i^*$, $P_i^* v_i^* = C_i k T_i^*$ and $\bar{r}N \Phi_i = r_i N_i$ the third term of equationB.17 can be easily converted to:

$$\bar{r}Nv^* \{ \Phi_1 P_1^* / \tilde{v}_1 + \Phi_2 P_2^* / \tilde{v}_2 - P^* / \tilde{v} \} = \Delta H_M \qquad 2.74$$

While using $\bar{r}NC = r_1 N_1 C_1 + r_2 N_2 C_2$ in the second term yields:

$$3kT \ r_1 N_1 C_1 \ln \ (\ \tilde{v}_1^{1/3} - 1 \ )/(\ \tilde{v}^{1/3} - 1 \ ) + 3kT \ r_2 N_2 C_2 \ln \ (\ \tilde{v}_2^{1/3} - 1)/(\ \tilde{v}^{1/3} - 1 \ ) \qquad B.18$$

or

$$3P_1^* V_1^* N_1 \tilde{T}_1 \ln \ (\ \tilde{v}_1^{1/3} - 1 \ )/(\ \tilde{v}^{1/3} - 1 \ ) + 3 \ P_2^* V_2^* N_2 \tilde{T}_2 \ln \ (\ \tilde{v}_2^{1/3} - 1 \ )/(\ \tilde{v}^{1/3} - 1) \qquad B.19$$

or

$$3\bar{r}Nv^* \{ P_1^* \Phi_1 \tilde{T}_1 \ln \ (\tilde{v}_1^{1/3} - 1)/(\ \tilde{v}^{1/3} - 1 \ ) + P_2^* \Phi_2 \tilde{T}_2 \ln \ (\tilde{v}_2^{1/3} - 1)/(\ \tilde{v}^{1/3} - 1 \ ) \} \qquad B.20$$

Equations B.19(or B.20) plus equation 2.74 are ^R_G given by equation 2.89 : The first term of equation B.17 represents the combinatorial part($-T\Delta S'_{Comb}$.) and will be replaced from the lattice theory.Hence,

$$\Delta F_M = \bar{r}NkT \ \{ (\Phi_1 \ / \ r_1)\ln \ \Phi_1 + (\Phi_2 / \ r_2) \ \ln \ \Phi_2 \}$$

$$+3\bar{r}Nv^* \ \{ \ \Phi_1 P_1^* \tilde{T}_1 \ln(\ \tilde{v}_1^{1/3} - 1 \ )/(\ \tilde{v}^{1/3} - 1) + \Phi_2 \ P_2^* \ \tilde{T}_2 \ \ln(\ \tilde{v}_2^{1/3} - 1)/(\ \tilde{v}^{1/3} - 1) \}$$

$$+ \ \bar{r} \ N \ v^* \{ \Phi_1 P_1^* / \ \tilde{v}_1 + \Phi_2 P_2^* / \ \tilde{v}_2 \ - P^* / \ \tilde{v} \ \} \qquad B.21$$

The chemical potential of component one in the mixture relative to the pure component is defined as:

$$\mu_1 - \mu_1^0 = -RT\,\{\ \delta\ \ln(Z\ /Z_1)/\delta\ N_1\}_{T,V,N_2}$$

$$= (\ \delta\ \Delta F_M\ /\delta\ N_1)_{T,V,N_2} + (\delta\Delta F_M\ /\delta\tilde{v})_{T,N_1 N_2}\cdot(\delta\tilde{v}\ /\delta N_1)_{T,V,N_2} \quad B.22$$

$$= RT\,\{\ \ln\ \phi_1 + (1-r_1/\ r_2)\ \phi_2\} + (V_1^{*}X_{12}\ /\ \tilde{v})\theta_2^2$$

$$+$$

$$+P_1^{*}V_1^{*}\,\{3\tilde{T}_1\ln\ (\ \tilde{v}_1^{1/3} - 1)/(\ \tilde{v}^{1/3} - 1)\ +(\tilde{v}_1^{-1} - \tilde{v}^{-1}) + P_1(\ \tilde{v} - \tilde{v}_1\ \}\quad B.23$$

Where $\tilde{P}_1\tilde{v}$ is the contribution of the second term in equation B.22 ,on the chemical potential, $(\delta\tilde{v}/\delta N_1)_{T,V,N_2} = V\ \delta(\bar{r}\ v^{*}N)^{-1}/\delta N_1 = -(\ \phi_1\tilde{v}\ /\ N_1)$.

Since this contribution is very small at ordinary pressures,it may be neglected, but it should be included at higher pressures.

B.111.   Partial Molar Residual Entropy of Mixing for Binary Mixtures

----

Differentiating equation 2.90 at constant N_2 gives:

$$T(\, \delta S/\delta\, N_1)_{T,P,N_2} = -P_1^* V_1^* \{3\, \tilde{T}_1 \ln\, (\, \tilde{v}_1^{1/3} - 1)/(\, \tilde{v}^{1/3} - 1)\} + \{\, (\, P_1^* V_1^* N_1 \tilde{T}_1 + P_2^* V_2^* N_2 \tilde{T}_2)/$$

$$(\, \tilde{v}^{2/3}\, (\, \tilde{v}^{1/3} - 1\,))\} \cdot (\delta\, \tilde{v}\, /\delta\, N_1) = T\, (\, \bar{S} - \bar{S}^o\,) \qquad \text{B.24}$$

where

$$P_1^* V_1^* N_1 \tilde{T}_1 + P_2^* V_2^* N_2 \tilde{T}_2 = r_1 N_1 C_1 k + r_2 N_2 C_2 k = \bar{r}\, NCk = \bar{r}\, N\, P^* v^* \tilde{T} \qquad \text{B.25}$$

$\delta\tilde{v}\, /\delta N_1$ is given by equation B.11. Application of equation B.13 procedure

here, will give relation 2.91 for TS_1^R .

Appendix   C

C.1.   The volume change of mixing calculated from equation 2.80 by   the

procedure explained in section 5.2.4. for mixtures of sec-octyl acetate in

ceroclor 45 and 52 at 64.5^oC are given in figure C-1. The state parameters
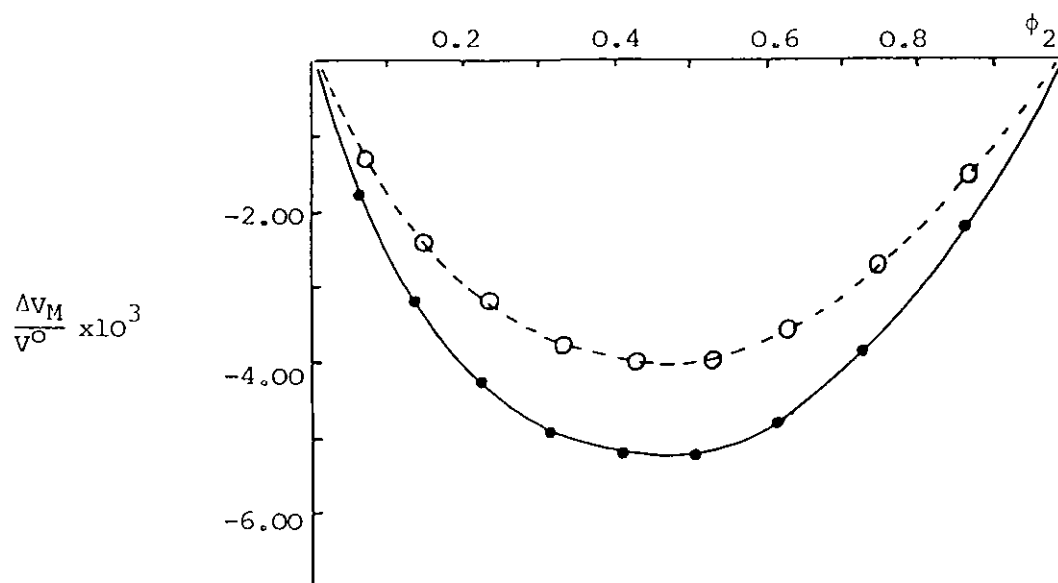
of the pure components are given in section 5.2.1.

FIG. C. 1. Theoretical values of $\dfrac{\Delta V_M}{V^O}$ calculated from Flory's equation of state theory at 64.5^OC. Full line represents the sec-octyl acetate-S52 mixtures and dashed line represents the sec-octyl acetate-S45 mixtures. Plotted against segmental fraction of ceroclors.

REFERENCES

Abe, A. and Flory, P.J., 1965. J. Amer. Chem. Soc. 87:9, 1838.

Abe, A. and Flory, P.J., 1966. J. Amer. Chem. Soc. 88:13, 2887.

Abu-Isa, I.A. and Myers, M.E., 1973. J. Polym. Sci. Chem. Ed., 11, 225.

Alexander, L.E., 1969. 'X-Ray Diffraction Methods in Polymer

    Science'. Wiley.

Allen, G., Gee, G. and Nicholson, J.P., 1960A. Polymer 1, 56, ibid.

    1961, 2, 8.

Allen, G., Gee, G., Mangaray, D., Sins, D. and Wilson, G.J., 1960B.

    Polymer 1, 467.

Ambron, D., 1980. NPL Report Chem., August.

Askadskii, A.A., Kalmakova, L.K., Tager, A.A., Slonimskii, G.L. and

    Korshak, V.V., 1977. Polym. Sci. USSR, 19:5.

ASTM, 1971. D1505-68, 1159.

Barandani, V., 1979. Macromolecules, 12, 883.

Baranyi, G.D. and Guillet, J.E., 1977. Macromolecules 11, 228.

Baranyi, G.D., Guillet, J.E., Jeberien, H.E. and Klein, J., 1980.

    Macromol. Chem., 181, 215.

Baranyi, G.D., 1981. Macromolecules, 14, 683.

Bennett, A.H., 1951. 'Phase Microscopy'. Wiley.

Bernstein, R.E., Cruz, C.A., Paul, D.R. and Barlow, J.W., 1977.

    Macromolecules 10, 681.

Billmeyer Jr., F.W., 1971. 'Textbook of Polymer Science'. Wiley.

Biroz, J., Zaman, L. and Patterson, D., 1971. Macromolecules, 4, 30.

Bondi, A., 1964. J. Phys. Chem. 68, 441.

Booth, C. and Pickles, C.P., 1973. J. Polym. Sci. Phys. Ed. 11, 595.

Brandrup, J. and Imergut, E.H., 1975. 'Polymer Handbook'. Wiley.

Brydson, J.A., 1978. 'Rubber Chemistry'. Appl. Sci. Pub.

Busnel, J.P., 1982. Polymer, 23, 137.

189

Cahn, J.W., 1975. J. Chem. Phys. $\underline{42}$, 93.

Canovas, A.A., Rubio, R.G. and Renuncio, J.A.R., 1982. J. Poly. Sci.
Phys. Ed. $\underline{20}$, 784.

Chahal, S.R., Kao, W.P. and Patterson, D., 1973. Faraday Transactions
$\underline{1}$, 1834.

Chang, T.S., 1939. Proc. Cambridge Philos. Soc., $\underline{38}$, 109.

Chong, C.L., 1981. Ph.D. Thesis, Imperial College.

Christner, G.L. and Thomas, E.L., 1977. J. Appl. Phys. $\underline{48}$, 4063.

Combs, L.L. and Dunne, L.J., 1982. J. Molecular Structure, $\underline{87}$, 375.

Coleman, M.M., Zarian, J., Varnell, D.F. and Painter, P.C., 1977. J.
Polym. Sci. Polym. Phys. Lett. Ed. $\underline{15}$, 745.

Coleman, M.M. and Zarian, J., 1979. J. Polym. Sci. Polym. Phys. Ed.
$\underline{17}$, 837.

Collins, E.A., Bares, J. and Billmeyer Jr., F.W., 1973. 'Experiments
in Polymer Science'. Wiley.

Cooper, D.R. and Booth, C., 1977. Polymer $\underline{18}$, 164.

Cowie, J.M.G., 1973. 'Polymers: Chemistry and Physics of Modern
Materials'. Intertext Book.

Cowie, J.M.G. and McEwen, I.J., 1979. Polymer, $\underline{20}$, 719.

Cowie, J.M.G. and Saeki, S., 1982. Unpublished.

Cruickshank, A.J.B., Windsor, M.L. and Young, C.L., 1966. Proc. R.
Soc. London, Ser. A, $\underline{295}$, 259.

Davis, D.D. and Kwei, 1980. J. Polym. Sci. Phys. Ed., $\underline{18}$, 2337.

Debye, P., 1959. J. Chem. Phys. $\underline{31}$, 680.

Deshpande, D.D.D., Patterson, D., Schreiber, and Su, C.S., 1974.
Macromolecules, $\underline{7}$, 530.

Demarzio, E.A. and Gibbs, J.M., 1959. J. Polym. Sci, $\underline{XL}$, 121.

Doube, C.D., 1979. Ph.D. Thesis, Imperial College.

Doube, C.D. and Walsh, D.J., 1979. Polymer, $\underline{20}$, 115.

Doube, C.D. and Walsh, D.J., 1980. Europ. Polym. J. $\underline{17}$, 63.

Dymond, J.H. and Smith, E.B., 1980. 'The Virial Coefficients of

Pure Gases and Mixtures'. Oxford Univ. Press.

Earnest Jr., T.R. and MacKnight, W.J., 1980. Macromolecules, $\underline{13}$, 844.

Eichinger, B.E. and Flory, P.J., 1968. Trans. Faraday Soc., $\underline{64}$,

2035, 2053, 2061, 2065.

Flory, P.J., 1941. J. Chem. Phys. $\underline{9}$, 660.

Flory, P.J., 1942. J. Chem. Phys., $\underline{10}$, 51.

Flory, P.J., 1965. J. Amer. Chem. Soc., $\underline{87:9}$, 1833.

Flory, P.J., Orwell, R.A. and Vrig, A., 1964. J. Amer. Chem. Soc.

$\underline{86}$, 3507, 3515.

Flory, P.J., Ellenson, J.L. and Eichinger, B.E., 1968. Macromolecules,

$\underline{1}$, 279, 285, 287.

Flory, P.J. and Hacker, H., 1971. Trans. Faraday Soc., $\underline{67}$, 2258.

Fox, T.G., 1956. Quoted from Pochan et al. (1979) paper.

Frensdroff, H.K. and Ekiner, O., 1971. J. Polymer Sci., A-1, $\underline{9}$, 205.

Fried, J.R., Karasz and MacKnight, W.J., 1978. Macromolecules, $\underline{11}$, 150.

Fujita, H. and Teramoto, A., 1982. J. Poly. Sci. Phys. Ed., $\underline{20}$, 893.

German, A.L. and Heikens, D., 1971. J. Polym. Sci. a-1, $\underline{9}$, 225.

German, A.L. and Heikens, D., 1975. Erup. Polym. J., $\underline{11}$, 555.

Gilmer, J., Goldstein, R.S. and Stein, R.S. Unpublished.

Gordon, M. and Taylor, J.S., 1952. J. Appl. Chem. $\underline{2}$, 493.

Hamada, F., Shiomi, T., Fujisawa, K. and Nakajima, A., 1980.

Macromolecules, $\underline{13}$, 729.

Hammer, C.F., 1971. Macromolecules, $\underline{4}$, 69.

Hedvig, P., 1977. 'Dielectric Spectroscopy of Polymer'. Adam Higler,

Bristol.

Hedvig, P. and Marossy, K., 1981. Die Angemandite Makromolekulare

Chemi, $\underline{79}$, 51.

Hichman, J.J. and Ikeda, R.M., 1973. J. Polym. Sci. Phys. Ed. $\underline{11}$, 1713.

Hildebrand, J.H. and Wood, S.E., 1933. J. Chem. Phys. 1, 817.

Hildebrand, J.H., 1953. Discu. Faraday Soc. No. 15, 9.

Hildebrand, J.H., Praunsnitz, J.M. and Scott, R.L., 1970. 'Regular
    and Related Solutions'. Van Nostrand Reinhold Co.

Hoy, K.L., 1970. J. Paint. Technol. 42, 76.

Huggins, M.L., 1941. J. Chem. Phys. 9, 660.

Huggins, M.L., 1942. Ann. N.Y. Acad. Sci. 43, 1.

Huggins, M.L., 1970. J. Phys. Chem., 74, 371.

ICI, BP, 497643.

Irvine, P. and Gordon, M., 1980. Macromolecules 13, 761.

Jacques, C.H.H. and Hapfenberg, H.B., 1974. Polym. Eng. Sci., 14, 441.

Kelley, F.N. and Bueche, F., 1961. J. Polym. Sci., 50, 549.

Kleintjens, L.A., Koningsveld, R. and Stockmayer, W.H., 1976. Br.
    Polym. J., 8, 144.

Kleintjen, L.A., Koningsveld, R. and Gordon, M., 1980. Macromolecules,
    13, 303.

Kokkonen, P., 1982. J. Chem. Thermody., 14, 585.

Koberstein, J., Russell, T.P. and Stein, R.S., 1979. J. Polym. Sci.
    Phys. Ed. 17, 1719.

Koningsveld, R., 1970. J. Macromolec. Sci. Phys. B17, 144.

Koningsveld, R. and Kleintjens, L.A., 1971. Macromolecules 4, 637.

Koningsveld, R. and Kleintjens, L.R., 1972. J. Polym. Sci. part C,
    39, 281.

Koningsveld, R., Kleintjens, L.A. and Schaffelers, H.M., 1974A. Pure
    Appl. Chem. 39, 1.

Koningsveld, R., Stockmayer, W.H., Kennedy, J.A. and Kleintjens, L.A.,
    1974B. Macromolecules, 7, 73.

Koningsveld, R. and Kleintjens, L.A., 1977. Br. Polym. J., 9, 212.

Koningsveld, R., Kleintjens, L.A. and Onclin, M.H., 1980. J. Macromol. Sci. Phys. B18(3), 363.

Kosai, K. and igashino, T., 1975. Nippon Setchaku Kiaki Shi, 11, 2.

Kowie, T.K., Nishi, T. and Roberts, R.F., 1974. Macromolecules, 7, 667.

Krause, S., 1978. Chapter Two of 'Polymer Blends'. Paul and Newman, ed.

Lipatov, Yu. S., Nesterov, A.E. and Ignotova, T.D., 1978. Europ. Polym. J., 18, 775.

Longuet-Higgins, H.C., 1953. Discu. Faraday Soc. No. 15, 73.

MacKnight, W.J., Karasz, F.E. and Fried, J.R., 1978. Chapter Five of 'Polymer Blend'. Paul and Newman, ed.

Marcincin, C., Romanov, A. and Pollak, V., 1972. J. Appl. Polym. Sci. 16, 2239.

McCrum, N.G., Read, B.E. and Williams, G., 1967. 'Anelastic and Dielectric Effect in Polymer Solids'. Wiley and Sons.

McGlashen, M.L. and Potter, D.J.B., 1962. Proc. R. Soc. London Ser. A, 267, 478.

Miller, A.R., 1942. Cambridge Philos. Soc., 38, 109.

McMaster, L.P., 1973. Macromolecules, 6, 760.

McMaster, L.P., 1975. Adv. Chem. Ser. 142, 43.

Meyer, M., Sande, J.V. and Uhlman, D.R., 1978. J. Polym. Sci. Phys. Ed. 6, 2005.

Murayama, T., 1978. 'Dynamic Mechanical Analysis of Polymeric Materials'. Elsevier.

Nesterov, Yc.A., Lipatov, Yu.S. and Ignatova, T.P., 1976. Polym. Sci. USSR, 18, 23.

Nicholson, D.J., 1958. Ph.D. thesis, Manchester University.

Nielsen, L.E., 1980. J. Polym. Sci., 42, 357.

Nishi, T. and Kwei, T.K., 1975. Polymer 16, 285.

Nishi, T. and Wang, T.T., 1975. Macromolecules 8, 227, 909

Olabisi, O., 1975. Macromolecules, 18, 316.

Olabisi, O., Robson, L.M. and Shaw, M.T., 1979. 'Polymer-Polymer Miscibility'. Academic Press.

Orwoll, R.A. and Flory, P.J., 1967. J. Am. Chem. Soc., 89, 6814, 6822.

Patterson, D., 1968. J. Polym. Sci. Part C., 16, 3379.

Patterson, D. and Delmas, G., 1970. Discuss. Faraday Soc. No. 49, 98.

Patterson, D., 1972. Pure and Applied Chem. 31, 135.

Patterson, D. and Robard, A., 1978. Macromolecules, 11, 690.

Paul, D.R. and Newman, S., 1978. 'Polymer Blends', Vol. I and II,
        Academic Press.

Paul, D.R., 1978. Chapter One of 'Polymer Blends', Paul and Newman, ed.

Paul, D.R. and Barlow, J.W., 1979. 'Multiphase Polymers', Adv.
        Chem. Ser., 176.

Perena, J.M., Fatou, J.G. and Guzman, J., 1980. Makromol. Chem.
        181, 1349.

Pikkarainen, L., 1982. J. Chem. Thermody. 14, 503.

Pochan, J.M., Beatty, C.L. and Pochan, D.F., 1979. Polymer, 20, 879.

Prest, W.M. and Porter, R.S., 1972. J. Polym. Sci. Phys. Ed. 10, 1639.

Prigogine, I., Trappeniers, N. and Mathot, V., 1953. Discu. Faraday
        Soc., No. 15, 93.

Prigogine, I., 1957. 'The Molecular Theory of Solutions', North-
        Holland Pub. Amsterdam.

Rabek, J.F., 1980. 'Experimental Methods in Polymer Chemistry', Wiley.

Reich, R. and Cohen, Y., 1981. J. Polym. Sci. Phys. Ed., 19, 1255.

Renuncio, J.A.R. and Prausnitz, J.M., 1976. Macromolecules, 9, 898.

Reynolds, W.B. and Conterine, P.J., 1961. US Pat. 2972, 604.

Robard, A. and Patterson, D., 1977. Macromolecules, 10, 121.

Rowlinson, J.S., 1970. Discu. Faraday Soc. 49, 30.

Saeki, S., Kumahara, N., Nakata, M. and Kaneko, M., 1975. Polymer
        16, 445.

Saeki, S., Kumahara, N. and Kaneko, M., 1976. Macromolecules 9, 101.

Sanchez, I.C. and Lacomb, R.H., 1976. J. Phys. Chem. 80, 2352, 2568.

Sanchez, I.C., 1978. Chapter Three of 'Polymer Blends', Paul and
        Newman, ed.

Sanchez, I.C. and Lacomb, R.H., 1978. Macromolecules, 11, 1145.

Sanchez, I.C., 1980. J. Macromol. Sci. Phys. B17(3), 565.

Scatchard, G., 1931. Chem. Rev., 8, 321.

Scatchard, G., 1937. Trans. Faraday Soc., 33, 160.

Schurer, J.W., de Boar, A. and Challa, G., 1975. Polymer, 16, 201.

Scott, R., 1949. J. Chem. Phys., 17, 268, 279.

Senich, G.A. and MacKnight, W.J., 1980. Macromolecules 13, 106.

Sharama, R., Sud, L.V. and Pillai, P.K.C., 1980. Polymer 21, 925.

Shih, H. and Flory, P.J., 1972. Macromolecules 5, 758, 761.

Shultz, A.R. and Flory, P.J., 1952. J. Amer. Chem. Soc., 74, 4760.

Small, P.A., 1953. J. Appl. Chem. 3, 71.

Smidsord, O. and Guillet, J.E., 1969. Macromolecules, 2, 272.

Stein, R.S., 1978. Chapter Nine of 'Polymer Blends', Paul and
        Newman, ed.

Storstrom, H. and Randby, B., 1971. 'Multiphase Polymers', Adv.
        Chem. Ser., 99.

Tabb, D.L. and Koening, J.L., 1975. Macromolecules, 8, 929.

Tager, A.A., Scholokhovich, T.I., and Bessonov, Ju. S., 1975.
        Europ. Polym. J., 11, 321.

ten Brinke, G., Eshuis, A., Roerdink, E. and Challa, G., 1981.
        Macromolecules, 14, 867.

Timmermans, J., 1960. 'Physical Chemical Constants of Pure Organic
        Compounds'. Elsevier.

Tompa, H., 1956. 'Polymer Solutions'. Butterworth, London.

Tripathi, J.B.P., 1979. Ph.D. Thesis, Imperial College.

van Aartsen, J.J., 1970. Europ. Polym. J., 6, 919.

van Aartsen, J.J. and Smolders, C.A., 1970. Europ. Polym. J., 6, 1105.

van Krevelen, D.W., 1972. 'Properties of Polymers'. Elsevier.

van Laar, J.J., 1910. Z. Physik. Chem. 72, 723.

Varnell, D.F., Runt, J.P. and Colman, M.M., Unpublished A.

Varnell, D.F., Maskala, E.J., Painter, P.C. and Colman, M.M.,

    unpublished B.

Vink, H., 1975. Europ. Polym. J., $\underline{11}$, 443.

Walsh, D.J. and McKeown, J.G., 1980. Polymer, $\underline{21}$, 1330.

Weeks, N.E., Karasz, F.E. and MacKnight, W.J., 1977. J. Appl.

    Phys. $\underline{48}$, 4068.

Wetton, R.E., MacKnight, W.J., Fried, J.R. and Karasz, F.E., 1978.

    Macromolecules, $\underline{11}$, 158.

Wood, L.A., 1958. J. Polym. Sci., $\underline{28}$, 319.

Zambrand, G., 1981. Ph.D. Thesis, Imperial College.

Ziska,J.J., Barlow, J.W. and Paul, D.R., 1981. Polymer, $\underline{22}$, 918.